

AD-A231 601

~~DTIC FILE COPY~~

REPORT DOCUMENTATION PAGE		DTIC FILE COPY	
1. AGENCY USE ONLY (Leave blank)		2. REPORT DATE 1990	3. REPORT TYPE AND DATES COVERED THESIS/EXERCISATION
4. TITLE AND SUBTITLE Features of the Raleigh Tornadic Storm Based on Analysis of Damage		5. FUNDING NUMBERS	
6. AUTHOR(S) John Thomas Roth		7. PERFORMING ORGANIZATION NAME(S) AND ADDRESS(ES) AFIT Student Attending: North Carolina State University	
9. SPONSORING / MONITORING AGENCY NAME(S) AND ADDRESS(ES) AFIT/CI Wright-Patterson AFB OH 45433-6583		10. SPONSORING / MONITORING AGENCY REPORT NUMBER AFIT/CI/CIA-90-145	
11. SUPPLEMENTARY NOTES			
12a. DISTRIBUTION / AVAILABILITY STATEMENT Approved for Public Release IAW 190-1 Distributed Unlimited ERNEST A. HAYGOOD, 1st Lt, USAF Executive Officer		12b. DISTRIBUTION CODE	
13. ABSTRACT (Maximum 200 words)			
<div style="text-align: right;"> DTIC SELECTE FEB 07 1991 S B D </div>			
14. SUBJECT TERMS		15. NUMBER OF PAGES 122	
		16. PRICE CODE	
17. SECURITY CLASSIFICATION OF REPORT	18. SECURITY CLASSIFICATION OF THIS PAGE	19. SECURITY CLASSIFICATION OF ABSTRACT	20. LIMITATION OF ABSTRACT

**FEATURES OF THE RALEIGH
TORNADIC STORM BASED ON
ANALYSIS OF DAMAGE**

by

John Thomas Roth

Captain, U.S. Air Force

A thesis submitted to the Graduate Faculty of
North Carolina State University
in partial fulfillment of the
requirements for the Degree of
Master of Science

Raleigh, NC

1990

112 pages

145

**FEATURES OF THE RALEIGH
TORNADIC STORM BASED ON
ANALYSIS OF DAMAGE**

by

John Thomas Roth

A thesis submitted to the Graduate Faculty of
North Carolina State University
in partial fulfillment of the
requirements for the Degree of
Master of Science

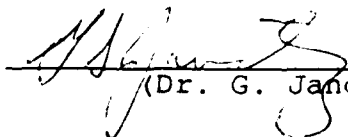
Department of Marine, Earth, and Atmospheric Sciences

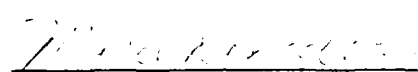
Raleigh, NC

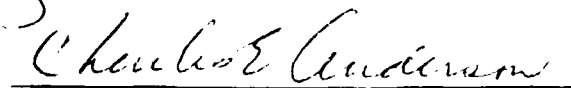
1990

APPROVED BY:




(Dr. G. Janowitz)


(Dr. M. Davidian)


(Dr. C. Anderson)
Chairman of Advisory Committee

<input checked="checked" type="checkbox"/>
<input type="checkbox"/>
<input type="checkbox"/>

Classification/	
Availability Codes	
Avail and/or	
Dist	Special
A-1	

ABSTRACT

ROTH, JOHN T. Features of the Raleigh Tornadic Storm based on Analysis of Damage. (Under the direction of Charles E. Anderson.)

The damage left by the tornado that moved across north Raleigh on 28 November 1988 indicates that more than just the tornadic vortex itself was responsible for causing it. The width of the damage track, in relation to the intensity of damage at its center, and the orientation of fallen trees indicate the presence of strong winds not directly associated with the tornado. Additional aberrations in the pattern of the damage suggest that microbursts, or small scale outflow areas, were also present in close proximity to the tornado.

A computer model was devised to simulate damage patterns caused by a tornado. Results from this model were examined and compared to the actual damage. By manipulating the input values so the output graphs look similar to the actual damage, the magnitude and direction of the ambient wind, and the location of microbursts, could be estimated. The results suggest the tornado was accompanied by ambient winds of at least 20 m s^{-1} , and microbursts in all quadrants relative to the tornado motion except the left front quadrant. The results, as well as the distribution of the damage itself, suggest that the intensity of the damage was increased by the presence of microbursts interacting with the tornado.

ACKNOWLEDGEMENTS

I would like to extend my appreciation to the United States Air Force Institute of Technology and Air Weather Service for making this research possible, and for providing moral and financial assistance to the effort.

I would also like to extend grateful thanks to my advisor, Dr. Charles Anderson, for all his guidance and support in conducting this research. I also wish to acknowledge the following people for their assistance: Kevin Schrab for his help in retrieving McIDAS data; Kevin and Ron Weglarz for their input into the mechanics of the computer model; Ron and Dr. Gerald Janowitz for their assistance with the mathematics of the model; Scott Funk for his preliminary research on the Raleigh tornado, including obtaining the Volens radar data and the Shearon Harris data; Dr. Gerald Watson, Dr. Al Riordan, and the students of Dr. Anderson's MEA 593A class in the spring 1989 for the early footwork of the damage survey. I also extend appreciation to the North Carolina Department of Transportation for its aerial photographs, and television stations WRAL and WTVD for their video tapes, which were of great value in mapping the damage, and the people at the National Weather Service office at the Raleigh-Durham airport for their assistance in obtaining local data.

TABLE OF CONTENTS

	<u>Page</u>
LIST OF TABLES.....	v
LIST OF FIGURES.....	vi
LIST OF ABBREVIATIONS AND SYMBOLS.....	ix
1. INTRODUCTION AND LITERATURE REVIEW.....	1
1.1 Overview.....	1
1.2 Thunderstorm Concepts.....	6
1.3 Squall Lines.....	10
1.4 Tornadoes.....	12
1.5 Tornado Damage.....	14
1.6 Downbursts and Microbursts.....	15
1.7 Radar Signatures.....	16
1.8 Long Track Tornadoes.....	17
2. RESEARCH OBJECTIVES AND METHODS.....	19
2.1 Objectives.....	19
2.2 Analysis of Tornado Damage.....	21
2.3 Additional Data.....	24
2.3.1 McIDAS Data.....	24
2.3.2 Radar Data.....	24
2.3.3 Other Data.....	25
3. METEOROLOGICAL SITUATION.....	26
3.1 Identification of Mesolow.....	26
3.2 Wind Data and Mesocyclone Circulation.....	28
3.3 Radar Imagery.....	31
3.4 Satellite Imagery.....	34
4. DETAILED DESCRIPTION OF THE DAMAGE.....	41
4.1 Overview.....	41
4.2 Chronology.....	43
4.3 Width of Track.....	44
4.4 Direction of Movement.....	45
4.5 Detailed Examination of Damaged Areas.....	45
Region 1.....	46
Region 2.....	49
Region 3.....	52
Region 4.....	54
Region 5.....	56
Region 6.....	57
Region 7.....	59

5.	DESCRIPTION OF DAMAGE MODEL.....	61
5.1	General Description.....	61
5.2	Flow Near a Tornado.....	62
5.3	Flow From a Nearby Microburst.....	65
5.4	Use of the Model.....	72
6.	RESULTS AND ANALYSIS.....	75
6.1	Model Output.....	75
6.2	Analysis of Damage Using Model Output Results...	75
6.3	Other Analyses of the Damage.....	95
7.	CONCLUSIONS AND FUTURE RESEARCH.....	102
7.1	Conclusions.....	102
7.2	Future Research.....	104
	REFERENCES.....	105
	APPENDIX.....	109

LIST OF TABLES

	<u>Page</u>
3.1 15 minute averaged pressure readings from the Shearon Harris plant.....	28
3.2 Portions of official weather observations from the NWS office at RDU.....	30
4.1 Probable chronology of tornado movement in Wake County.....	44

LIST OF FIGURES

	<u>Page</u>
1.1 County outlines of the northern piedmont area of North Carolina.....	2
1.2 Locations of tornadoes in the November, 1988 North Carolina/Virginia outbreak.....	3
1.3 Location of tornado damage track in north Raleigh.....	5
1.4 Diagram of three-dimensional airflow patterns in a classical supercell thunderstorm.....	8
1.5 Surface airflow patterns in a tornado producing supercell thunderstorm.....	9
1.6 Schematic diagram of the splitting of an intense thunderstorm cell.....	11
2.1 Locations of tornado reports in Wake County.....	23
3.1 Microbarograph traces from (a) NCSU and (b) RDU, showing "V" notches around 0100, and frontal passage around 0500.....	27
3.2 Wind trace from the Shearon Harris plant.....	29
3.3 Transcriptions of PPI scope photographs from the Volens radar.....	32
3.4 Transcription of PPI scope from Marseilles IL radar at 2215 GMT, 3 April 1974.....	35
3.5 Enhanced infrared GOES satellite picture at time 0501 GMT.....	36
3.6 Same as Figure 3.5, time 0531 GMT.....	37
3.7 Same as Figure 3.5, time 0601 GMT.....	38
3.8 Same as Figure 3.5, time 0631 GMT.....	39
4.1 Locations of the regions of the damage track in north Raleigh referred to in the text.....	42
4.2 Damage map of Region 1.....	47
4.3 Damage map of Region 2.....	50

4.4	Damage map of Region 3.....	53
4.5	Damage map of Region 4.....	55
4.6	Damage map of Region 6.....	58
5.1	Computer flow chart of damage simulation model.....	63
5.2	Horizontal velocity profile generated by a model microburst.....	67
5.3	Schematic surface flow associated with various types of microbursts.....	70
5.4	Doppler radar velocity profile from a microburst producing storm in the JAWS experiment.....	71
6.1	Model output for a tornado with a 30 m s^{-1} ambient wind from same direction as tornado movement.....	78
6.2	Model output with 20 m s^{-1} ambient wind from direction 20° less than (i.e. backed direction) that of tornado movement.....	79
6.3	Model output with 25 m s^{-1} ambient wind from direction 30° less than that of tornado movement.....	80
6.4	Damage west of Glenwood Avenue.....	81
6.5	Model output with 20 m s^{-1} ambient wind and a microburst to right front of tornado.....	82
6.6	Damage in Region 2.....	84
6.7	Model output with microburst to left rear of tornado, with little interaction between the two.....	86
6.8	Model output with microburst to left rear of tornado, but much closer initially than in Figure 6.7.....	88
6.9	Damage in Region 4.....	89
6.10	Damage in Region 6.....	90
6.11	Model output with microburst to rear and immediate right of tornado.....	91
6.12	Model output with no microburst, with ambient wind 25 m s^{-1} from direction 40° less than tornado movement direction.....	92

6.13	Composite showing model output with two microbursts.	94
6.14	Model output showing microburst to right front of circulation center, with no tornado damage present.....	96
6.15	Locations of microbursts along damage track in north Raleigh.....	97
6.16	Close-in view of damage at the end of Old Deer Trail.....	99
6.17	Tornado relative locations of microbursts in the Teton-Yellowstone tornado of 1987.....	101

LIST OF ABBREVIATIONS AND SYMBOLS

AGL	(elevation) above ground level
b	radius of microburst outflow boundary
b ₂	greatest distance between effective center of microburst outflow and microburst boundary
EST	Eastern Standard Time
FAA	Federal Aviation Administration
ϕ	velocity potential function
Γ	vortex circulation strength
GMT	Greenwich Mean Time
GOES	Geostationary Orbiting Environmental Satellite
ILM	Wilmington, NC airport identifier
LEWP	line echo wave pattern
m	sink strength of tornado
MCAS	Marine Corps Air Station
McIDAS	Man-computer Interactive Data Acquisition System
MSL	(elevation above) mean sea level
NCSU	North Carolina State University
NOAA	National Oceanic and Atmospheric Administration
NWS	National Weather Service
PPI	Plan Position Indicator (radar scope)
ψ	potential streamfunction
r _v	radius of tornadic vortex
RDU	Raleigh-Durham airport identifier
s	distance from center of tornado

s1	distance from center of microburst outflow boundary
s2	distance from effective center of microburst outflow
SHPP	Shearon Harris power plant
U _A	x-direction component of ambient wind
U _v	x-direction component of tornado velocity
V _A	y-direction component of ambient wind
V _M	maximum microburst outflow wind speed
V _R	maximum radial component of tornadic surface wind
V _T	maximum tangential component of tornadic surface wind
V _v	y-direction component of tornado velocity
VIP	video integrating processor
VQN	Volens, VA radar site identifier
x ₀ ,y ₀	center of tornadic vortex
x ₁ ,y ₁	center of microburst outflow boundary
x ₂ ,y ₂	effective center of microburst ouflow

1. INTRODUCTION AND LITERATURE REVIEW

1.1 Overview

In the early morning hours of 28 November 1988 a series of tornadoes crossed parts of central and eastern North Carolina and southern Virginia. The strongest of the storms formed west of Raleigh, near the Raleigh-Durham International Airport (RDU), and moved across densely populated areas of north Raleigh on a path that would cover over 130 kilometers across Wake, Franklin, Nash, and Halifax counties of North Carolina (Storm Data, 1988). See Figure 1.1 for the locations of counties in the northern piedmont of North Carolina. It was one of several tornadoes that hit in North Carolina and surrounding states that night; Figure 1.2 shows the locations of tornadoes in this outbreak.

The event was characterized by Storm Data as "an odd-season, odd-hour, odd-location outbreak", referring to the fact that tornadoes are relatively uncommon in November, after midnight, and in the southeastern United States. It was also unusual in that it was a fast mover, and that the classic radar signatures of tornadic storms were not observed, or formed only after the event was already underway, hindering the warning process. As this event was so unusual, from the standpoint that most research done on more common types of tornadoes, it provided a good

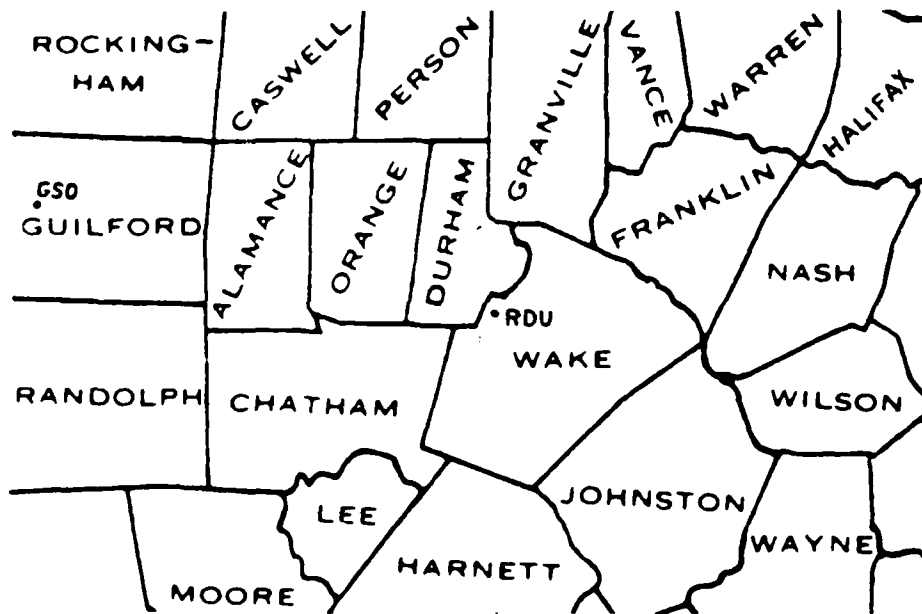


Figure 1.1 County outlines of the northern piedmont area of North Carolina.

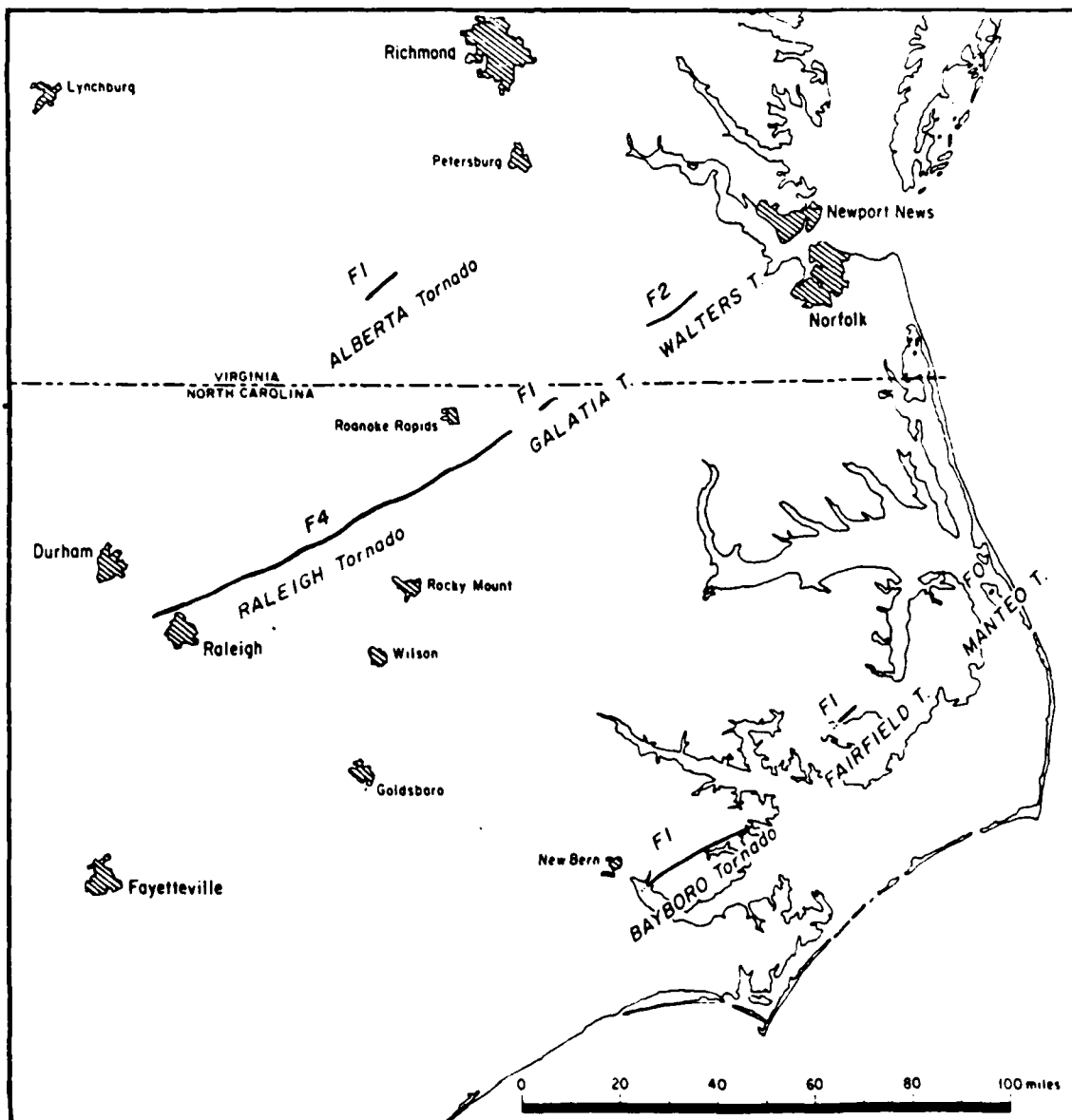


Figure 1.2 Locations of tornadoes in the November, 1988 North Carolina/Virginia outbreak. (Storm Data, 1988)

opportunity to study some of the features associated with such storms that do not follow normal patterns.

The weather situation on the evening of the 27th had a cold front moving over the Apalachian mountains, with an unseasonably warm and moist tropical air mass covering the coastal plain and into the eastern Piedmont region. A weak boundary region divided the tropical air from the cooler air just east of the front. This boundary had been sliding northwestward during the evening; moving northwest of the Raleigh area by 2000 EST. A squall line had formed east of the front in the western Piedmont area, and was moving eastward toward the tropical air. As the line intercepted the boundary and came into contact with the tropical air, it intensified. The Raleigh tornado developed from one of the cells in the squall line.

The path of the tornado across Wake County ran from northern Cary, through William B. Umstead State Park, across the northern subdivisions of Raleigh, and continued between Wake Forest and Rolesville, and on into Franklin County. Figure 1.3 shows the path of the tornado damage in north Raleigh. The Raleigh tornado was rated F4 on the Fujita scale. It attained this strength only briefly on several occasions as it crossed through north Raleigh. Over most of its path through this area, it was generally F2, although its intensity was variable, and it may have even dissipated in certain spots. High winds, heavy rain, vivid lightning, and

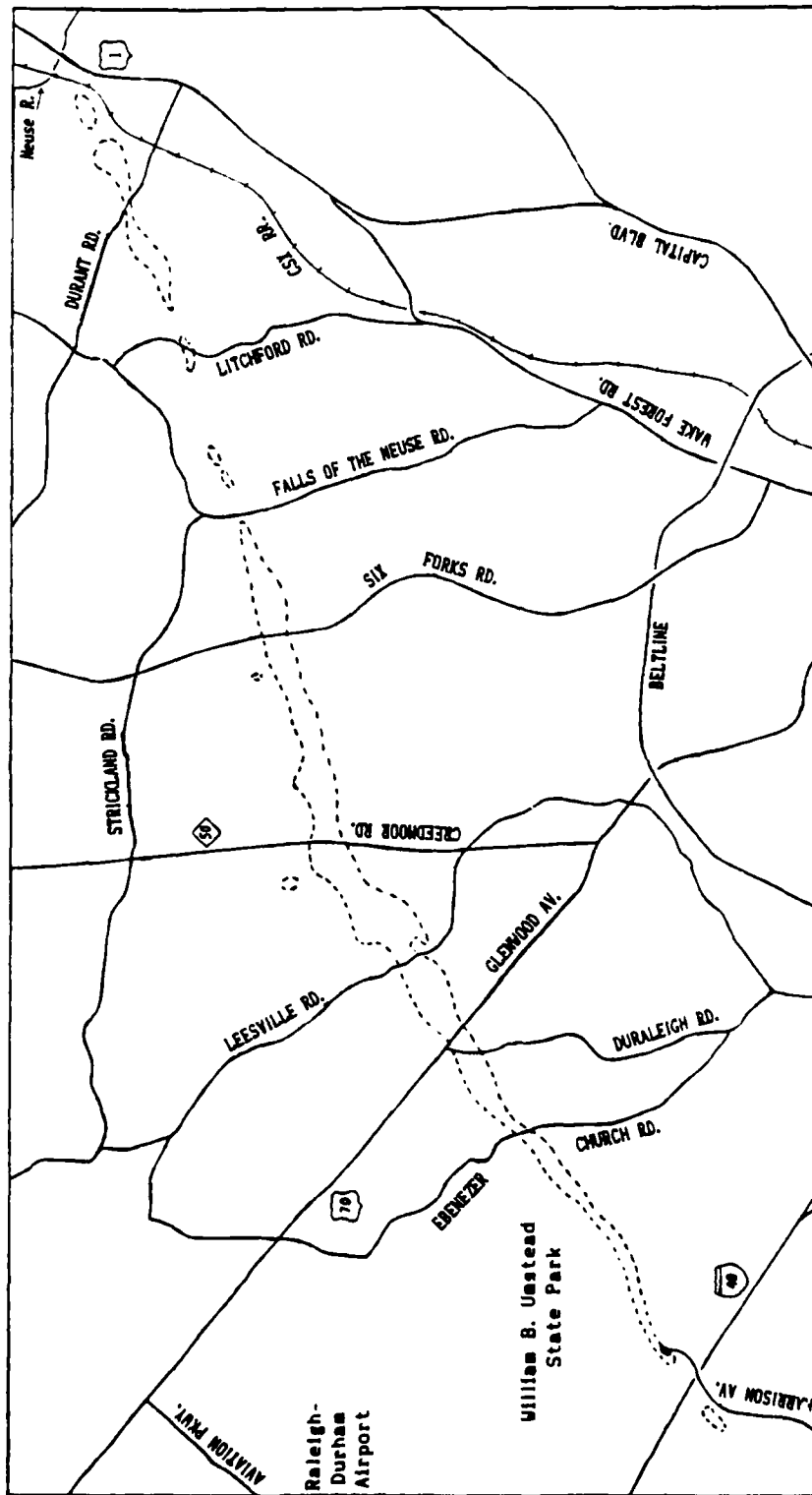


Figure 1.3 Location of tornado damage track in north Raleigh.

a loud roaring noise were occurring in association with this storm.

Interviews with eyewitnesses conducted after the fact have revealed some of the characteristics of the storm. Nearly all near the path of the storm center reported hearing a loud roaring noise in conjunction with the high winds, and many reported driving rain also occurring at the same time. Some reports of strong winds and driving rain came from more than a kilometer away from the center of the damage path. Also almost universal were reports of frequent, almost strobe-like lightning flashes in the minutes leading up to the high wind. Many reported hearing no thunder, although that could be a function of continuous thunder rumbling being confused with the wind noises. One respondent reported a break between the end of the lightning and beginning of the winds, and one reported hail.

1.2 Thunderstorm Concepts

Thunderstorms have long been the subject of fascination and of study. Although some studies were done before World War II, the present understanding of thunderstorms began in the late 1940s. The major project during this period was the volume on thunderstorms by Byers and Braham (1949). The concept was advanced that thunderstorms consisted of cells, each with its own life cycle, each consisting of an updraft and a downdraft. The updraft predominates in the early stage

of the cell's life, and the downdraft, caused by the accumulation of rain in the cell, becomes predominant as the cell passes maturity, and eventually causes its death. These storms move with the mean winds over the low to middle troposphere.

Though this representation works well for most thunderstorms, it was noted early on (Byers, 1942) that some thunderstorms moved to the right of the mean wind, as well as lasting longer. Browning (1964) advanced an explanation to account for these cells, which he termed supercells. These storms develop when the environmental wind shears strongly in the vertical. The supercell is a large convective cell able to maintain itself in a nearly steady state for several hours due to physical separation of the updraft and downdraft as a result of environmental vertical wind shear. Figures 1.4 and 1.5 show schematic diagrams of supercell thunderstorms. The updraft in a sheared environment normally has a pronounced cyclonic rotation due to tilting of horizontal vorticity (Miller, 1975). As the updraft accelerates in the area of maximum buoyancy, between the cloud base and the level of nondivergence, vertical vorticity is enhanced through stretching of vortex tubes, and thus a strong mid-level vortex is formed (Benton and Shapiro, 1988). In addition to classic supercells, other types of "supercell" thunderstorms may form, depending on how much moisture is available in the environmental inflow (Moller and Doswell, 1988).

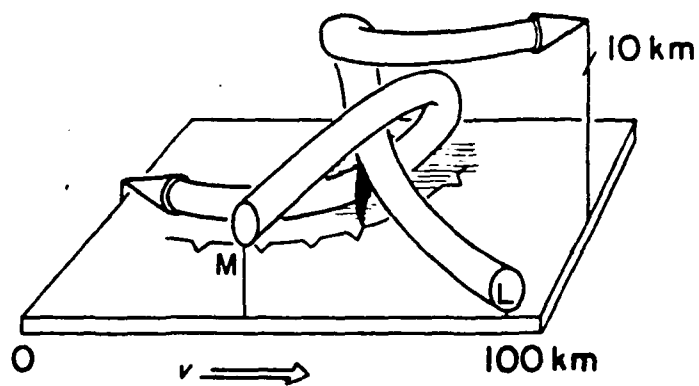


Figure 1.4 Diagram of three-dimensional airflow patterns in a classical supercell thunderstorm. "L" indicates low-level inflow, "M" indicated mid-level inflow. (Browning, 1964)

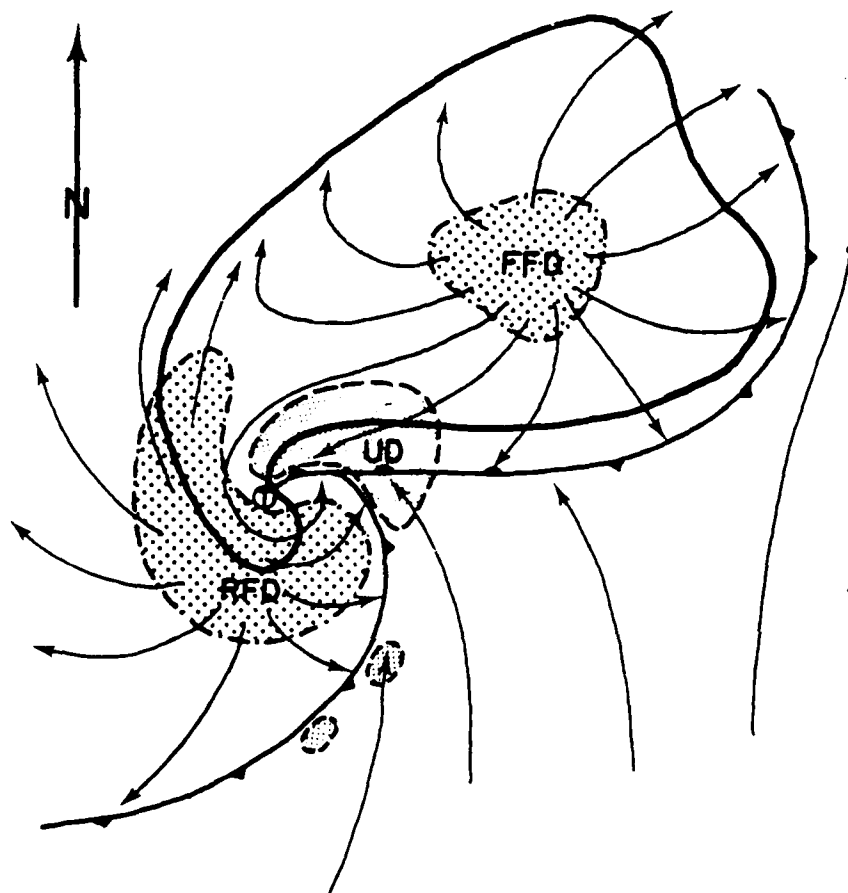


Figure 1.5 Surface airflow patterns in a tornado producing supercell thunderstorm. "FFD" is the forward flank downdraft, "UD" is the updraft, "RFD" is the rear flank downdraft. The dark line delineates the area of heaviest precipitation. (Lemon and Doswell, 1979)

The initial updraft in a sheared environment actually develops a pair of counterrotating vortices, rather than just one (Miller, 1972, Wilhelmson and Klemp, 1978). The developing downdraft can split the updraft, and the cell itself splits, with one part moving to the right of the mean wind, and one to the left (Rotunno and Klemp, 1982), see Figure 1.6. The right moving cell, which rotates cyclonically, will normally become the dominant one when the wind veers with height.

1.3 Squall Lines

Squall lines are lines of convection that maintain themselves for long periods of time. Rotunno *et al* (1988) identify two types of squall line. One is characterized by a continuing series of transitory cells that form and die in a periodic fashion. The other is a line of semi-independent supercells. Smull and Houze (1985), examining an Oklahoma case, detected sloped cells in the line, so that the updrafts and downdrafts were separated by a gust front. The area where air was flowing in to the line from the rear showed up as a low reflectivity notch on the radar pushing into a large area of stratiform precipitation behind the line.

Contrary to previous theory, recent evidence suggests that there is a continuum, rather than a distinct separation, between the multicell and supercell type of thunderstorm systems (Vasiloff and Brandes, 1984). The implication is

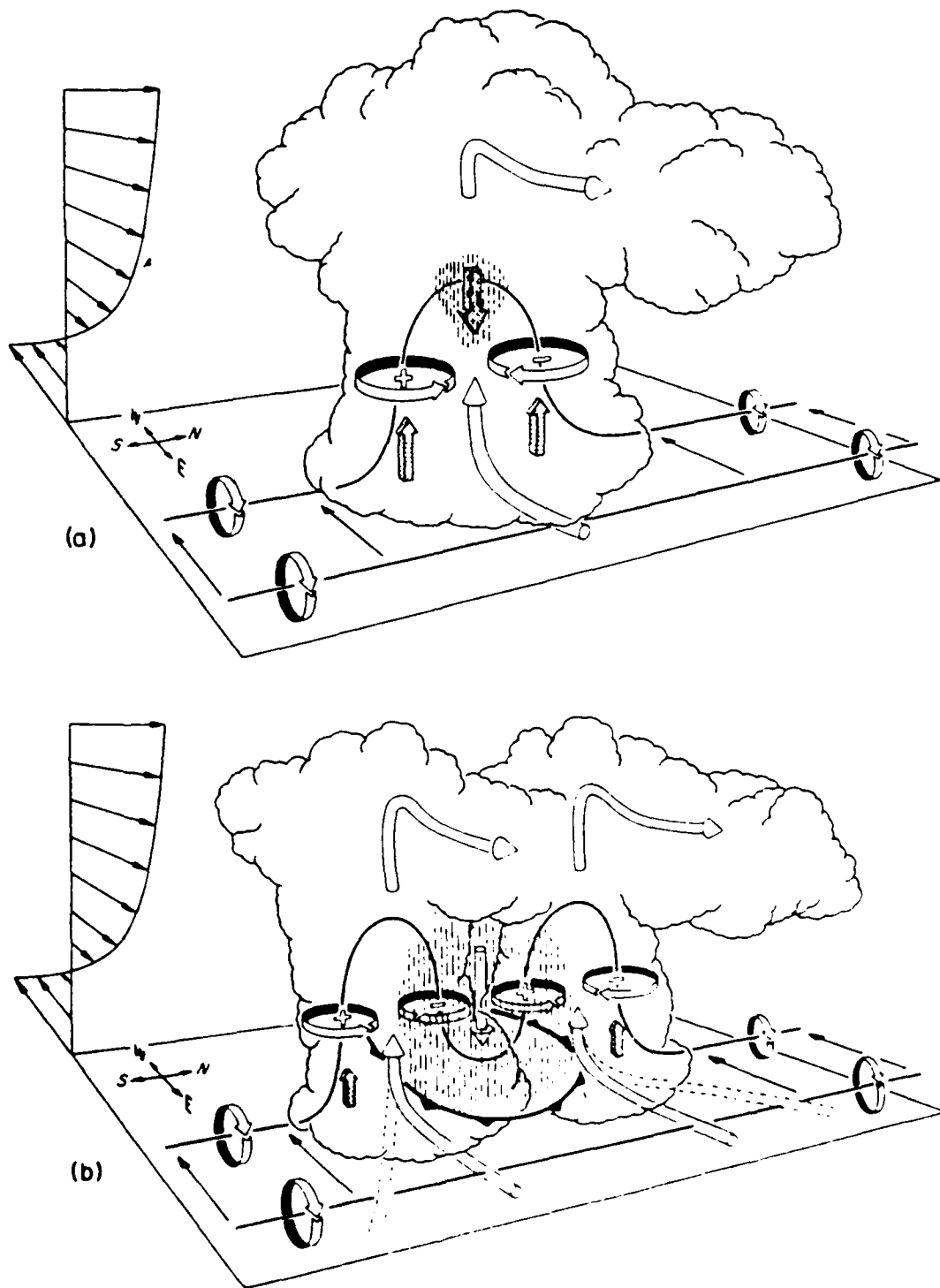


Figure 1.6 Schematic diagram of the splitting of an intense thunderstorm cell. The thin lines represent vorticity filaments, the cylindrical arrows represent airflows. (Klemp, 1987)

that it is possible to have something between a multicell and a supercell organization within a squall line.

1.4 Tornadoes

Most tornadoes, including nearly all the stronger ones, come from supercell storms (Klemp, 1987). Lemon and Doswell (1979) described in detail the surface features associated with a supercell thunderstorm developing into its tornadic phase. It is analogous to a synoptic scale cyclone as it begins to occlude (see Figure 1.5).

The key to the transition into the tornadic phase occurs when the steady state nature of the supercell is changed by a second downdraft forming to the rear of the main updraft (RFD in Figure 1.5). This coincides with the collapse of overshooting cloud tops and the weak echo region of the radar echo. Actual tornado formation occurs when the low-level vorticity rapidly increases to a value much higher than the mid-level value.

Lemon and Doswell (1979) and Brandes (1984b) indicated that the tornado forms when the mid-level vortex moves to the updraft/rear downdraft boundary, causing concentration of vertical vorticity at lower levels due to convergence. Barnes (1978a) and Lemon and Doswell (1979) suggested that the rear downdraft induces the tornadic development, while Brandes (1984a), Klemp (1987) and Benton and Shapiro (1988)

suggest that both phenomena are results of dynamic pressure associated with an intense updraft.

Prior to tornado formation, vertical vorticity near the surface is less than half the mid-level vorticity value. Fujita (1973) has argued that rotating downdrafts occurring in conjunction with collapsing cloud tops can account for low-level vorticity intensification, along with observed ground damage patterns. These microburst and downburst winds can produce tornado-like vortices even without mesocyclone influences (Brandes, 1975; Forbes and Wakimoto, 1983), enhanced by the vertical motions that are associated with the leading edge of a gust front (Goff, 1976).

Brandes (1984b) disputes the downflow explanation, saying that downflow is divergent, and thus reduces the magnitude of vertical vorticity. He argues instead that the mesocyclone intensification at low levels results from convergence near the core of the updraft, and that as the vorticity spins up, the upward pressure gradient force sustaining the updraft is reduced, and a rear downdraft is induced (Brandes, 1984a).

Klemp (1987) suggests that low-level vorticity enhancement results from the leading gust front moving into the path of the updraft inflow. This results in increasing the horizontal vorticity parallel to the inflow due to increased baroclinicity. The horizontal vorticity is tilted into the vertical as the inflowing air enters the updraft.

Burgess and Donaldson (1979) have indicated that small tornadoes can develop in strong vertical wind shear situations when the parent storm is still developing.

1.5 Tornado Damage

Tornado damage, being the most visible and long-lived effect of the storm, has been studied for a long period of time, by the engineering community as well as meteorologists. One of the earliest detailed studies was by Letzmann (1923). He made hand calculations based on varying several factors such as translational speed and angle of inflow, and calculated a number of various damage and debris patterns. Later studies have increased knowledge of the nature of tornado damage; for example, Fujita et al (1967), which identified six types of damage created by tornadoes.

Although caused by whirling winds, the damage left by tornadoes need not show a spiral or cycloidal pattern. Reynolds (1959) argued that if the vortex translation along the ground was at a high enough speed, relative to the speed of wind circulating about the vortex, the the wind on the side left of the motion, blowing opposite the direction of translation, will not be strong enough to cause damage. Thus nearly all the damage left by the storm would be in the direction of translation, and could be mistaken for straight-line winds.

Several different patterns of damage can result, based on the angle of inflow, the ratio of rotational speed to translational speed, and the radial variation of wind speed (Letzmann, 1923, Minor et al, 1982). These are characterized commonly by most of the damage occurring on the right side of the path, and a singularity line (damage orientation converges or reverses direction). This type of damage was the prevalent pattern noted in north Raleigh.

Barnes (1978b) noted that in a series of tornadoes that hit parts of Oklahoma in 1970, the damage occurred in a series of curving swaths, which was attributed to two separate vortices around a parent tornadic circulation. Fujita (1973; 1978; 1989) has observed that areas of downflow can occur in the vicinity of tornadoes; significantly modifying the pattern of damage. Forbes and Wakimoto (1983) have also noted areas of damage separated from the main damage track, which they termed "blow-down spots", to the right of the tornado path.

1.6 Downbursts and Microbursts

Although downdrafts are an essential part of any thunderstorm cell, the intensity with which they interact with the ground can vary considerably. The term "downburst" was coined by Fujita (1976) to describe a downdraft intense enough to cause a hazard to aircraft. The term was later expanded to include any downdraft whose outflow was strong

enough to cause damage at the ground (Fujita and Wakimoto, 1981). The term "microburst" refers to the same phenomenon on a smaller scale; a microburst is a downburst with a maximum diameter of four kilometers.

To learn more about these phenomena, several studies have been done over the last few years. The studies, such as the Joint Airport Weather Studies (JAWS) project in Colorado (McCarthy et al, 1982), used Doppler radar and extensive meso-networks of observing stations. These studies have increased knowledge about the structure of these downflows. Additional studies have shown that a smaller scale microburst may occur within a larger downburst, or macroburst (Fujita and Wakimoto, 1981, Sinclair et al, 1988). Although the existence of such phenomena near tornadoes has been suggested in ground damage surveys, little study has been done to indicate their exact relationship in a tornadic storm.

1.7 Radar Signatures

Although no classic hook-shaped echo was noted on radar with this storm system (NOAA, 1988), Forbes (1981), based on a statistical study of the April 1974 superoutbreak, has pointed out that a number of distinctive echo types can be associated with tornadic storms. The characteristics of these echoes are: (1) a hook or appendage at the right-rear flank of the main portion of the echo, or a line echo wave pattern (LEWP), (2) echo reflectivity with intensity of VIP

(video integrating processor) level 4 or higher, (3) main portion of the echo with a single core of high reflectivity, and an outer portion with an oval or bullet shape. Radar pictures from the 1974 outbreak (in Agee et al, 1976) show several of these types of echoes associated with families of tornadoes in Indiana.

1.8 Long Track Tornadoes

Many of the mechanisms which contribute to the formation of tornadoes also contribute to their eventual destruction. Thus, to examine a long-lived tornado, one must examine which factors can contribute to the extension of a tornado's lifetime. Anderson and Gunning (1982) have indicated three factors which contribute to sustaining a tornado. These are mesoscale convergence in the surface flow, mesoscale advection of storm-scale vorticity, and mesoscale confluence of surface flow streamlines.

Fujita (1989) has argued that the occurrence of microbursts in the vicinity of a tornado produces torque, adding angular momentum to the flow at the surface, and thus can sustain a tornadic circulation across even mountainous terrain. This factor is most efficient if the center of the microburst is some distance from the tornado center, and the outflow from the microburst flows into the tornado. In addition to imparting angular momentum to the system, it could also counteract the dissipation of vertical vorticity

by the divergence of the outflow. With the outflowing air moving toward the tornado center, it has the effect of reconcentrating the vorticity back to the center of the mesocyclone.

Fujita (1973) has also postulated that sustenance and severity of tornadoes may be enhanced when the temperature lapse rate near the surface becomes more stable, such as after sunset or after cooler downdraft air entrainment occurs. This is because stable air is less likely to rise prematurely, i.e. before it gets to the main updraft.

Much lightning was observed in conjunction with this storm, and it is possible that lightning may contribute energy to a storm by adding heat, although there is no consensus on this matter (Davies-Jones and Golden, 1975). Also, if a strong mesocyclone is present, a long-lived "tornado" may not be a single tornado but a family of tornadoes produced by a single parent storm (Agee et al, 1976).

2. RESEARCH OBJECTIVES AND METHODS

2.1 Objectives

The principal objectives of this research are to learn about the Raleigh tornado and its parent storm from the data available, primarily the damage left behind. As previously mentioned, the Raleigh tornado had a number of unusual features. Additionally, the storm developed in an area that was, for most of the previous evening, only a marginal severe weather environment. This is why no watch was issued and no other preparations were taken. Also, the tornado formed quickly after the initial cell intensification. Thus, anything that can be learned about its structure can help in analyzing its anomalies.

In order to analyze a tornado it requires close examination of all evidence left in its wake. One problem with an after-the-fact case study such as this is that data are relatively sparse; the only extensive source of data is the damage left behind by the storm. Other data sources in similar research were lacking in this situation, often just because of bad luck. For example, the WSR-74 radar at RDU was out of order at the time of the storm, although it is likely that many of its features would have been lost in ground clutter due to the fact that the cell moved right over the radar site. Wind recording devices at both RDU and NCSU were also out of order. Of course, there was no Doppler radar available to verify winds. Thus, this research must

rely on inferences made from what was available, in particular the damage left by the storm.

Taking note of the storm's anomalous features, several questions arise. Why did the storm form when it did? What were the mechanisms that caused the tornado to form? How did it behave over its path on the ground? What factors influenced its motion and evolution? Why did it last as long as it did? Why were there no classic tornado signatures? What was the relation of the squall line and boundary line to the tornado's evolution?

In attempting to answer some of these questions, this research is based on the following hypothesis: the Raleigh tornado was accompanied by strong environmental (i.e. outside the primary tornado circulation) winds occurring near the vortex. An ambient wind with a similar speed and direction as tornado propagation, and several areas of strong outflow, or microbursts, appeared to have been present. These wind flows, although not directly associated with the tornado itself, can account for some of the damage patterns it left behind. These flows may also have contributed to some of the unusual feature of the storm, such as why it formed as quickly as it did after the thunderstorm cell intensified, and why it lasted as long as it did.

2.2 Analysis of Tornado Damage

The primary source of data for this research was the damage caused by the tornado in north Raleigh. Because of the time of day it hit and the fact that there was no warning, no reliable visual accounts were received from eyewitnesses, nor were there any films or photographs. Still, the damage left by a tornado is a very useful indicator of the ground level wind flow in the vicinity of the tornado (Minor et al, 1982). Many minor features that would otherwise not be detected will show up in damage and debris fields. Some disadvantages of using damage as evidence include perishability, as cleanup and rebuilding begin soon afterwards, and the fact that, especially in built-up areas, differences in apparent damage (e.g. a lightly damaged building next to a flattened building) are often not due to actual differences in the wind field. Whether a structure fails, and where its debris settles, is determined not only by the speed and direction of the wind, but also the duration of the peak winds, the presence of mechanically induced turbulence in the flow, the integrity and construction of the structure, and the angle at which the wind hits the walls (Mehta et al, 1976; Minor et al, 1982). The ideal wind field portrayal would be a uniform field of targets, such as trees or cornstalks.

Ground surveys were conducted by NCSU personnel across much of the damage path in north Raleigh from Ebenezer Church

Road near Umstead Park to Durant Road south of the Neuse River. Emphasis was placed on the more heavily damaged areas in north Raleigh, chiefly between Glenwood Avenue and Lead Mine Road, and east of Six Forks Road. Mapping was done, showing locations of tree falls, damaged buildings, and debris scatter. These maps are reproduced in Chapter 4. Interviews of willing witnesses were also conducted. The locations of interviewed people, including in-person and telephone interviews, are shown in Figure 2.1.

In addition to ground surveys, aerial views of damage were available from several sources, and were used to supplement the ground surveys. The North Carolina Department of Transportation provided aerial photographs taken by a mapping camera from an airplane flying at 6000 feet above mean sea level (MSL). The series of twelve photographs covered the area from Ebenezer Church Road east of Umstead Park to US 1 and the CSX railroad tracks just south of the Neuse River. Also used were video tapes provided by WRAL-TV and WTVD-TV stations, in particular a segment of the WRAL tape featuring a helicopter survey of the damage path through north Raleigh from Umstead Park to Falls of the Neuse Road.

The maps made of the damaged areas were compared to similar studies of damage in the literature. Also a computer model was developed to simulate the damage patterns left behind by a passing tornado vortex. The model can vary the size, wind speeds, propagation speed, and environmental wind

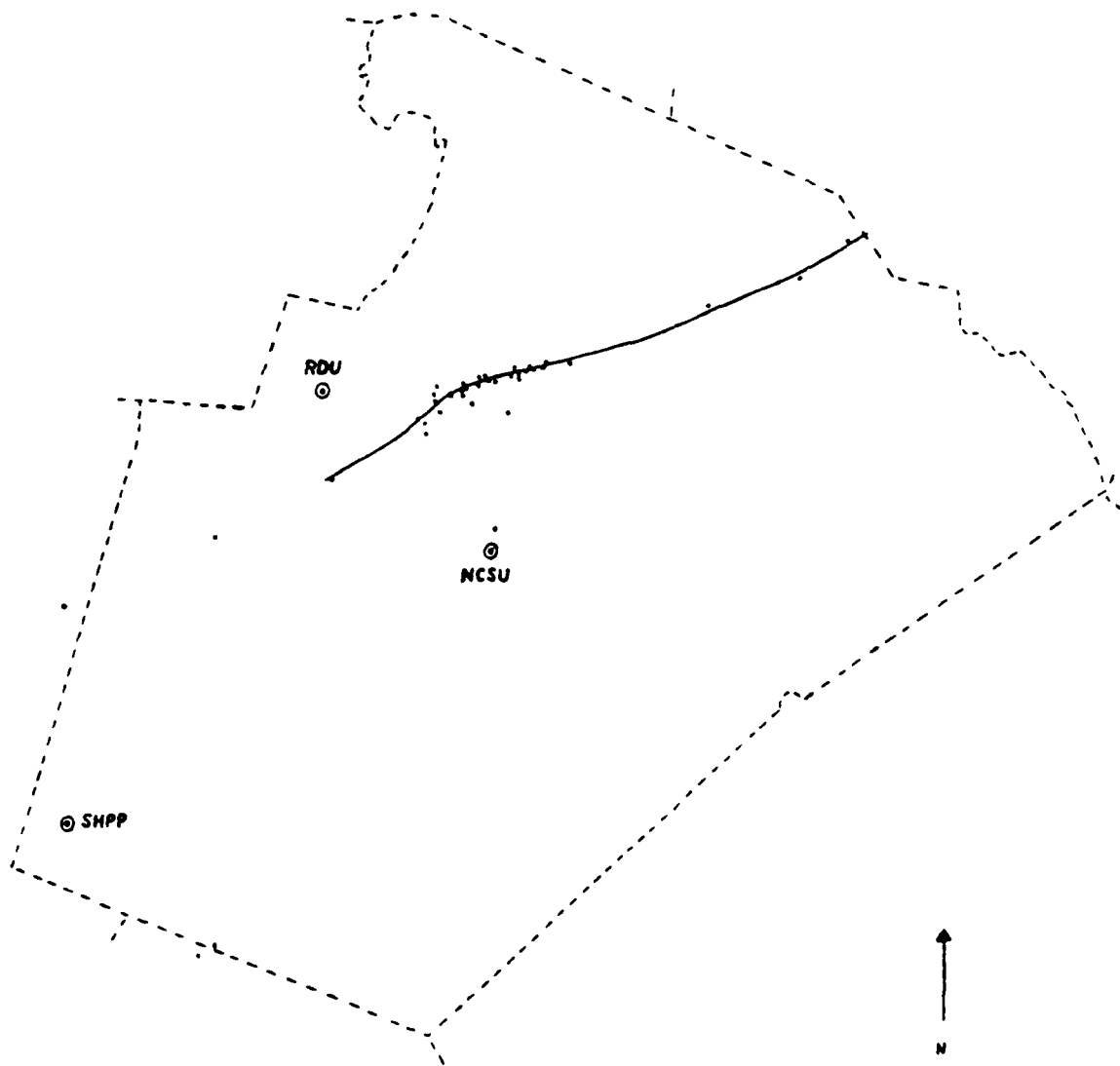


Figure 2.1 Locations of tornado reports in Wake County. The circled dots are locations where weather data are available: RDU (NWS office at the airport), NCSU (North Carolina State Univ.) and SHPP (Shearon Harris power plant). Line shows tornado path.

profile to determine the characteristics of the tornado as it moved across Wake County.

2.3 Additional Data

2.3.1 McIDAS Data

Additional sources of data included the surface and upper air reports from conventional reporting stations, the values from which were stored on meteorological data (MD) files on the McIDAS system. McIDAS (Man-computer Interactive Data Acquisition System), located at the Space Science and Engineering Center at the University of Wisconsin at Madison, has the ability to receive real-time satellite and conventional data reports and use them to plot reported data and produce analyses. These data can be stored in MD files for further use and manipulation in the future. A remote McIDAS work station is located at NCSU. GOES satellite imagery was also available on the McIDAS system.

2.3.2 Radar Data

Also used in this research were 16 millimeter radar films from the Volens, VA (VQN) and Wilmington, NC (ILM) radars provided by the National Climatic Data Center in Asheville. These films show pictures of position plan indicator (PPI) scans from the radars taken at intervals of five to ten minutes. Additionally, the MF7-60 radar report form from Volens was compared to the films to help determine echo and echo height locations.

The Volens radar pictures were transcribed from the film onto a map of local area county outlines for the purpose of refining locations of the echoes. A map from the Volens radar station showing county outlines was used for this purpose.

2.3.3 Other Data

Data from the weather observation tower at the Shearon-Harris power plant of Carolina Power and Light at New Hill, NC was also used. The meteorological tower is located on the plant site at 60 meters above ground level (AGL). The location of the plant is indicated on Figure 2.1. The data received included a wind trace and fifteen minute averaged pressure readings.

Other sources of data included observation forms from the National Weather Service (NWS) office at RDU, which lists all surface observations, including synoptic network transmissions, and other data such as precipitation amounts, sunshine and wind data. Microbarograph pressure traces from the North Carolina State University weather observatory and reporting stations across North Carolina and surrounding states were also examined.

3. METEOROLOGICAL SITUATION

3.1 Identification of Mesolow

The Raleigh tornado appears to have been associated with a strong mesolow that formed along the boundary line marking the northwestward extent of the unseasonable tropical airmass. This boundary lay to the northwest of Raleigh most of the evening. The mesolow pressure pattern was evident on barograph traces taken at RDU and NCSU, and from the 15-minute averaged readings taken at the Shearon Harris power plant station. The barograph tracings, shown in Figure 3.1, both indicate a general fall in the overall pressure with the approach of the cold front that passed the Raleigh area around 0500 (all times EST unless otherwise indicated), but show a "V"-shaped notch superimposed on the larger pattern. The depth of this notch is 2.5 to 3.0 millibars. This feature began around 0030 when the pressure began to fall sharply, and it ended around 0130 when the pressure leveled off after rising rapidly. The lowest pressure occurred at or shortly after 0100. The Shearon Harris readings, listed in Table 3.1, show a similar evolution.

An important point to make about this anomalous pressure pattern is that it was a localized mesoscale feature. Pressure traces from other weather stations around the state and neighboring states showed a pattern of a slow pressure fall with a sudden jump at the time of squall line passage.

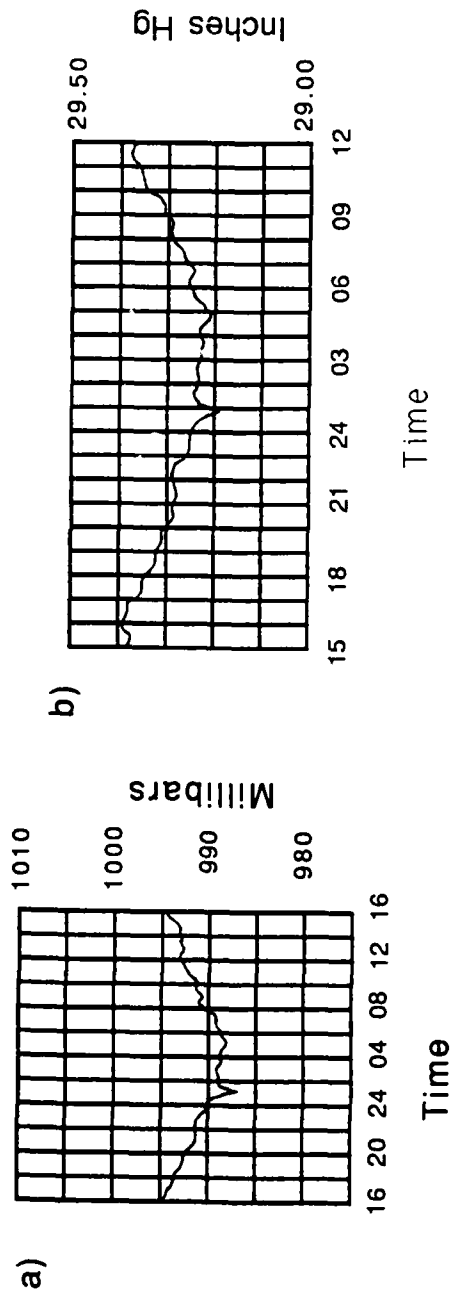


Figure 3.1 Microbarograph traces from (a) NCSU and (b) RDU, showing "V" notches around 0100, and frontal passage around 0500. All times EST.

TABLE 3.1 15 minute averaged pressure readings from the Shearon Harris plant (Time is GMT, pressure in inches of mercury).

0400	29.41	0515	29.39	0630	29.38
0415	29.41	0530	29.37	0645	29.38
0430	29.41	0545	29.34	0700	29.38
0445	29.40	0600	29.33	0715	29.38
0500	29.39	0615	29.36	0730	29.38

This was the pattern noted at Charlotte and Greensboro. The "V" notch was observed only at Norfolk, VA and Cherry Point MCAS, NC (near New Bern). The Norfolk "V" notch, which was recorded at 0400, was a reflection of the same system that spawned the Raleigh storm.

3.2 Wind Data and Mesoscale Circulation

Reliable wind data for the storm are somewhat harder to obtain, as both the RDU and NCSU wind recording devices were out of order that night.

The wind trace from the Shearon-Harris plant, shown in Figure 3.2, shows a gradual veering of the wind, indicating that the center of the mesocyclone was some distance away, and passed to the north of the plant. The shift in wind direction occurred over the same period as the pressure notch described above. The center of the mesocyclone (circulatory winds) and the center of the mesolow need not be coincident (Barnes, 1978a). In this case, however, they appear to be close.

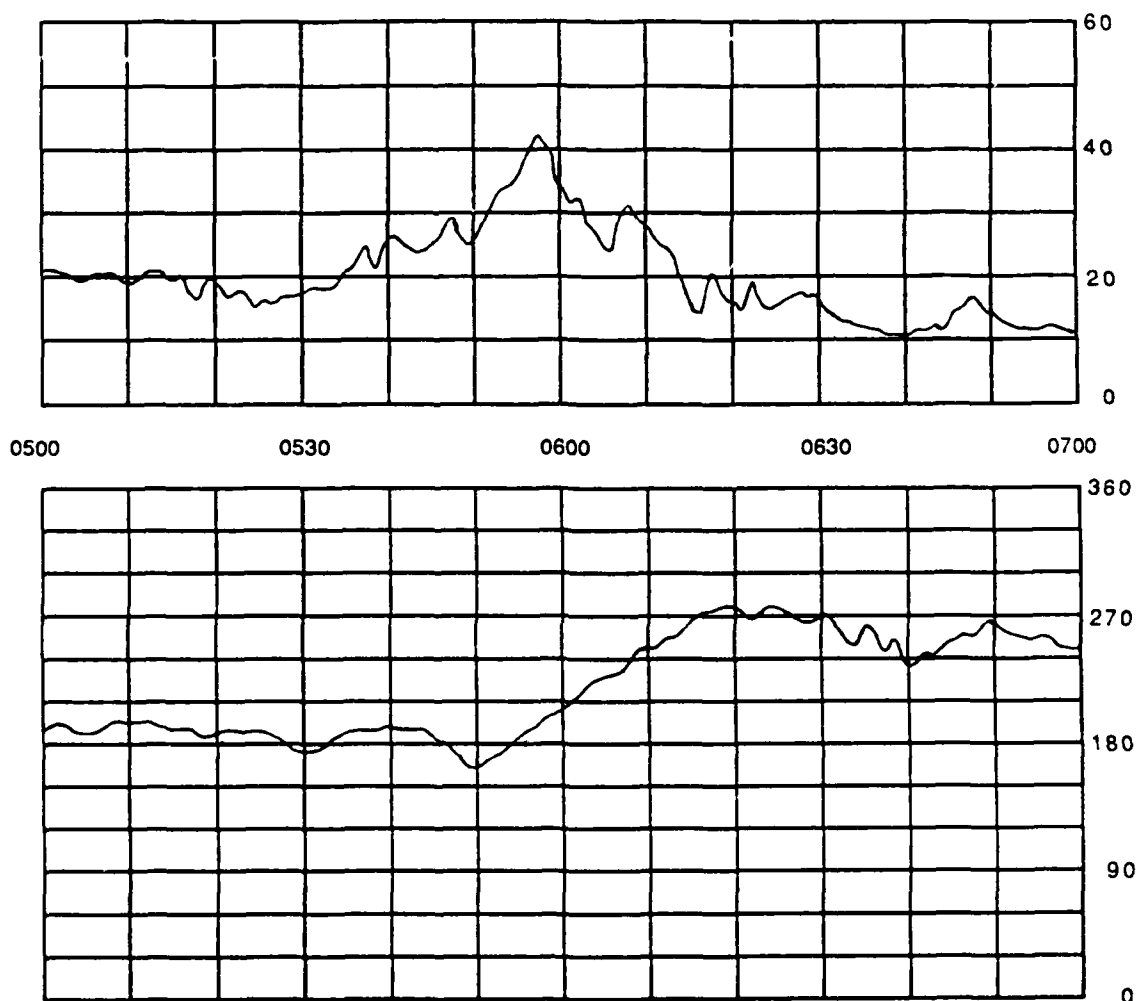


Figure 3.2 Wind trace from the Shearon Harris plant. The top part indicates wind speed in miles per hour, the bottom part wind direction in degrees azimuth. Time is GMT.

Although continuous wind readouts were not available at RDU, the NWS observers were able to receive wind data from the FAA control tower for use in weather observations. Excerpts from the official RDU observations are listed in Table 3.2. Altimeter settings are included because sea level pressure readings are calculated only for the record hourly observations. Of note are the directions of the wind before and after the passage of the mesoscale feature. The wind shift from a southeasterly to a west-northwesterly direction in a twelve minute span indicates a strongly confluent wind field, as well as the center of confluence passing very near the station. There is no real indication as to whether the winds were veering or backing as the feature passed, so it is not known if it passed to the north or south of the station. Also, as noted in the remarks, the time of greatest windshift and of lowest pressure occurred nearly simultaneously.

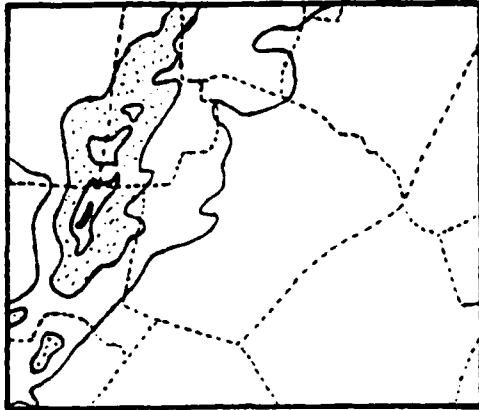
TABLE 3.2 Portions of official observations from the NWS office at RDU. Pres. WX is present weather, SLPres. is sea level pressure (millibars), Alstg. is altimeter setting, Dir/sp is wind direction in degrees azimuth and speed in knots, PRESFR/PRESRR is pressure falling/rising rapidly. Times are EST.

Time	Pres. WX	SLPres.	Alstg.	Dir/sp	Remarks
2350	-	1006.3	29.73	190/14	-
0052	TRW-	1004.5	29.68	150/08	FQT LTG, PRESFR
0104	TRW+	-	29.67	290/21	FQT LTG, PRESRR
				GUST 33	WIND SHIFT 0101
0138	TR-	-	29.72	270/10	FQT LTG
0155	-	1005.7	29.71	240/04	LOWEST PRES 1003.3

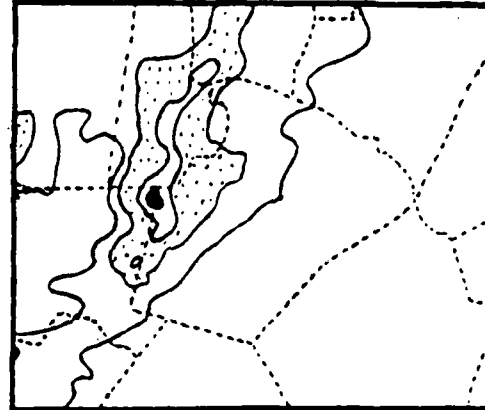
3.3 Radar Imagery

The development of the storm, as viewed on the Volens (VQN) WSR-74S 10-cm radar, began with the development of a squall line between 2300 and 2330. In the beginning, none of the echoes were strong in intensity. Between 0015 and 0045, one of the echoes intensified as it moved over southern Randolph into central Chatham counties of North Carolina. At the same time, the line became less organized as the cells to the south of the strengthening cell weakened. The area of level 3 echo expanded and began to separate into two separate cells. This occurred over Chatham and Durham counties around 0045. The Raleigh tornado developed in association with the southern cell. This cell began to move ahead of the northern one, and the pattern began to resemble a line echo wave pattern.

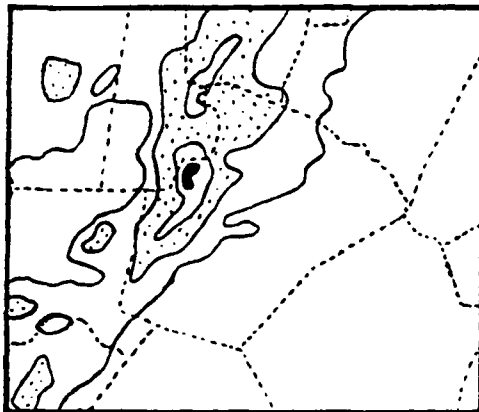
Transcriptions of the Volens radar pictures taken at the time the tornado formed and moved across Wake County are shown in Figure 3.3. The transcriptions are superimposed on local county outlines for reference. The splitting of the level three echo can be seen in these pictures, although the echoes are connected on the 0056 and 0113 pictures. The southern cell moves from northwestern Chatham County to northeastern Wake County, and the northern cell moves from southwestern Durham County to eastern Granville County.



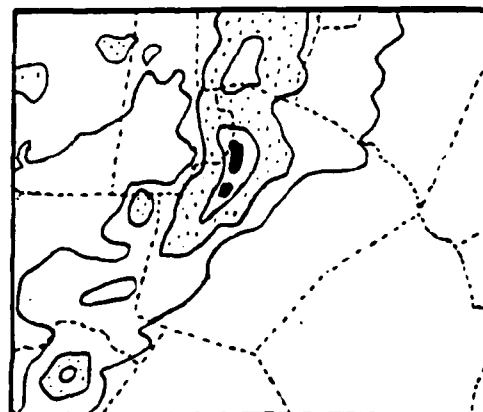
0049



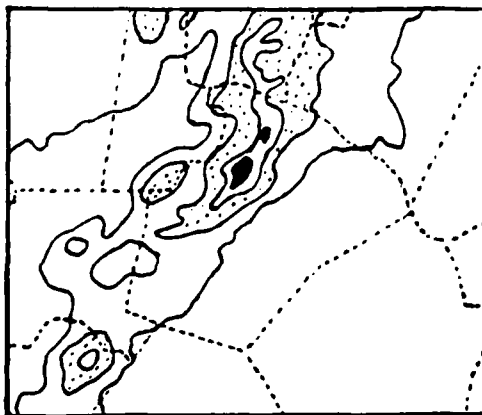
0056



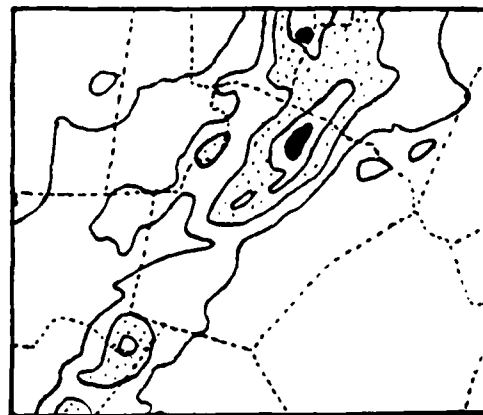
0104



0108



0113



0121

Figure 3.3 Transcriptions of PPI scope photographs from the Volens radar. Shown are VIP levels: 1 and 3 are plain, 2 is dotted, 4 is black. Times are EST.

A feature of the Raleigh storm cell echo during this time is its comma shape, most noticeable in the level three echo on the 0104 and 0121 pictures. This shape is probably a result of mid-level entrainment of dry air. The dry air entrainment results in a lower reflectivity notch between the comma "head" and "tail".

A notable feature of the line during this time is that the center of highest reflectivity shifted incrementally to the south on two separate occasions. The first occurred around 0030, shortly after the first level 4 echo appearance. The second occurred between the 0108 and 0113 pictures. The second shift might have been the cause of the VQN radar operator reporting to the Raleigh forecaster that the cell was diminishing (NOAA, 1988).

The Wilmington (ILM) radar showed a similar pattern, although in less detail, due to the fact that it was farther away. During the formation of the Raleigh tornado, the line of storms was just moving into the 125 nautical mile (231.5 km) range of the WSR-57 radar. Also, because of the distance involved, the elevation of the echoes observed in Wake county was about 4000 meters, as compared to about 1800 meters observed from the VQN radar (using an antenna elevation angle of 0.2 to 0.3 degrees). The ILM pictures showed an elongated level 3 echo beginning at 0033, with level 4 first appearing at 0049. The echo was essentially featureless on the

Wilmington pictures, but does indicate level 4 reflectivity was detected at 4000 meters elevation with this cell.

The radar pattern was similar to the pattern observed in northern Indiana on the Marseilles, IL WSR-57 radar during the April 1974 outbreak, as described by Agee et al (1976). A transcription of that radar picture is shown in Figure 3.4 for comparison. As in the Raleigh case, a long-path tornado developed out of a squall line, and the cell producing the tornado moved ahead of the rest of the line.

3.4 Satellite Imagery

The infrared imagery from the GOES (Geostationary Operational Environmental Satellite) shows the evolution of the Raleigh storm during the time of the tornado; see Figures 3.5 to 3.8. The main feature is the large anvil initially covering the central third of North Carolina At 0501 GMT, with a small area of overshooting tops (the gray area) in the south central portion of the anvil. This was a transitory and recurring feature for most of the previous evening (NOAA, 1988).

Between 0501 and 0601 GMT (midnight and 0101 EST) the overshooting tops expanded and cooled, shown by the darker black area, indicating that the overshooting tops had grown considerably and were much higher than before. Then, between 0601 and 0631 the tops lowered, indicated by the reduced areas of black and dark gray, and continued to do so

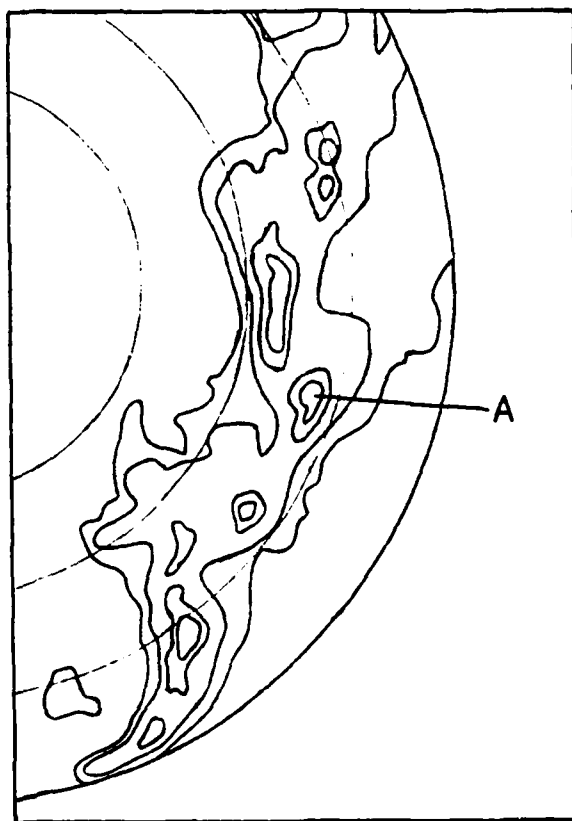
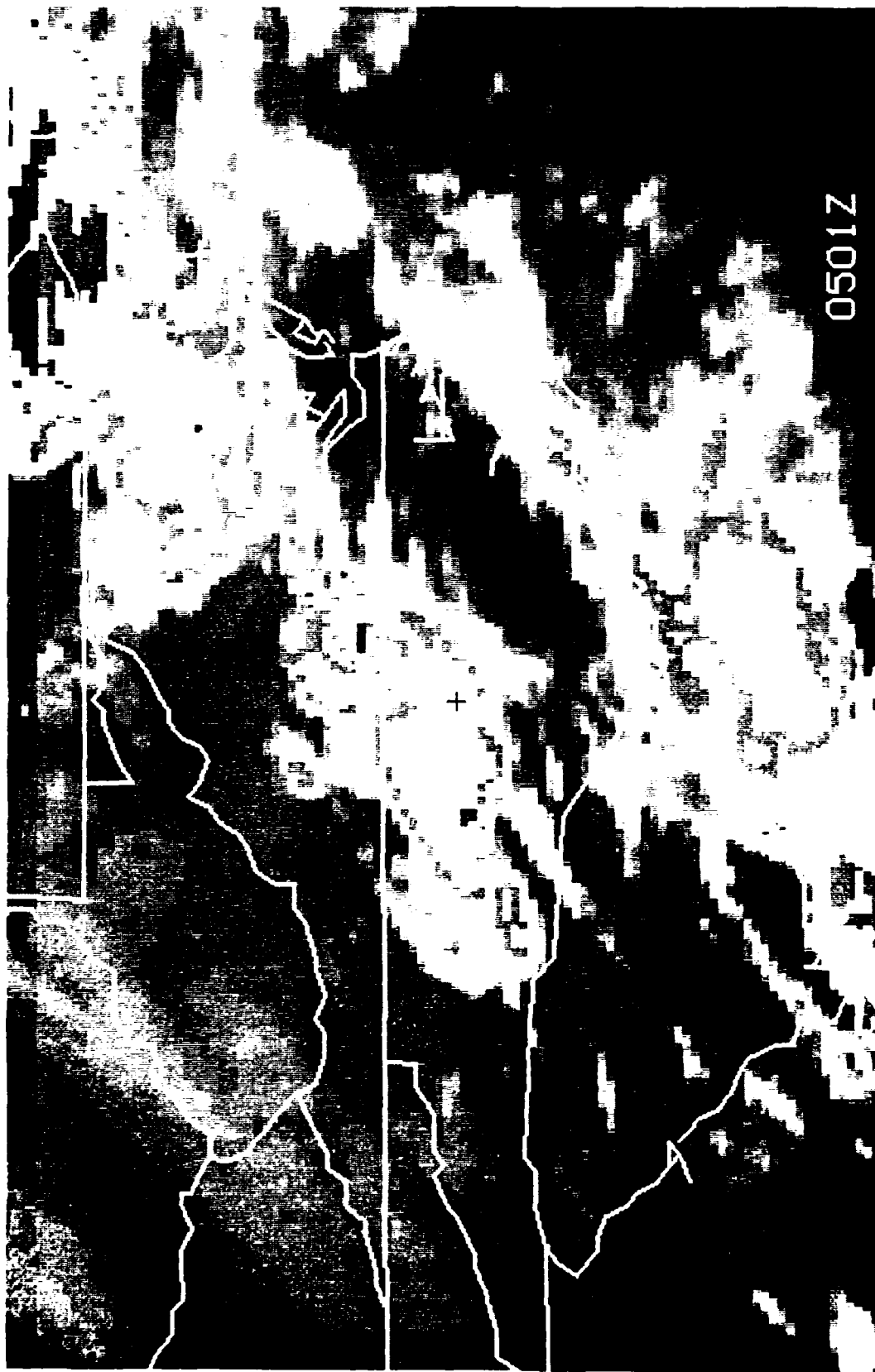


Figure 3.4 Transcription of PPI scope from Marseilles IL radar at 2215 GMT, 3 April 1974. The cell marked "A" produced a long-lived family of tornadoes. (from Agee *et al*, 1976)



0501Z

Figure 3.5 Enhanced infrared GOES satellite picture at time 0501 GMT. The location of RDU is shown by the "+" cursor.

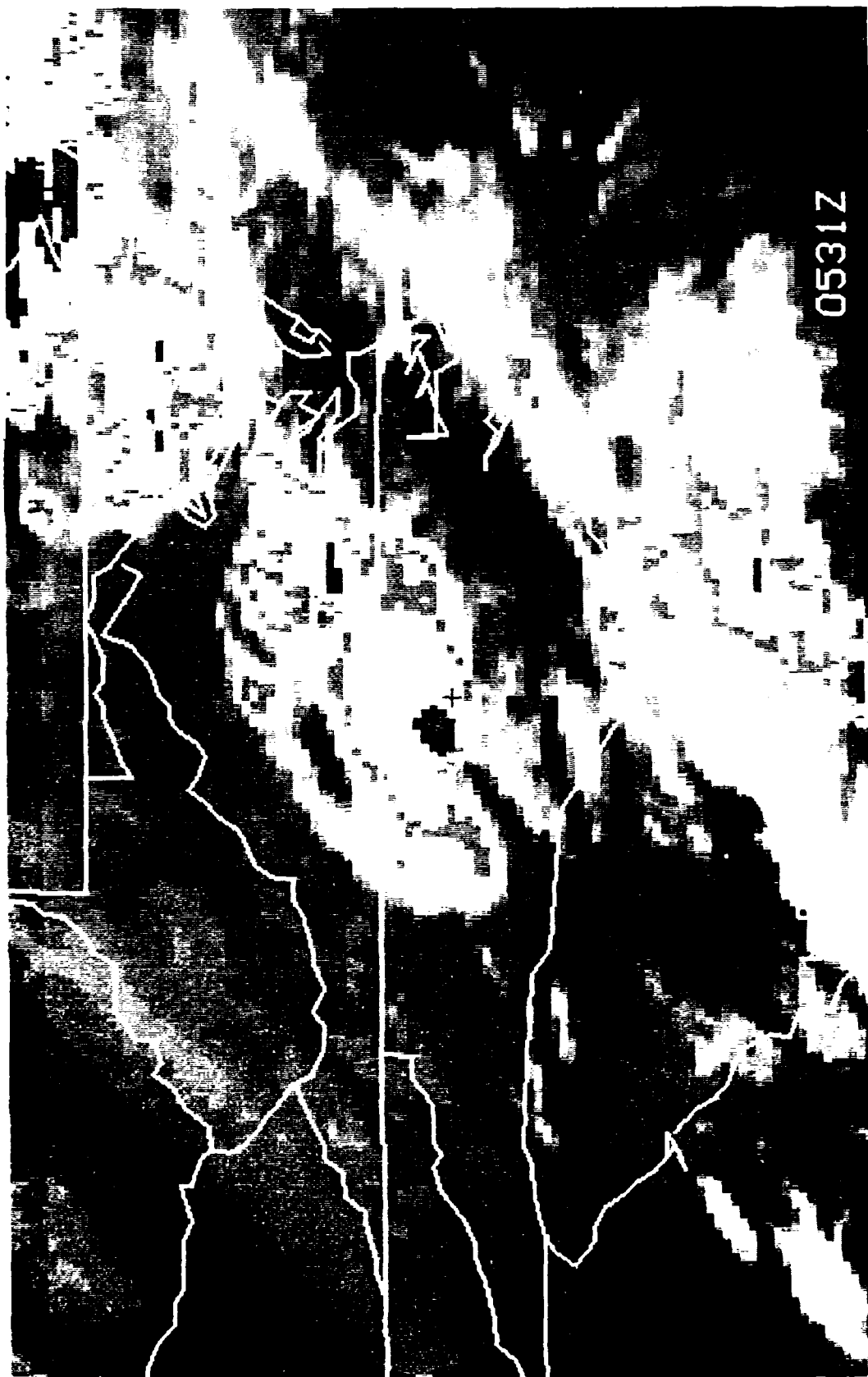


Figure 3.6 Same as Figure 3.5, time 0531 GMT.

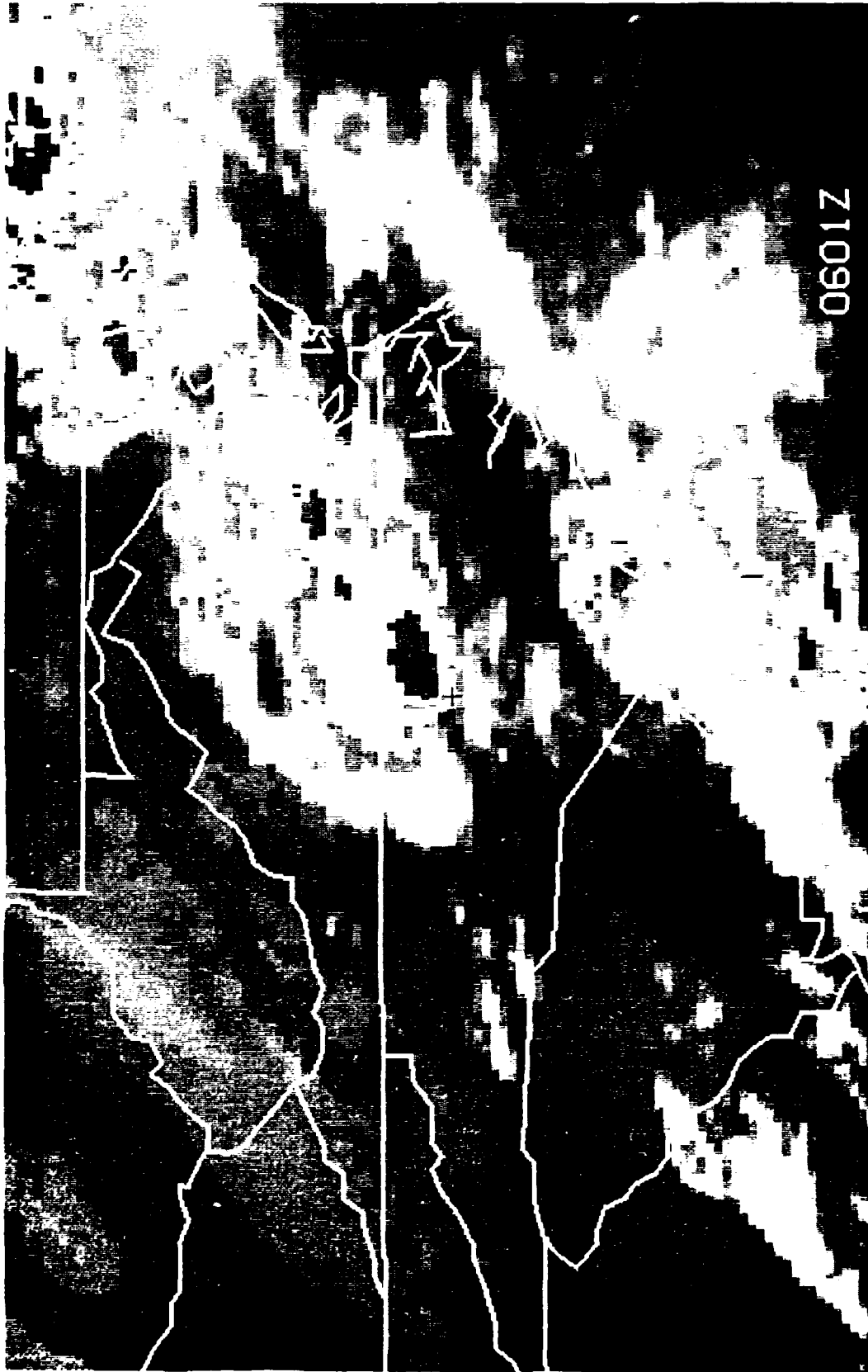


Figure 3.7 Same as Figure 3.5, time 0601 GMT.

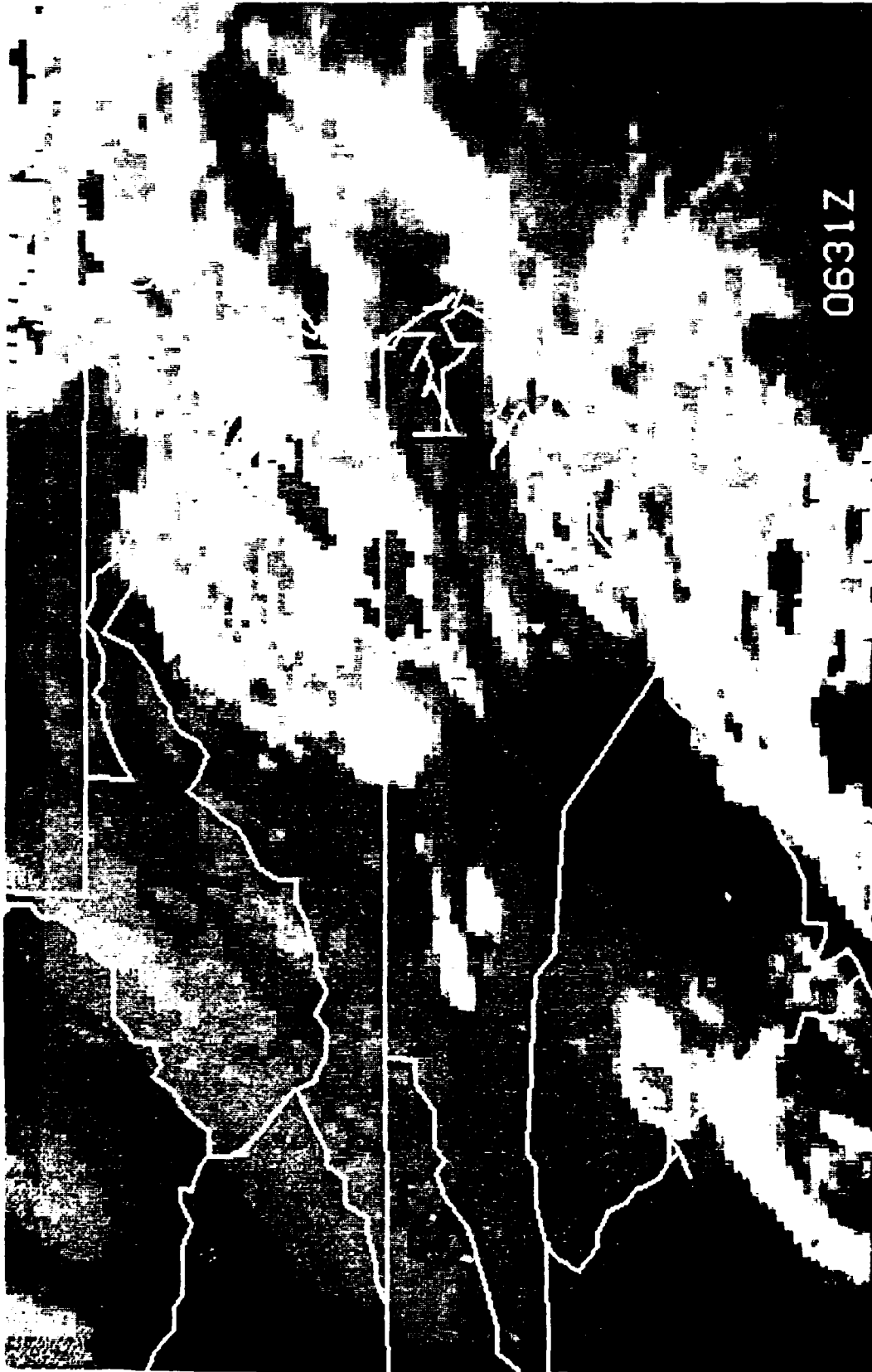


Figure 3.8 Same as Figure 3.5, time 0631 GMT.

afterward. The collapse of overshooting cloud tops is often accompanied by tornadoes and downbursts (Fujita, 1973), although in this case the tornado was forming, if not already formed, by the time the maximum cloud tops were occurring (0100 EST).

4. DETAILED DESCRIPTION OF THE DAMAGE

4.1 Overview

Mention has already been made of some of the features of the north Raleigh damage track. At this point a detailed examination of the track will be done. Firstly, particulars of the track will be examined; then close-up features of the damage will be examined, dividing the track up into several regions of particular characteristics. The locations of these regions are shown in Figure 4.1.

Minimal damage began occurring by the time the storm was in northern Cary, near the Interstate 40-Harrison Avenue interchange. A few hundred feet to the northeast in Umstead Park, considerable damage to trees indicated that the tornado vortex was fully in contact with the ground at this point. As it crossed Glenwood Avenue (US 70), (see Figure 4.1) it rapidly intensified, and F3 damage began occurring. A K-mart store and several apartment and townhouse buildings were destroyed in this area. The storm then weakened slightly but, after crossing Leesville Road, it reached its maximum intensity (Regions 2 and 3). The damage path was over one kilometer wide at this point, its greatest width in Wake county. After it crossed Creedmoor Road (NC 50), it weakened, and for the remainder of its path through north Raleigh and Wake County, it remained fairly weak (F1 to F2) but occasionally intensified for brief periods.

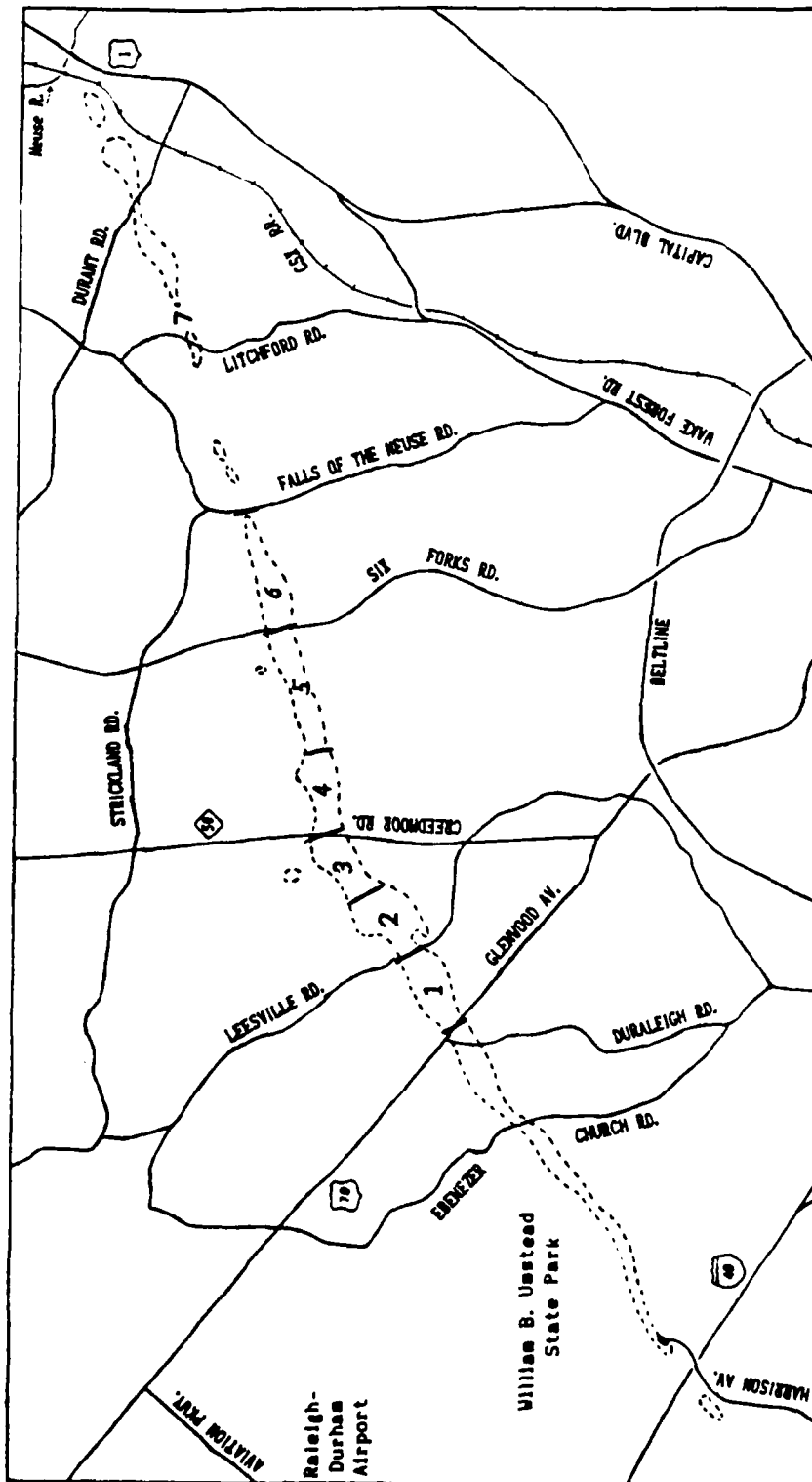


Figure 4.1 Locations of the regions of the damage track in north Raleigh referred to in the text.

4.2 Chronology

A chronology of the storm is somewhat problematic. The lack of warning prevented alerting storm spotters. Due to the late hour when the storm hit, it was dark and many people were asleep, and interviews conducted after the fact may have been affected by memory inaccuracy and clocks not being accurately set. So, reports of times may be of dubious accuracy. Excerpts from the official log of the National Weather Service office at RDU had estimated the storm location between Duraleigh Road and US 70 at 0100 (all times EST unless otherwise specified), and at Sawmill and Mine Shaft Roads at 0105 (NOAA, 1988). However, a report from a Raleigh police officer patrolling US 70 (News and Observer, 1989) and the station log at the fire station on Davis Circle (Anderson, 1990) both indicated the storm passing Glenwood Avenue (US 70) at 0108. The official RDU observations had the lowest pressure and wind shift occurring at or just after 0100. Based on these reports and personal correspondences conducted over the next few months, a best estimate of a chronology of the storm is shown in Table 4.1. Based on this sequence, the forward speed of the storm through north Raleigh and Wake County was about 25 meters per second (55 to 60 m.p.h.).

TABLE 4.1 Probable chronology of tornado movement in Wake County. All times are EST.

0050 - Entering Wake County north of US Hwy 64*
0100 - East of Morrisville between Hwys 54 and 40*
0105 - In Umstead State Park between Hwys 40 and 70
0110 - Crossing Creedmoor Road
0115 - Crossing Litchford Road
0120 - East of US Hwy 1 and Neuse River
0125 - North of Town of Rolesville

* Vortex aloft, damage not occurring on the ground

4.3 Width of Track

The width of the damage varied over its course through Wake County. In Umstead Park up to Glenwood Avenue, the width was between 450 and 500 meters. As it crossed Glenwood, it widened considerably as its southern boundary bulged southward (Region 1). It widened to about 750 meters at Pleasant Grove Church Road, and was between 1000 and 1050 meters wide across the Brookhaven - Hampton Oaks area (Regions 2 and 3). It narrowed to about 850 meters in the Hidden Valley - Greystone Village area (east of Creedmoor Road -Region 4), and remained about this width up to the eastern part of Region 6, where it narrowed to about 350 meters. East of Falls of the Neuse Road (Region 7), the damage became sporadic, with a width of up to 450 meters. Approaching US Highway 1 at the Neuse River, the damage was around 500 meters wide, and remained at a similar width to the northeast.

4.4 Direction of Movement

The direction of movement was generally northeastward, with some small changes and at least one significant change in direction. In Umstead State Park, the damage indicates movement from 240° azimuth, slowly backing to 232° by the time it reached Glenwood Avenue, and continued this heading as far as Leesville Road. The path becomes somewhat obscured at this point, but there appears to be a northward shift of the center and a change in direction. By the time it reached the Hampton Oaks subdivision (Region 3), it had veered significantly and was heading from 258° when it crossed Creedmoor Road. It slowly acquired a more northwardly component as it moved to the east. Its heading backed to 250° when it crossed Falls of the Neuse Road and returned to 240° when it crossed US 1.

4.5 Detailed Examination of Damaged Areas

The pattern of the damage left by the tornado was primarily characterized by tree falls, debris, etc, converging towards a line near the center of the path and generally in the direction of tornado movement, characteristic of a fast moving tornadic storm (Reynolds, 1959, Minor et al, 1982). This pattern was noted almost exclusively in the trees in Umstead Park, but several anomalies to this pattern occurred farther along the track, most notably in the area where the tornado was at its maximum

destructiveness. In this area are indications of strong asymmetric inflows. This phenomenon was noted at a few other places as well, though not as strong, being evident in modifications in the tree-fall pattern. A detailed examination of several regions along the damage path follows, with particular attention given to the "normal" damage pattern in this storm and anomalous features found in a particular region. In each figure, the tornado movement is left to right.

Region 1: Glenwood to Leesville (Figure 4.2). In this region the K-mart store at Townridge Square Shopping Center was destroyed, as were three buildings in the Cooper's Pond apartment complex, three townhouses on Sunscape Lane, and several houses to the northeast. The basic pattern of damage in this area was a continuation of the pattern that had begun in Umstead Park, primarily tree falls converging towards a line near the actual path of the vortex. The main changes in the damage that occurred in this area, aside from the increase in strength of the wind evident in the destroyed buildings, included a noticable southward bulge in the right side boundary of damage, and a corresponding increase in the area of tree falls and debris south of the convergence line. Throughout this expanded area, the main pattern continued to be convergence toward the same line, with tree falls and debris from the destroyed and damaged buildings (the K-mart and the Cooper's Pond buildings) being blown northward.

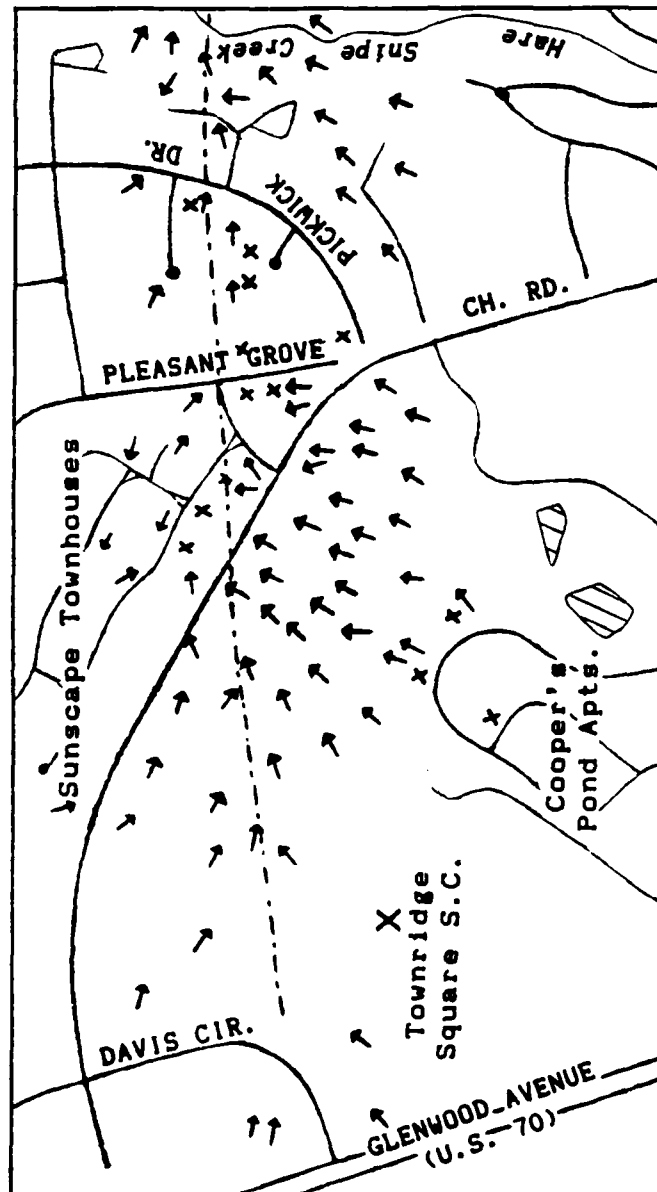


Figure 4.2 Damage map of Region 1. X's indicate destroyed buildings, arrows indicate the direction of fallen trees. Dashed line shows location of damage convergence line. Note: Leesville Road is just off the right edge of this map.

Also, for the first time, a significant number of trees were blown by a wind with an easterly component. This occurred on the northern portion of the damage track from around Pleasant Grove Church Road to Leesville Road. Within this area, the number of trees so affected was still a minority, with the majority still following the afore-mentioned converging pattern.

An examination of some of the notable features of the damage in this area must begin with an odd occurrence at the Cooper's Pond Apartments. Between two of the destroyed buildings sits a building that was barely touched. This can probably be explained by the fact that it was sheltered by the building next to it. The buildings are oriented in a mainly east-west direction, and the spared building sits down lower than the building to the south of it, which suffered extensive damage. The destructive wind was blowing from the south, so the spared building had just enough shelter from the higher terrain and buildings south of it to be spared, while the next building to the north, across the street and closer to the center of the storm, was leveled.

The destroyed Sunscape Townhouse buildings all sat in a row and were fully exposed to the wind. They also sat right near the line of damage convergence, with the last building, right in the center of the line, was twisted off its foundation and blown northeastward into the street. The

houses that were destroyed were all within 100 meters of the convergence line.

Region 2: Leesville to Ray/Lynn Intersection (Figure 4.3). This area seemingly represents a sharp break from the previous general damage pattern of the storm. The definite damage convergence line abruptly ends at Leesville Road and reappears only in the wooded area north of the Calibre Oaks Apartments, and even here it is not nearly as obvious as it was previously. And, it sits about 200 meters to the left (northwest) of its extrapolated position (based on the previous region).

The area southeast of Ray Road does continue the previous pattern of southerly inflow to the right of the path center. The overall width of the damage at its greatest at this point. In particular, tree damage was observed in the creek valley that runs through the Brookhaven subdivision, continuing all the way to Lynn Road. This valley lies about 500 meters to the southeast of the center of the damage path. Light damage occurred throughout the area between the creek and Ray Road, generally blown toward the north and northeast.

A notable event was that most of the buildings in the Calibre Oaks complex were extensively damaged, while the nearby Autumn Chase apartment complex was largely undamaged. This was probably due to the tornado weakening as it passed near Autumn Chase, while Calibre Oaks was affected by a strong easterly flow as well as the tornado.

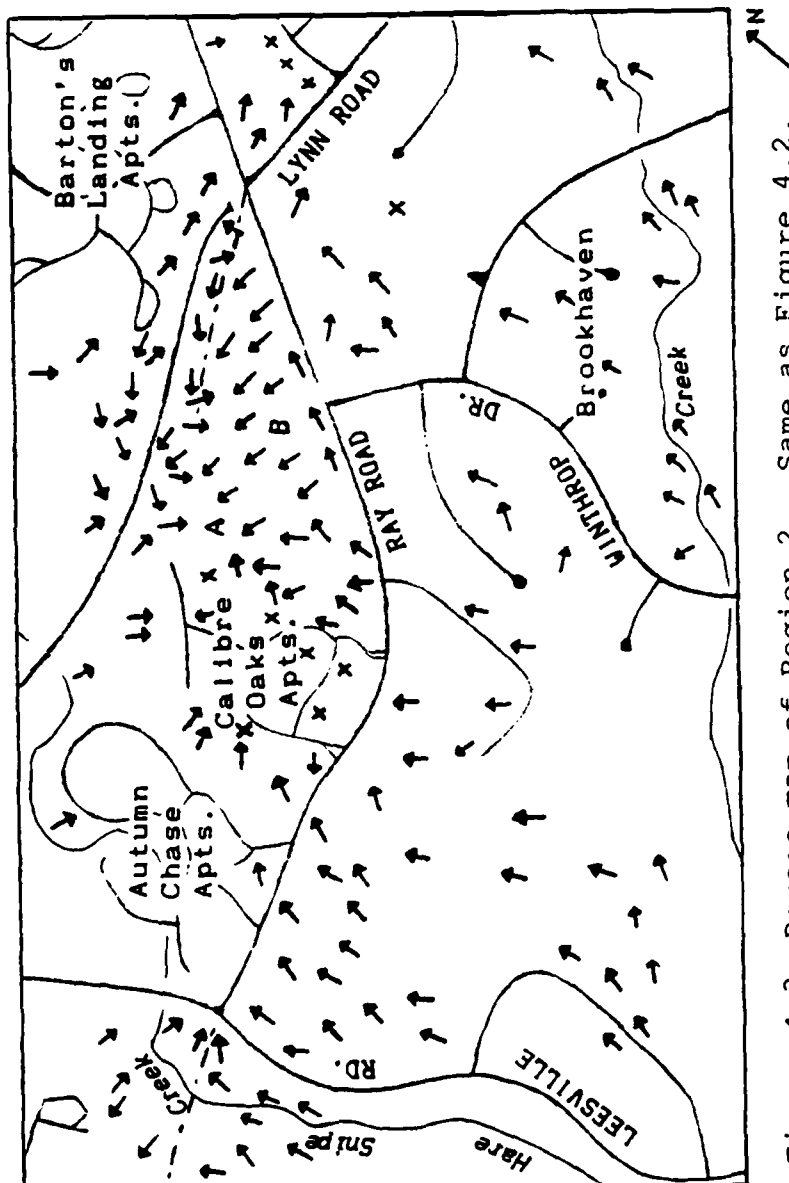


Figure 4.3 Damage map of Region 2. Same as Figure 4.2.

The most interesting feature of this area is this pronounced easterly inflow, most evident in the wooded area between Calibre Oaks and the intersection of Ray and Lynn Roads, marked "B" in Figure 4.3. In this area, nearly every large tree and many small ones were leveled. Although some trees, particularly near the unfinished (at the time) section of Lynn Road north of Calibre Oaks, were down towards the northeast or east, the vast majority of the trees were blown down towards the west. The wind direction indicated by the fallen trees was from 80°.

Damage indicating an easterly wind component was also evident north of Lynn Road and west of the Barton's Landing apartments, although it was not as predominant, and more trees were blown down toward the east. A close-up inspection of the tree falls along this stretch of Lynn Road shows that the trees blown down toward the west fell first, with the ones blown toward the east fallen over the others. In the Barton's Landing complex, at the northern fringe of the damage path, the damage was less severe and dominated by northwesterly to westerly winds.

Just north of the Calibre Oaks complex in the wooded area is a concentrated spot, marked "A" on Figure 4.3, of seemingly random tree fall in many directions. An aerial view of this feature looks very much like a similar feature photographed from the air in the 1987 Teton-Yellowstone tornado (Fujita, 1989, Fig. 12), although the swirling

appearance is not as prominent. This was the first of at least two such features noted along the damage path in north Raleigh.

Region 3: Ray and Lynn to Creedmoor (Figure 4.4). In this area the storm reached its maximum intensity. On Three Bridges Circle, the largest area of F4 damage occurred, and this was the location of the first fatality in Raleigh (News and Observer, 1989). The damage indicated a powerful southerly flow across Lynn Road and Three Bridges Circle, becoming more east-southeasterly direction farther north within Three Bridges Circle. Many houses around Three Bridges Circle were destroyed, their debris blown to the north and northwest. The easterly wind component is no longer evident beyond Three Bridges Circle and Mill Ridge Road, except for sporadic trees fallen toward the west-northwest farther along the track. An isolated area of light damage was also noted about 600 meters to the north of the tornado damage (off Figure 4.4).

Across the creek valley and into the West Wood town houses, the pattern of convergence toward a line becomes reestablished as the dominant one. An unusual feature was noted in the wooded area south of the West Wood complex. The primary pattern here is the expected one of mainly southerly to southwesterly inflow toward the convergence line. However, a small region in the wooded area was largely untouched while the surrounding territory on all sides had

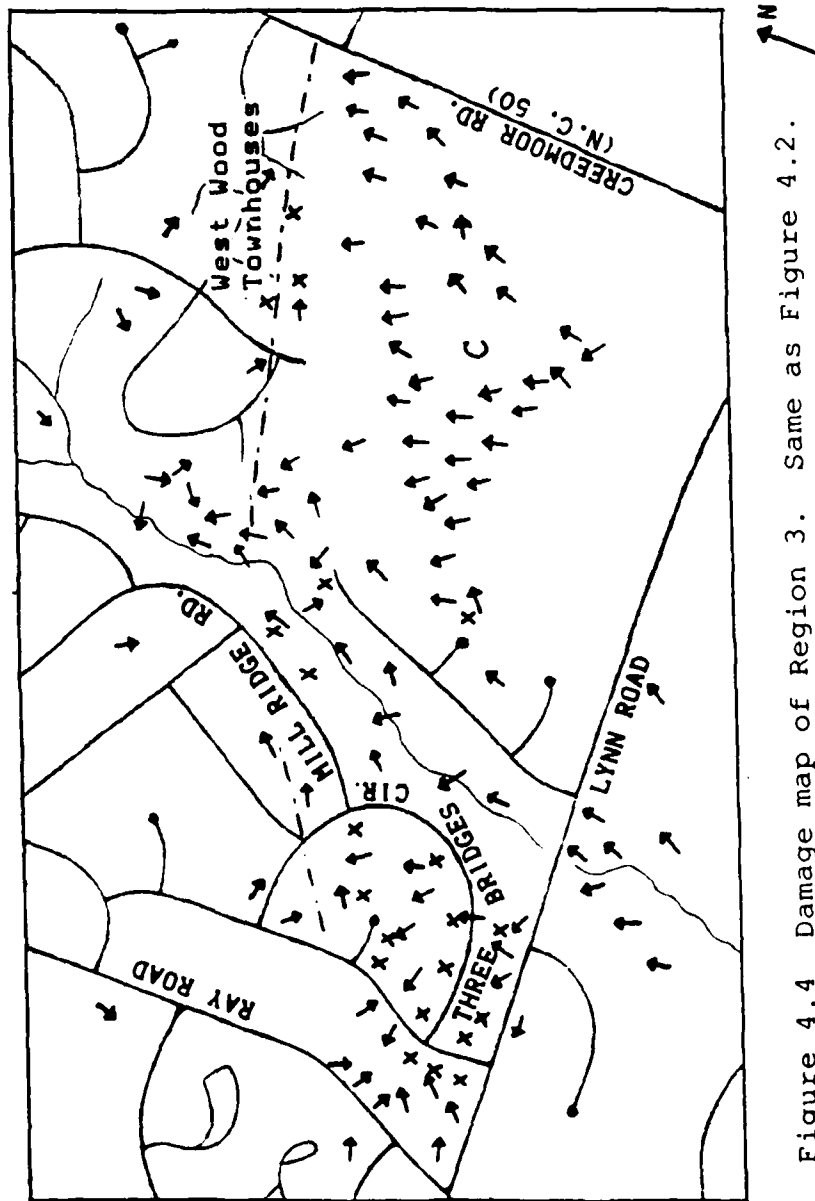


Figure 4.4 Damage map of Region 3. Same as Figure 4.2.

considerable tree damage. This region, marked "C" on Figure 4.4, is about sixty meters in diameter and sits on relatively high terrain about 250 meters south of the line of convergence. Aerial photos show the greatest tree damage to the west of this region and along narrow valleys in a "Y" shaped swath. Although the tree damage is greatest in the lower areas, this was probably not due to a channeling effect, as the valleys lie primarily east-west while the main flow was southerly.

Region 4: Creedmoor Road to Greystone Lake (Figure 4.5). In this area the storm lost some of its strength, but still caused considerable damage. The Asbury United Methodist Church on Creedmoor Road was destroyed, as were several houses near Greystone Lake. The pattern of convergence toward a line was evident here, with some notable exceptions, as will be discussed. The convergence line ran from near the Asbury church to along and just south of Valley Lake Drive to Greystone Lake at the southern inlet that protrudes to the southwest. One house overlooking this inlet was flattened.

A noteworthy feature of this region was another area of damage occurring to a greater extent in valleys than on higher ground. Two houses on Rangecrest Road and a wooded area in front of them sustained minimal damage. This location is marked "D" on Figure 4.5. Those houses sat atop high ground over a culvert carrying a small creek toward

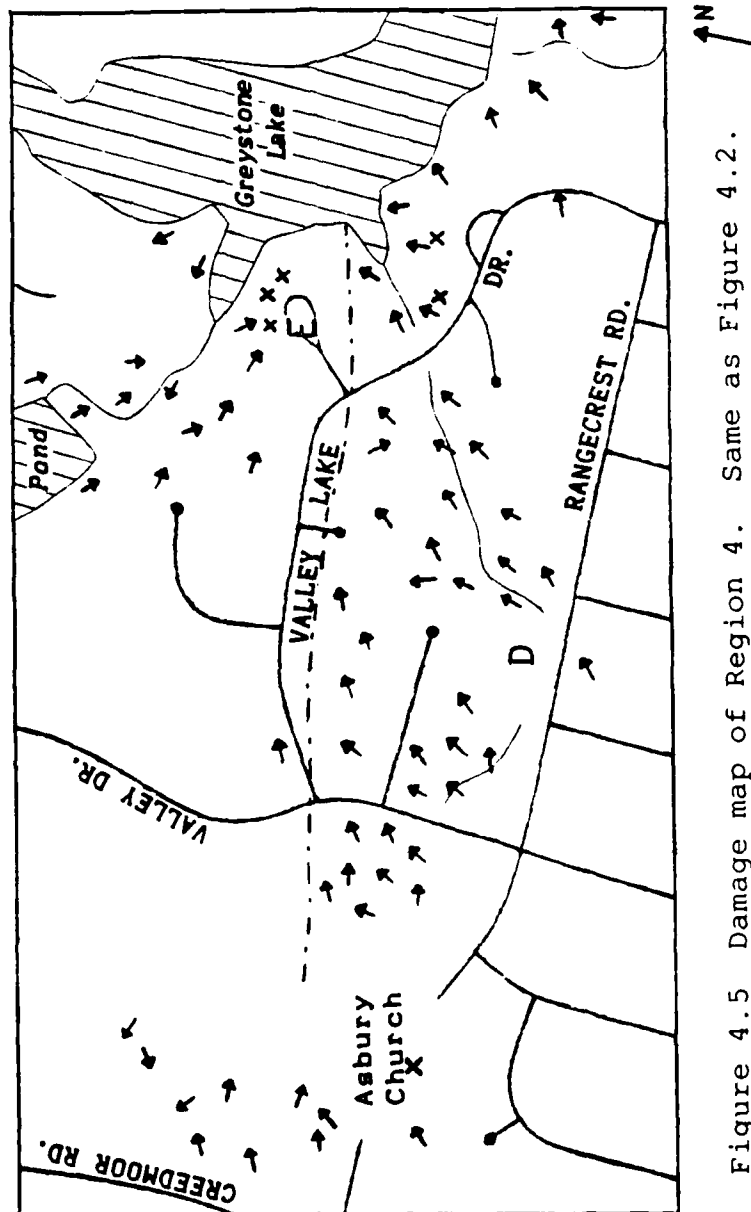


Figure 4.5 Damage map of Region 4. Same as Figure 4.2.

Greystone Lake. In the valley northeast of these houses, where the creek flows out of the culvert, much more extensive tree damage occurred, and continued through the valley toward the lake. Channeling may have been involved here, as the direction of the flow as evidenced by the tree fall had a component in the same direction as the valley orientation.

Another feature noted here was a strong northwesterly flow to the north of the main damage path. This was evident in downed trees from near the pond east of Valley Drive towards Greystone Lake, culminating in the destruction of three houses on Lookout Point Court ("E" on Figure 4.5). This was the only incident in north Raleigh of winds strong enough to destroy structures that blew from the northwest. Debris was also piled up at the southeast corner of the lake near the earthen dam, although that could be expected even in the absence of the strong inflow, as the winds to the rear of the tornado would blow it this way.

Region 5: Greystone Lake to Six Forks Road. This region was relatively uneventful, in terms of perturbations to the basic damage pattern. Several incidents of major damage did occur, but the storm had weakened as it passed through this region. A house on Wedgeland Drive on the east shore of Greystone Lake was destroyed--leading to Raleigh's second fatality (News and Observer, 1989)--and several houses in line to the east were severely damaged. This, and two houses heavily damaged on Mine Shaft Road near Sawmill, were

the only major deviations from the relatively weak, mostly F1 to low F2, damage following the convergence to a line pattern in this region. Also, another area of isolated damage north of the main track was observed in the creek valley north of Sawmill Road.

Region 6: Six Forks Road to Ravenscroft School (Figure 4.6). A sudden and drastic, though short-lived, intensification of the storm occurred as it passed through this area. A widening of the damage path and obscuring of the convergence line pattern were noted here.

As the storm was crossing Six Forks Road, it picked up strength causing significant damage to the Celebration and Peachtree Market shopping centers and some townhouses on Crown Oaks Drive. At Alison Court, a short cul-de-sac off Mourning Dove Road (marked "G" on Figure 4.6), tremendous damage occurred, with nearly all the houses being destroyed. One was moved nearly intact into the middle of the street. The overall pattern of damage at this point had most of the trees down to the north (within about 40 degrees of north), while the structural damage and debris was toward the east-northeast, the direction of the tornado's movement. Some divergent flow was noted south of Mourning Dove Road, from near Peachtree Market to the townhouse complexes south of Mourning Dove Road. East of Alison Court, several more houses were destroyed as the storm center moved into the creek valley.

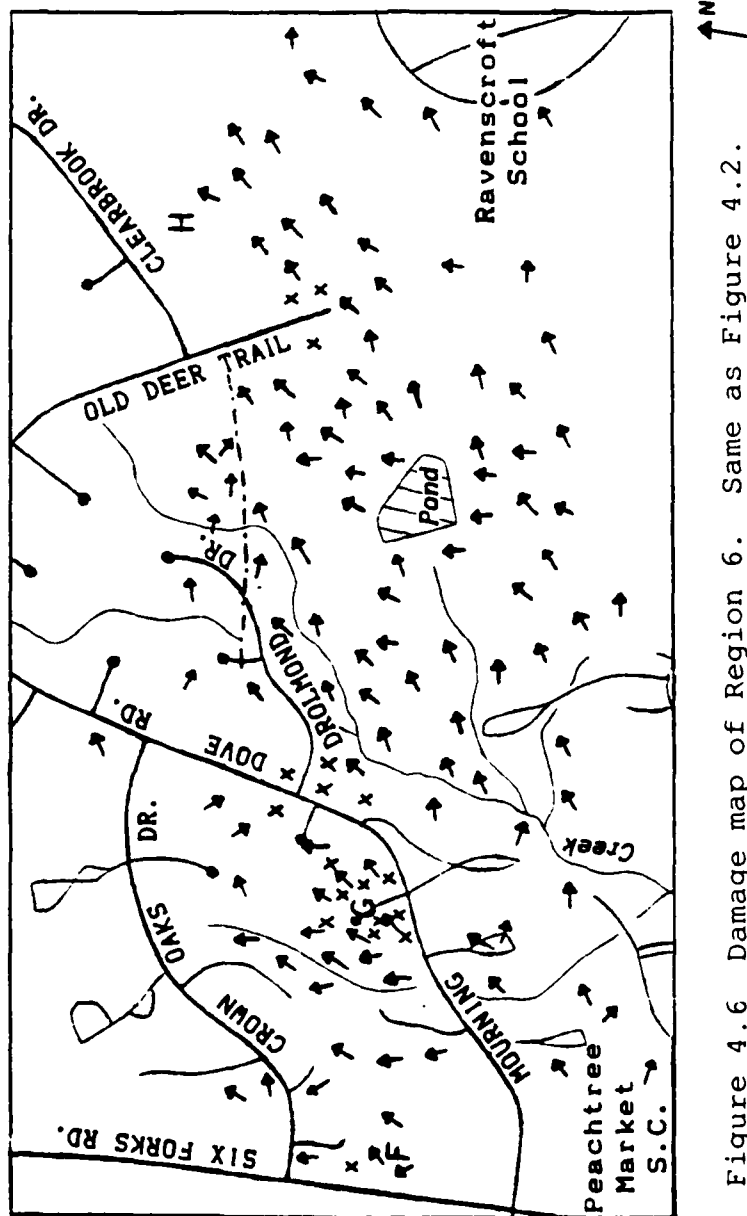


Figure 4.6 Damage map of Region 6. Same as Figure 4.2.

In the wooded area, the convergence to a line pattern began to reform between Drolmond Drive and Old Deer Trail. Over half the trees were downed and a slight structure by the pond was destroyed. There was a vast area to the right (south) of the convergence line where tree damage was evident, nearly 500 meters. The trees in this area were blown mostly toward the north to northeast.

At Old Deer Trail, three of the last four houses at the end of the street were destroyed. An oddity was that the one that was spared was the one at the very end of the street, and it was surrounded by downed trees. East of the Old Deer Trail and Clearbrook Drive intersection, in the wooded area behind the houses, was another confined area with tree falls in many different directions without any apparent pattern as to what fell first ("H" on Figure 4.6). Another area with trees down in several directions was located in a wooded area just east of Six Forks road, between Crown Oaks Drive and Mourning Dove road ("F" on Figure 4.6), although the tree fall directions in this area did not appear to be as random.

Beyond Old Deer Trail, the tree damage grew weaker, and the path narrowed. By the time it reached Ravenscroft School and Falls of the Neuse Road, the major damage to North Raleigh was just about over, although the storm itself would still go on for many miles.

Region 7: Falls of the Neuse Road to the Franklin County border. Damage was minimal and sporadic between Falls

of the Neuse and Litchford Roads, indicating the storm weakened considerably and may have dissipated temporarily at this point. Damage was observed again east of Litchford Road and on towards the US 1 bridge over the Neuse River. This damage, as viewed from aerial photographs, was patchy. The storm continued northeastward across the Neuse River into sparsely populated areas, strengthening at least one more time in Wake County, just before reaching the Franklin County border, where it destroyed several buildings.

5. DESCRIPTION OF DAMAGE MODEL

5.1 General Description

Much of the focus of this research has been on the damage in north Raleigh, and what can be surmised from it about the tornado. To aid in damage feature identification, a model was devised which would reproduce the damage patterns left behind by a tornado passing across a grid, with a damageable target at each gridpoint. Each target is assigned a threshold value, the magnitude of wind speed required to cause the target to sustain damage, randomly within a certain range. If the calculated wind speed at any time exceeds the threshold value for that point, the point is assigned damage. Each point can sustain damage only once, as in the case of a tree being blown over.

The target at each point is assigned a certain value of damage on a random basis. The values used are based on failure thresholds for different types of trees (Fujita, 1978), and the prevailing types of trees in the Raleigh area (Forest Service, 1969). Based on these, the points were assigned values based on wind speeds from 40 to 70 meters per second. Higher values could be used to simulate damage to buildings.

The model is kinematic, meaning there is no time dependence in the flow field. To simulate movement across the grid, a series of time steps are used. During each time step, a flow field is calculated using the equations

described below, and damage is assigned as appropriate. In the next time step, the tornado center (x_0, y_0) is moved, and wind flow and damage are recalculated. The damage is cumulative, so that all damage is accounted for after the last time step, and is plotted into a graphics output file. A flow chart for the model is shown in Figure 5.1.

5.2 Flow Near a Tornado

The model begins by assigning each point on the grid a value based on the actual distance from the tornado center, which is initially set to $(0,0)$. The distance between grid points is determined by input parameters.

To simulate the near-surface horizontal windfield in the vicinity of a tornadic vortex, a two-dimensional potential flow approach was used. It assumes an axisymmetric vortex structure, a steady state wind field, level terrain with uniform roughness, no interaction between gridpoint targets, and non-turbulent flow. The tornado vortex is assumed to be moving with constant velocity, whose x- and y-components are U_V and V_V respectively. The model uses inviscid complex potential flow theory. For a complex argument z where $z=x+iy$, it uses a complex potential function

$$F(z)=\phi+i\psi$$

where ϕ is the velocity potential and ψ is the streamfunction of the flow. To simulate a free cyclonic vortex with inflow

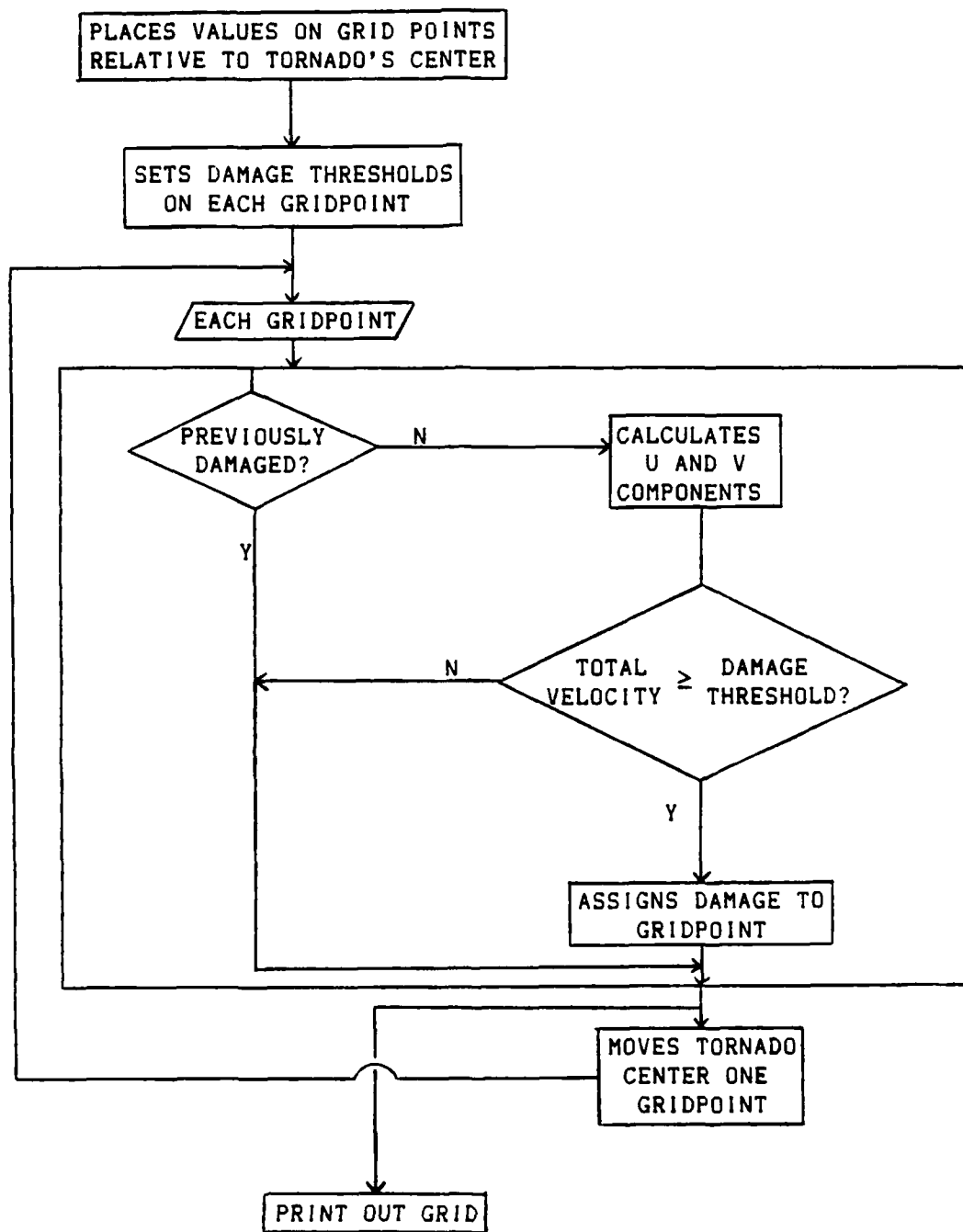


Figure 5.1 Computer flow chart of damage simulation model.

in an ambient wind field, a form of the potential function can be used that is composed of the sum of three components; a point sink at the center of the vortex (to produce inflow), a vortex circulation component (to produce rotation), and an ambient wind component. The function used is

$$F(z) = -\frac{m}{2\pi} \ln(z-z_0) - \frac{i\Gamma}{2\pi} \ln(z-z_0) + (U_A - iV_A)z$$

The formulas of the three components are from Batchelor (1984) and are additive, and

m is the strength of the point sink

Γ is the vortex circulation strength

U_A and V_A are the u and v components of the ambient wind

z_0 is center of the vortex = $x_0 + iy_0$

Then the streamfunction ψ is just $\text{Im}[F(z)]$, which can be expressed as

$$\psi = -\frac{m}{2\pi} \arctan\left(\frac{y-y_0}{x-x_0}\right) - \frac{\Gamma}{2\pi} \ln[(x-x_0)^2 + (y-y_0)^2]^{1/2} + U_A y - V_A x$$

Then the u and v components of the total velocity can be obtained by taking the y and x partial derivatives

$$u = \frac{\partial \psi}{\partial y} = \frac{-m(x-x_0) - \Gamma(y-y_0)}{2\pi[(x-x_0)^2 + (y-y_0)^2]} + U_A$$

$$v = -\frac{\partial \psi}{\partial x} = \frac{-m(y-y_0) + \Gamma(x-x_0)}{2\pi[(x-x_0)^2 + (y-y_0)^2]} + V_A$$

So, if s is the distance from the vortex center point (x_0, y_0) , $s = [(x-x_0)^2 + (y-y_0)^2]^{1/2}$, it follows that $|\vec{V}| = [u^2 + v^2]^{1/2}$, and $|\vec{V}| \propto 1/s$.

Within the vortex itself the assumptions of solid body rotation and uniform vertical velocity are used, so that the tangential and radial velocity components vary linearly with distance from the center. If V_R and V_T are, respectively, the maximum radial and tangential velocity components associated with the tornadic vortex occurring at distance r_v from the vortex center, then r_v can be considered the radius of the vortex, and for $s \leq r_v$,

$$u = \frac{-(x-x_0)V_R - (y-y_0)V_T}{r_v} \quad v = \frac{(x-x_0)V_T - (y-y_0)V_R}{r_v}$$

And here, $|\vec{V}| \propto s$. The vortex thus has a Rankine-like velocity profile, which is not an unreasonable assumption in assessing ground damage (Minor et al, 1982).

5.3 Flow from a Nearby Microburst

The damage patterns in north Raleigh imply that some microbursts were occurring in the vicinity of the tornado. To investigate this, a microburst was introduced into the model. In order to simulate a microburst occurring near the tornado, the simple potential flow model no longer holds. To account for this, the same basic velocity functions as calculated above are used, except the ambient, or external,

wind components now vary with position. A microburst outflow centered at (x_1, y_1) with an outflow radius b is designed to approximate the wind fields seen in theoretical microburst models and in results from actual Doppler radar measurements taken during field experiments. Then, within the outflow boundary, the microburst winds replace the ambient wind (U_A, V_A) in the external wind components u_{EXT} and v_{EXT} as described below.

The microburst wind profile uses a circular boundary with a point source at its center. The velocity is weighted so that it increases linearly with s_1 , the distance from the center, to reach a maximum value V_M at $b/2$ (half the outflow radius). As s_1 increases further, the outflow speed remains constant at V_M up to $s_1=0.9b$. From $s_1=0.9b$ to $s_1=b$, the outflow component goes to 0, while an external component is added that increases from 0 to (U_A, V_A) at $s_1=b$. In this way, first-order continuity is preserved. This formula is an approximation of the outflow radial profile generated from microburst models; see Figure 5.2. As time in the model progresses, the outflow radius b increases at a rate of one third the maximum outflow wind speed, and the maximum outflow speed V_M decreases with $1/b$. The rate of increase in b is less than the outflow speed due to the development of horizontal vortices at the rim of the outflow boundary, which contribute an increase in the horizontal speed at the surface (Fujita, 1985).

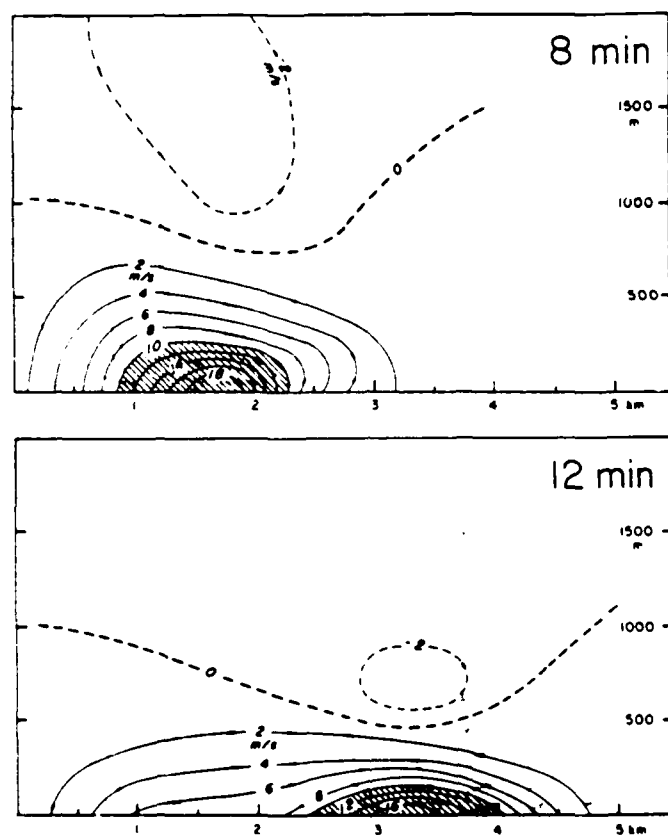


Figure 5.2 Horizontal velocity profile generated by a model microburst. (Krueger and Wakimoto, 1985)

Thus, the external wind functions in the wind equations can now be expressed as

$$u_{EXT}(x,y) = \begin{cases} V_M \frac{2(x-x_1)}{b} & 0 \leq s_1 \leq 0.5b \\ V_M \frac{x-x_1}{s_1} & 0.5b < s_1 \leq 0.9b \\ 10 \left(1 - \frac{s_1}{b}\right) V_M \frac{x-x_1}{s_1} + U_A \left(1 - 10 \left(1 - \frac{s_1}{b}\right)\right) & 0.9b < s_1 \leq b \\ U_A & s_1 > b \end{cases}$$

$$v_{EXT}(x,y) = \begin{cases} V_M \frac{2(y-y_1)}{b} & 0 \leq s_1 \leq 0.5b \\ V_M \frac{y-y_1}{s_1} & 0.5b < s_1 \leq 0.9b \\ 10 \left(1 - \frac{s_1}{b}\right) V_M \frac{y-y_1}{s_1} + V_A \left(1 - 10 \left(1 - \frac{s_1}{b}\right)\right) & 0.9b < s_1 \leq b \\ V_A & s_1 > b \end{cases}$$

This microburst model assumes that the downrushing air has no horizontal momentum and is irrotational. In reality, however, this is often not the case. Fujita (1985) has noted that microbursts associated with mesocyclones have cyclonically curved outflow. Additionally, the fast movement and high ambient wind speeds observed with the Raleigh system suggests a high magnitude horizontal velocity component in

the microburst's downflow, resulting in an asymmetric outflow at the surface. See Figures 5.3 and 5.4.

With no systematic study of microbursts in close proximity to tornadoes available, an intuitive approach was used. The tornado velocity (U_V, V_V) was added onto the basic point source outflow, with half of it contributing to a circulatory motion centered at the tornado center, which is assumed to be the center of rotation of the parent mesocyclone. Additionally, a recalculated effective outflow center (x_2, y_2) is calculated based on the difference between the storm's translational speed and the outflow speed. The radial wind variation is then calculated based on the distance from the effective outflow center. Defining this distance $s_2 = [(x-x_2)^2 + (y-y_2)^2]^{1/2}$ and defining the maximum distance from (x_2, y_2) to the microburst outflow as b_2 equal to $[(x_1-x_2)^2 + (y_1-y_2)^2]^{1/2}$, and the outflow winds $U_{MICRO}(x, y)$ and $V_{MICRO}(x, y)$ as

$$U_{MICRO} = \begin{cases} V_M \frac{x-x_1}{s_1} \frac{2s_2}{b_2} + U_V + \frac{1}{2} \left(\frac{-U_V(x-x_0) + V_V(y-y_0)}{s} \right) & s_2 \leq 0.5b_2 \\ V_M \frac{x-x_1}{s_1} + U_V + \frac{1}{2} \left(\frac{-U_V(x-x_0) + V_V(y-y_0)}{s} \right) & 0.5b_2 < s_2 \leq b_2 \end{cases}$$

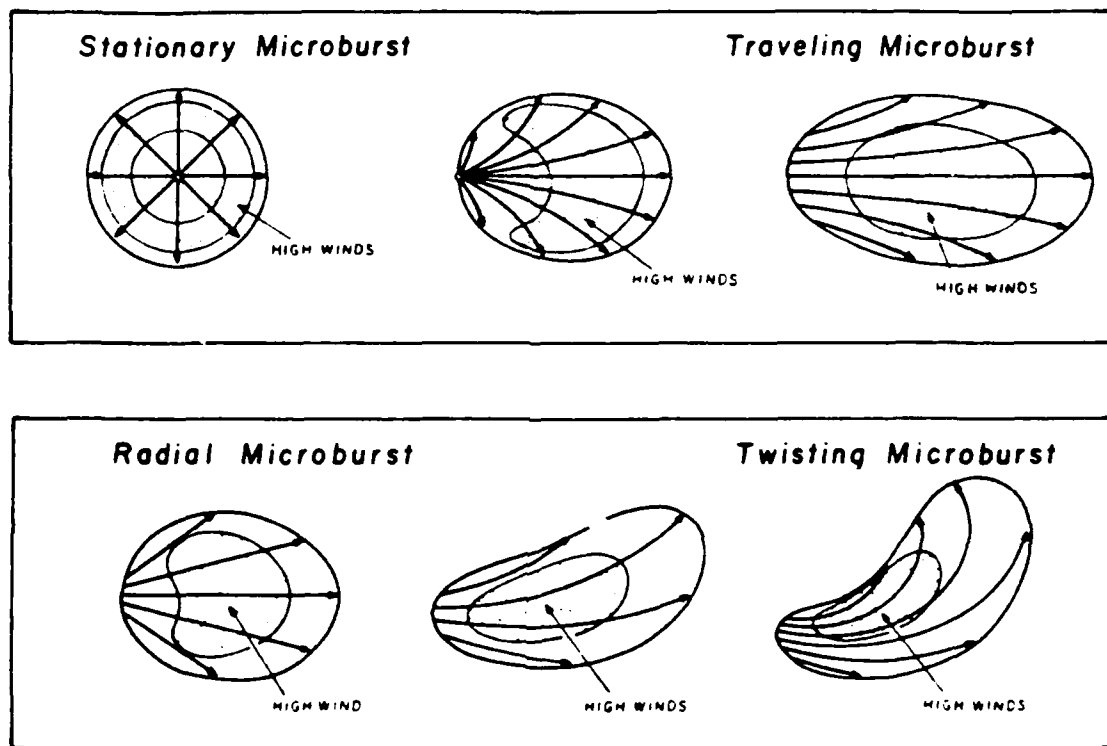


Figure 5.3 Schematic surface flow associated with various types of microbursts. (Fujita, 1985)

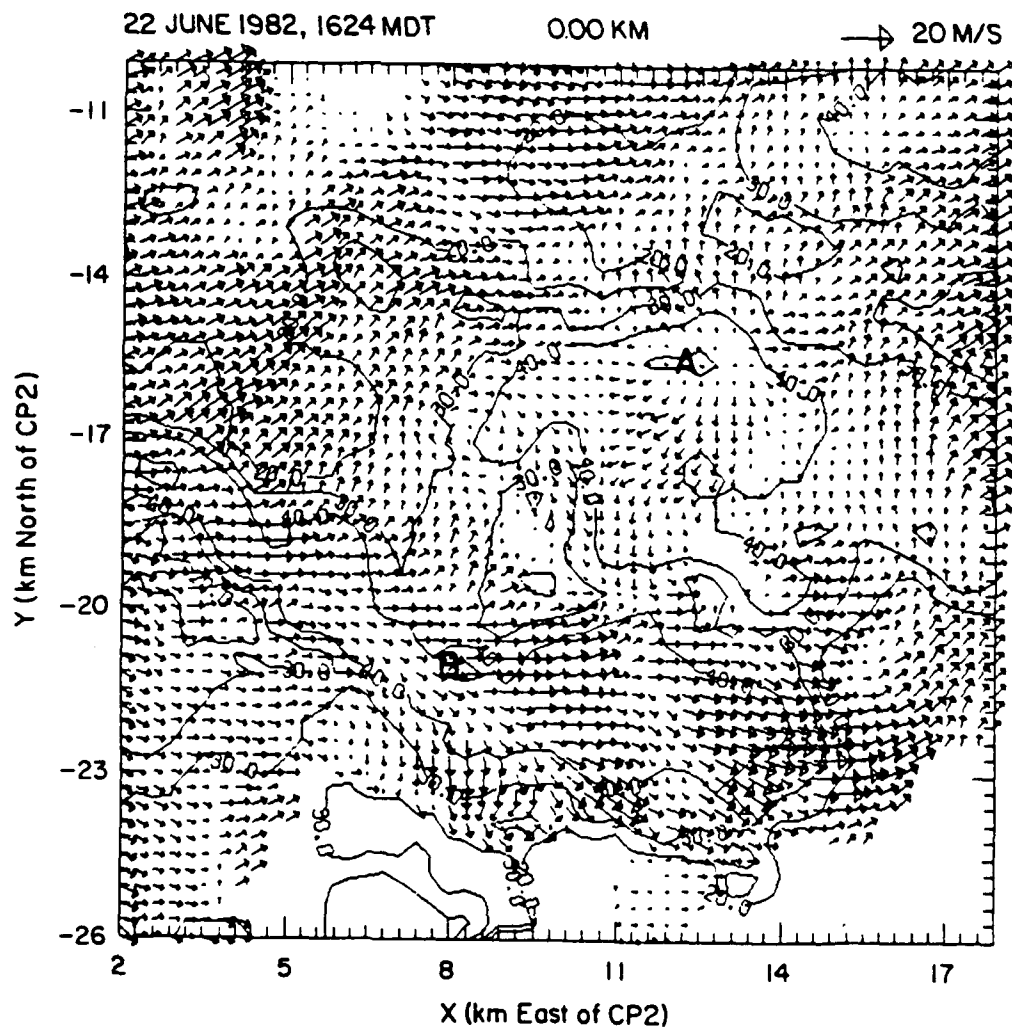


Figure 5.4 Doppler radar velocity profile from a microburst producing storm in the JAWS experiment. Note the translational wind component in microburst B. (Hjelmfelt, 1984)

$$V_{\text{MICRO}} = \begin{cases} V_M \frac{y-y_1}{s_1} \frac{2s_2}{b_2} + v_V + \frac{1}{2} \left(\frac{U_V(y-y_0) - V_V(x-x_0)}{s} \right) & s_2 \leq 0.5b_2 \\ V_M \frac{y-y_1}{s_1} + v_V + \frac{1}{2} \left(\frac{U_V(y-y_0) - V_V(x-x_0)}{s} \right) & 0.5b_2 < s_2 \leq b_2 \end{cases}$$

Then the external wind functions become

$$u_{\text{EXT}} = \begin{cases} U_{\text{MICRO}} & 0 \leq s_1 \leq 0.9b \\ U_{\text{MICRO}} \left(10 \left(1 - \frac{s_1}{b} \right) \right) + U_A \left(1 - 10 \left(1 - \frac{s_1}{b} \right) \right) & 0.9b < s_1 \leq b \\ U_A & s_1 > b \end{cases}$$

$$v_{\text{EXT}} = \begin{cases} V_{\text{MICRO}} & 0 \leq s_1 \leq 0.9b \\ V_{\text{MICRO}} \left(10 \left(1 - \frac{s_1}{b} \right) \right) + v_A \left(1 - 10 \left(1 - \frac{s_1}{b} \right) \right) & 0.9b < s_1 \leq b \\ v_A & s_1 > b \end{cases}$$

Though this model is still crude, it represents a good flow field approximation for the purpose of analyzing damage patterns. Numerous different input values were attempted to try and simulate the observed damage in north Raleigh.

5.4 Use of the Model

In order to simplify the calculations, the storm movement is assumed to be in the negative y-direction. Thus U_V is equal to zero, and so several terms drop out of some of the above expressions. Also, the movement of the (x_0, y_0)

point can be made to adjacent gridpoints with the grid value of x_0 being constant. The output grid, turned on its side, represents a left to right moving tornado moving across the grid, similar in orientation to the damage illustrations in the previous chapter.

The input parameters are designed to use values directly observed or estimated from the damage. The only real guesswork involves trying to place the microburst. The model prompts the following parameters

- Starting gridpoint (based on number of time steps)
- Vortex radius
- Number of gridpoints per vortex radius
- Speed and direction of vortex propagation
- Maximum winds from tornado
- Ratio of rotation component to inflow component
- Number of time steps to run
- Speed and direction of ambient wind
- If microburst is present
- Random number seed (to set damage threshold values)

As can be seen, the model runs with or without a microburst present. If there is a microburst, the following additional parameters are asked for

- x- and y-coordinates of microburst center
- maximum velocity associated with the microburst
- initial outflow radius

All other values used in the model (m , Γ , V_R , V_T , s , etc) are calculated from the input values.

6. RESULTS AND ANALYSIS

6.1 Model Output

The main purpose of the model is to simulate a tornado moving through a field of damageable targets in order to detect features that can be identified from the damage that might not be intuitively obvious. Results from running the model, given the model's inherent limitations, can be used to identify features of the tornado and of the winds around it.

Some care was used in interpreting the model output in comparison to the actual damage. The model contains no terrain or ground roughness variations, so changes in the flow due to these effects will not show up in the model output. Additionally, assuming the "ambient" wind component is uniform throughout the field of the grid may not be correct. Attempts to change the ambient component with time as the tornado was moved across the grid modified the results slightly, but were no more conclusive than not changing it.

6.2 Analysis of Damage Using Model Output Results

The tornado's speed, according to eyewitness accounts and radar imagery, was about 25 meters per second, and this value was used throughout the model runs. In order to reproduce the types of damage patterns seen in Raleigh, an "ambient wind", a wind of scale larger than the tornado, must have been present in the flow field. A speed of at least 20 meters per second is required. Increasing the speed beyond

this value does little to additionally modify the pattern of damage near the center of the path, except to reorient the arrows even more in the direction of the wind. What it does is to modify the width of the damage track. As the ambient wind increases, the width of the damaged area increases, reaching infinity (i.e. the scale of the ambient wind flow) when the magnitude of the wind reaches the minimum threshold of failure of the targets.

The direction of a 20 m s^{-1} wind needs to be in the same direction as the tornado propagation, within 30° , left to right (relative to tornado's motion), and 20° , right to left, or the damage in the model becomes dissimilar to the actual damage. Thus if the tornado was moving from 250° , the direction of the ambient wind must be at least 230° and at most 280° . Increasing the ambient wind to 25 m s^{-1} allows 30° variation either way.

Because of the way the model is designed, the actual width of the tornado (in meters) is not a determining factor in the output, only its width on the grid field (in gridpoints). Thus, the size of the vortex can be estimated by the width of the damage in the output, in gridpoints. Based on the width of the damage from the model output, the diameter of the vortex based on a 20 m s^{-1} wind would be about 150 meters; it would be closer to 100 meters based on a 30 m s^{-1} ambient wind.

Figures 6.1 and 6.2 show tree fall patterns similar to the damage observed just west of Glenwood Avenue. The actual damage has a greater number of trees down to the right of the convergence line, indicating at least one of the following possibilities. The ambient wind is higher than 20 m s^{-1} , or the direction is more southerly than the tornado propagation. The best fit here appears to be 210° at 25 m s^{-1} . Output using this value is shown in Figure 6.3. See Figure 6.4 for comparison to actual damage.

East of Glenwood Avenue, the damaged area expands to the south, evidenced by the damage at Cooper's Pond. It is obvious that an increased southerly wind speed developed south of the tornado path. This could be attributed to an increase in the strength of the tornado itself, i.e. the sink strength. Since there is little difference in the pattern of damage at the center of the path, this effect is likely not due to changes in the wind field outside the tornado.

Convincing evidence of a microburst is observed in the few kilometers northeast of Leesville Road. A strong microburst, centered near the creek and Winthrop Drive, would account for the damage in the creek valley, 500 meters or more from the main storm track, as well as the striking anomalies in the damage from the tornado itself. Figure 6.5 shown the model results from placing a microburst with a 500 meter outflow radius about 600 meters to the right of the tornado path and, initially, about 800 meters ahead of the

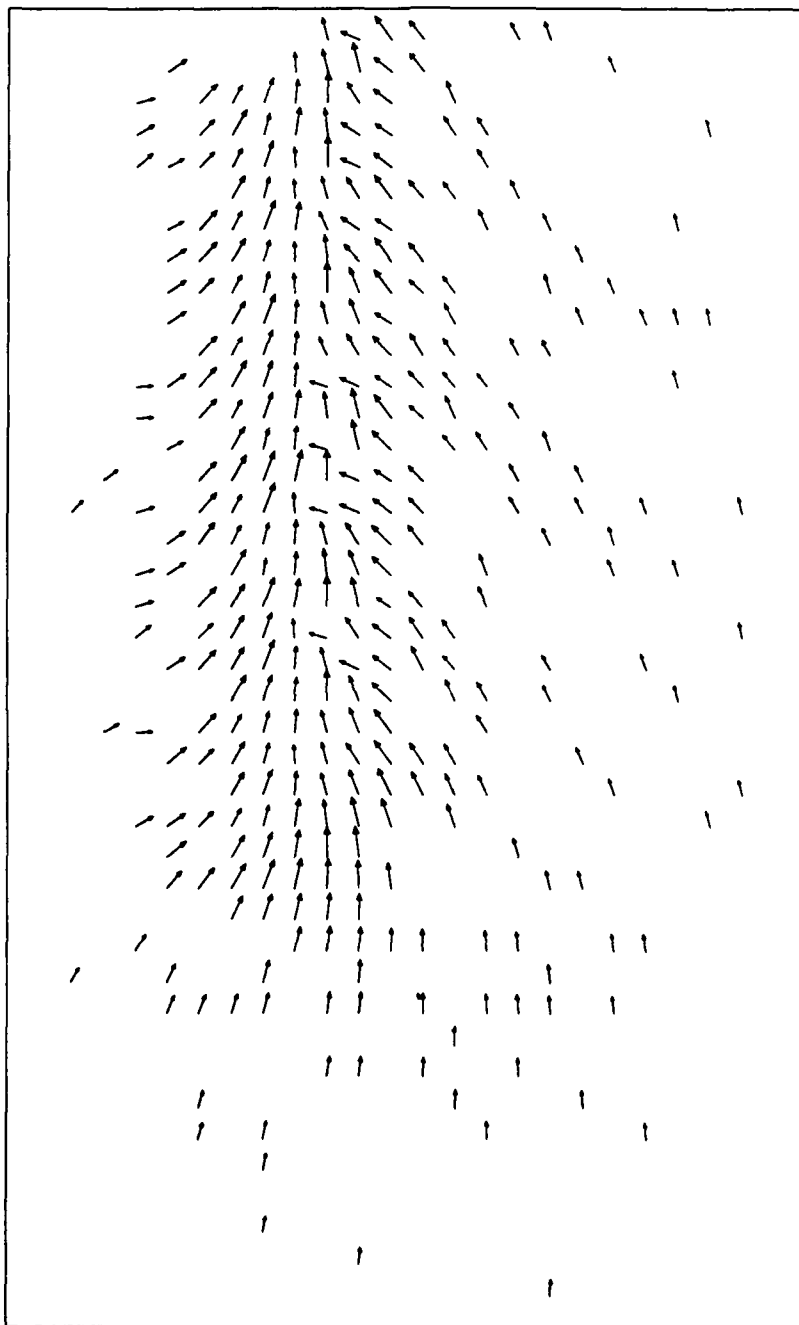


Figure 6.1 Model output for a tornado with a 30 m s^{-1} ambient wind from same direction as tornado movement.

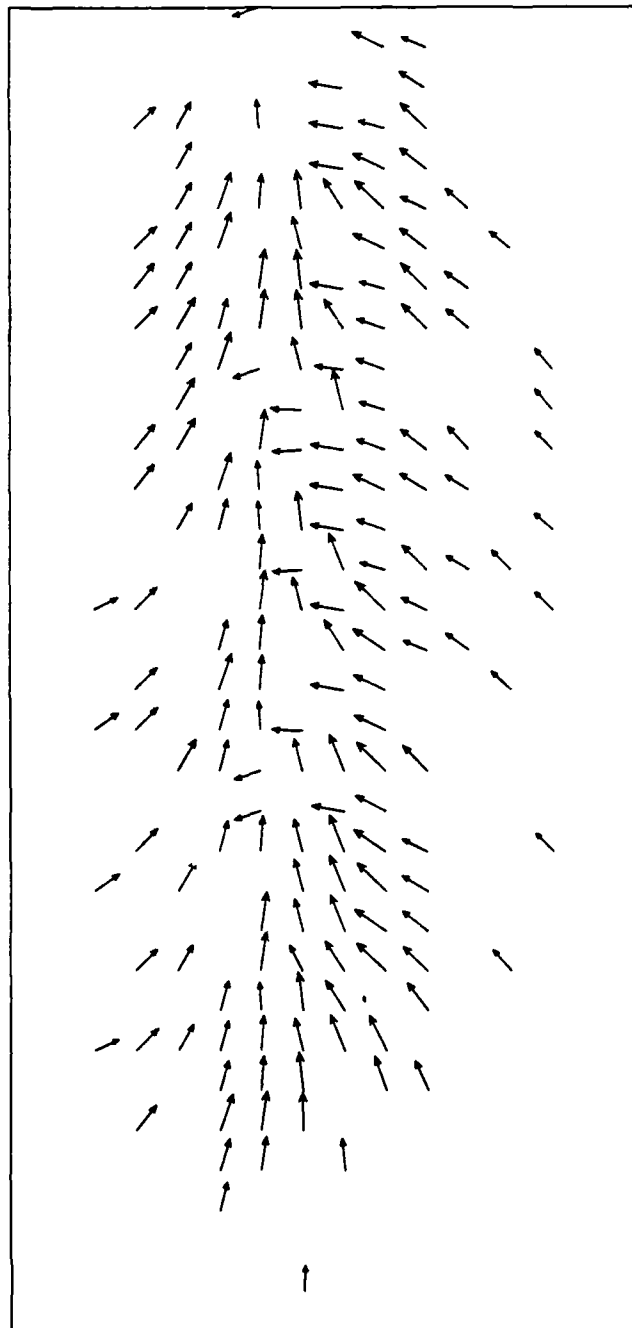


Figure 6.2 Model output with 20 m s^{-1} ambient wind from direction 20° less than (i.e. backed direction) that of tornado movement.

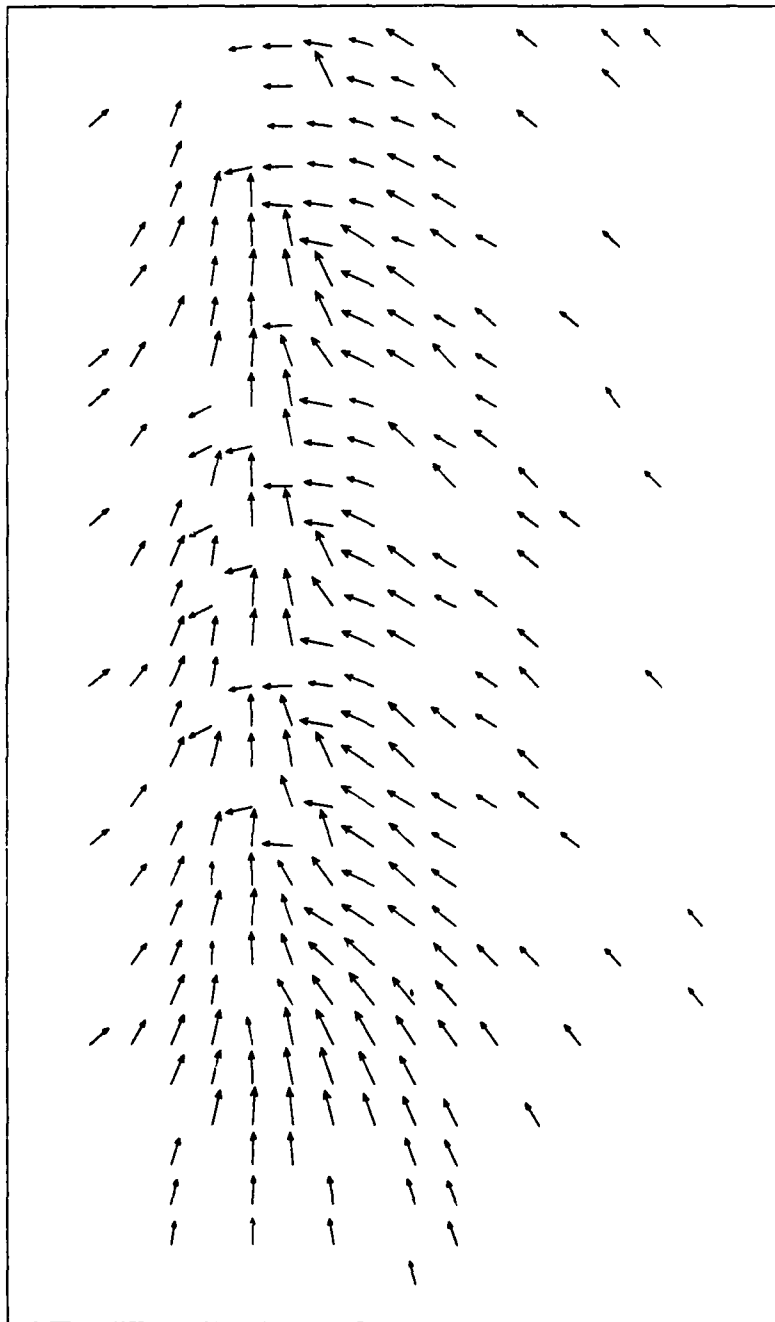


Figure 6.3 Model output with 25 m s^{-1} ambient wind from direction 30° less than that of tornado movement.

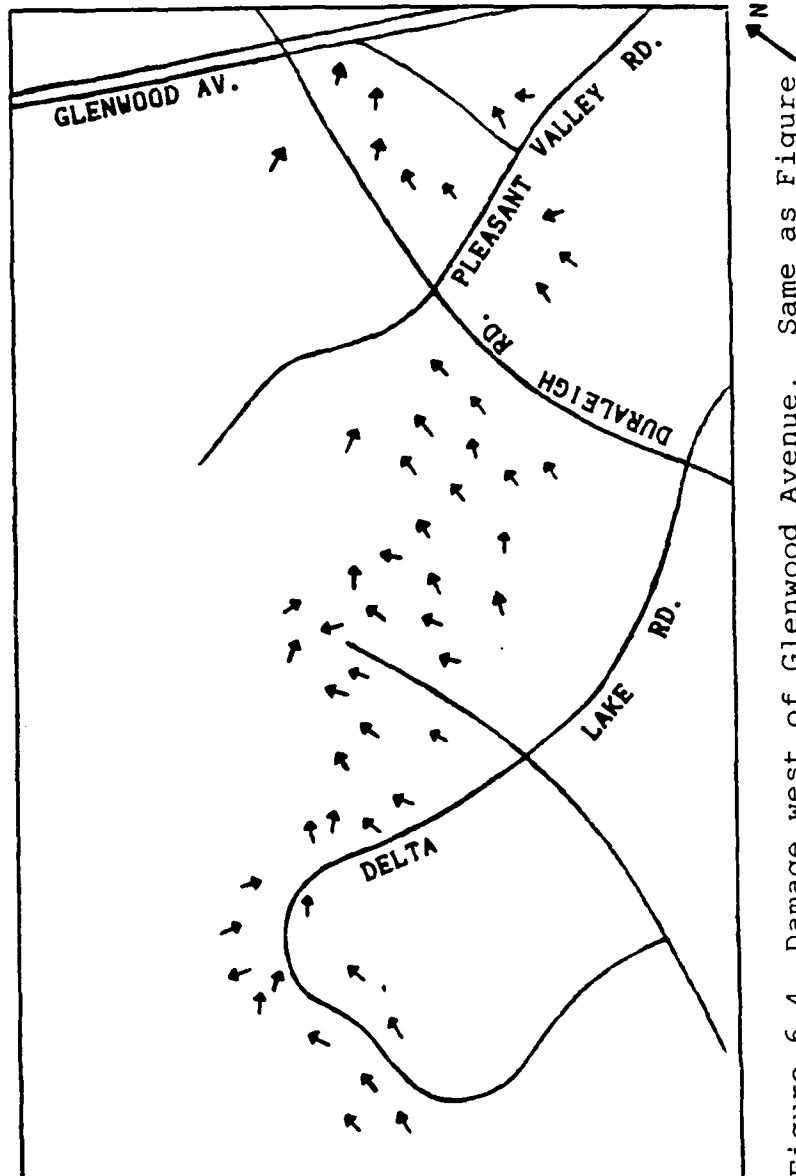


Figure 6.4 Damage west of Glenwood Avenue. Same as Figure 4.2.

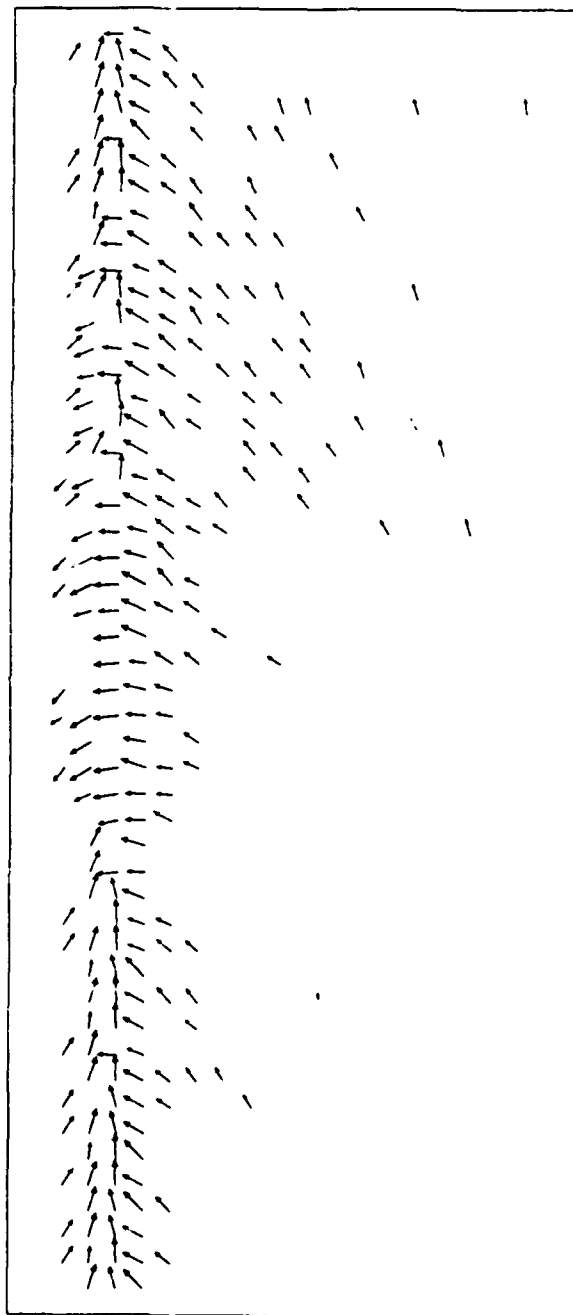


Figure 6.5 Model output with 20 m s^{-1} ambient wind and a microburst to right front of tornado. Tornado moves past microburst center, resulting in modification of the damage pattern. Microburst (MB) coordinates (10,25), initial tornado coordinates (25,50). Note, in all model runs, axes are sideways, so x-axis points upward and y-axis points to left.

tornado. The modified damage pattern shows strong winds now blowing across the line of propagation from right to left, with a component against the propagation evident on the left side of the center. This is similar to the actual pattern observed along Ray and Lynn Roads, shown in Figure 6.6.

The model underestimates the apparent strength of the easterly flow between Calibre Oaks and Barton's Landing, although it does well with the direction. The model assumes a homogeneous microburst, where in reality that is not always the case. Fujita and Wakimoto (1981) identified smaller scale areas of increased intensity within microbursts, which they termed "burst swaths". It is possible that one of these swaths was responsible for the strong flow towards the tornado. This could be the cause of similar asymmetric inflows observed in photographic accounts of other tornadoes (Hoecker, 1960, Golden and Purcell, 1977).

The excessive damage to the houses on Three Bridges Circle may have been due to another burst swath, although this may have been governed by terrain considerations as well. The affected area sits on a slope facing the south (the direction of the wind), and there were few trees or high-profile buildings immediately across Lynn Road, which is why there was little damage on the south side of Lynn Road.

As for the area of trees toppled over each other ("A" in Figure 6.6), the model did not reflect this. This may be due to the inherent limitations of the model, or it may have been

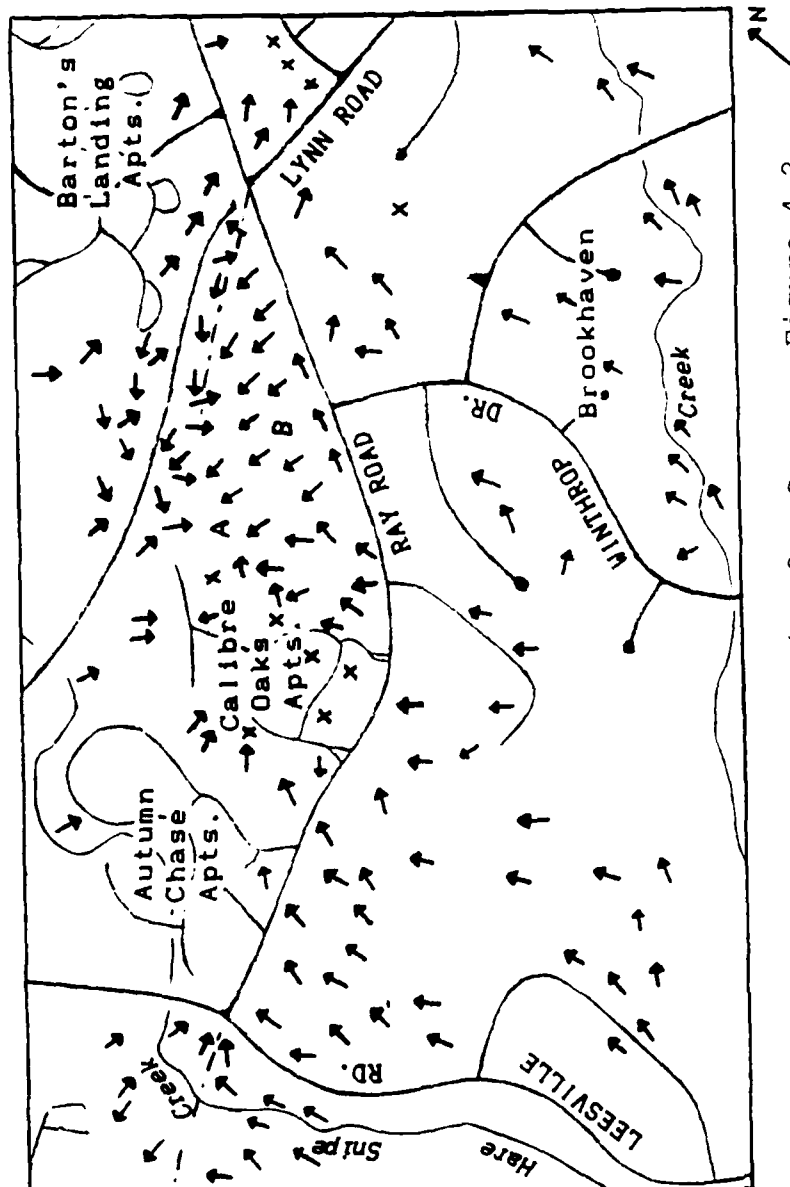


Figure 6.6 Damage in Region 2. Same as Figure 4.2.

a problem of scaling. The dimensions of the grid were too small to show much detail along the center of the damage track and still fit in a microburst. Still (see Figure 6.5), there is some indication of this type of swirl right near where the microburst-influenced damage begins to take over.

Another phenomenon noted in the damage near this area was an isolated area of damage about 600 to 700 meters to the left of the damage track center. This could be accounted for by a microburst occurring after the passage of the tornado. Figure 6.7 shows the output results obtained by placing a microburst to the left-rear of the tornado, far enough away to prevent the microburst flow from reaching the tornado's highest winds. Without having the tornado near enough to affect the outflow, the only evidence is some relatively light damage separated from the main damage caused by the tornado. This feature was also noted again farther along the track. Regarding Figure 6.7, because of the way the model is set up, the tornado and microburst begin simultaneously at the beginning of the model run. Hence, the tornado damage on the output diagram appears to be downstream of the microburst damage. In actuality, the tornado damage would have occurred across the length of the diagram.

East of Creedmoor Road, in the Greystone Village subdivision, another microburst appears to have occurred, this one to the left of the tornado. Unlike the one described in the preceeding paragraph, this one was close

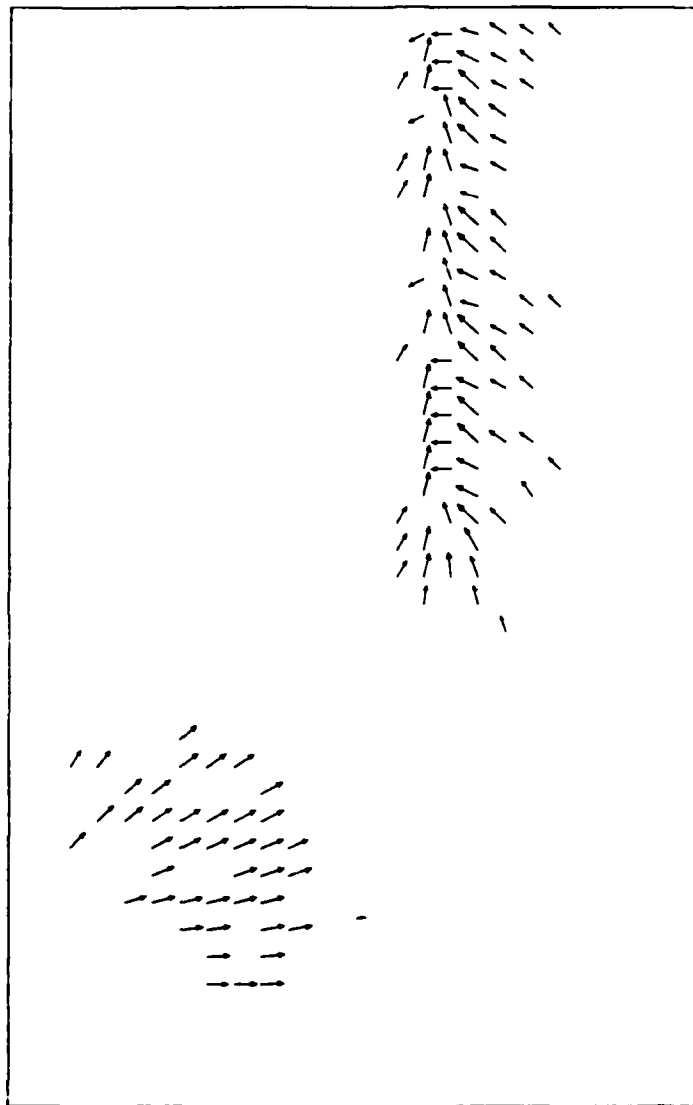


Figure 6.7 Model output with microburst to left rear of tornado, with little interaction between the two. The tornado damage would actually occur all the way across the bottom of the diagram. MB coordinates (40,35), initial tornado coordinates (25,20).

enough to interact with the tornado. Figure 6.8 shows the output from a model run with a microburst just to the left-rear of the tornado. The strongest damage is in a diagonal from the left rear of the tornado. This result agrees with the observed pattern to the northwest of Greystone Lake, probably aided by channeling effects in the creek valley, culminating with the destruction of the houses on Lookout Point Court, see Figure 6.9.

The other area of primary concern was the region east of Six Forks Road. This was very difficult to approximate using the model. The damage indicates divergent flow south of Mourning Dove Road, which certainly implies a microburst was present at some point, see Figure 6.10. One possibility was a microburst occurring behind and to the right of the tornado. Figure 6.11 illustrates this. This does a reasonable job in the area to the right of the storm track, albeit with a little too much of a left-to-right component. It does not do well at all near the center of the damage path.

Another possibility is a microburst initially to the right-front of the tornado, similar to, but smaller than, the one described above (Figure 6.5). Or it could be a shift in the ambient wind to a more southerly direction, and/or a strengthening of that wind. Such a senario is depicted in Figure 6.12. Each of these could better account for the generally south to north orientation of the trees near the

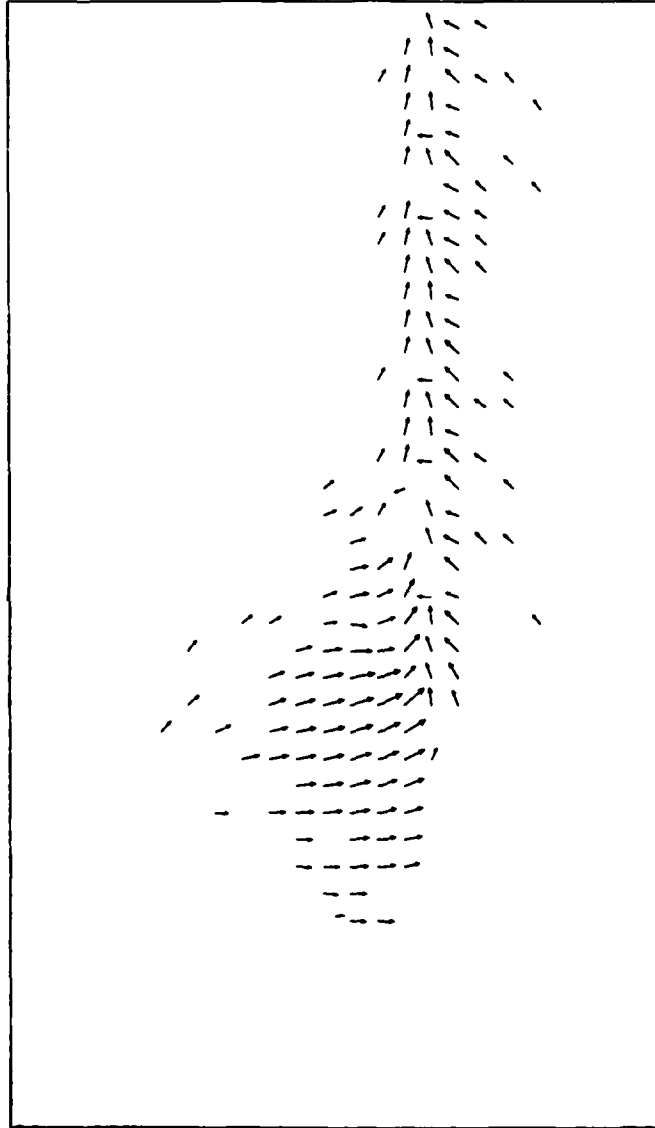


Figure 6.8 Model output with microburst to left rear of tornado, but much closer initially than in Figure 6.7. MB coordinates (35,30), initial tornado coordinates (25,25).

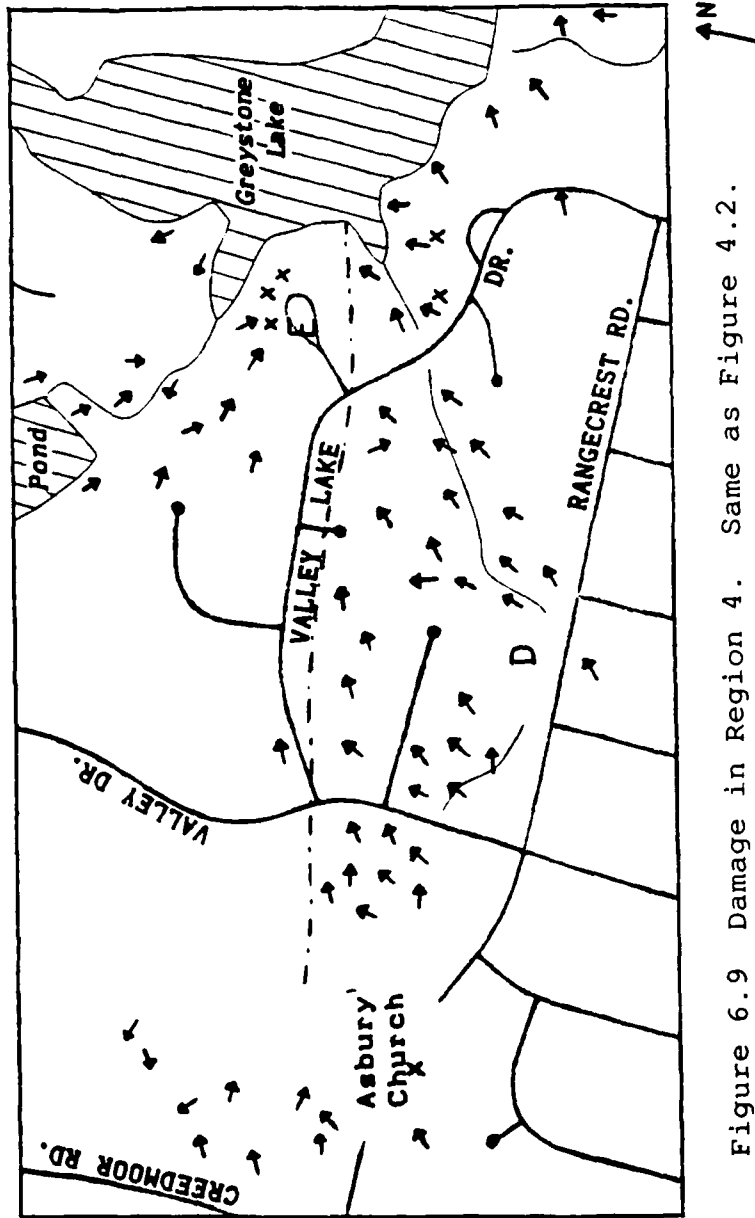


Figure 6.9 Damage in Region 4. Same as Figure 4.2.

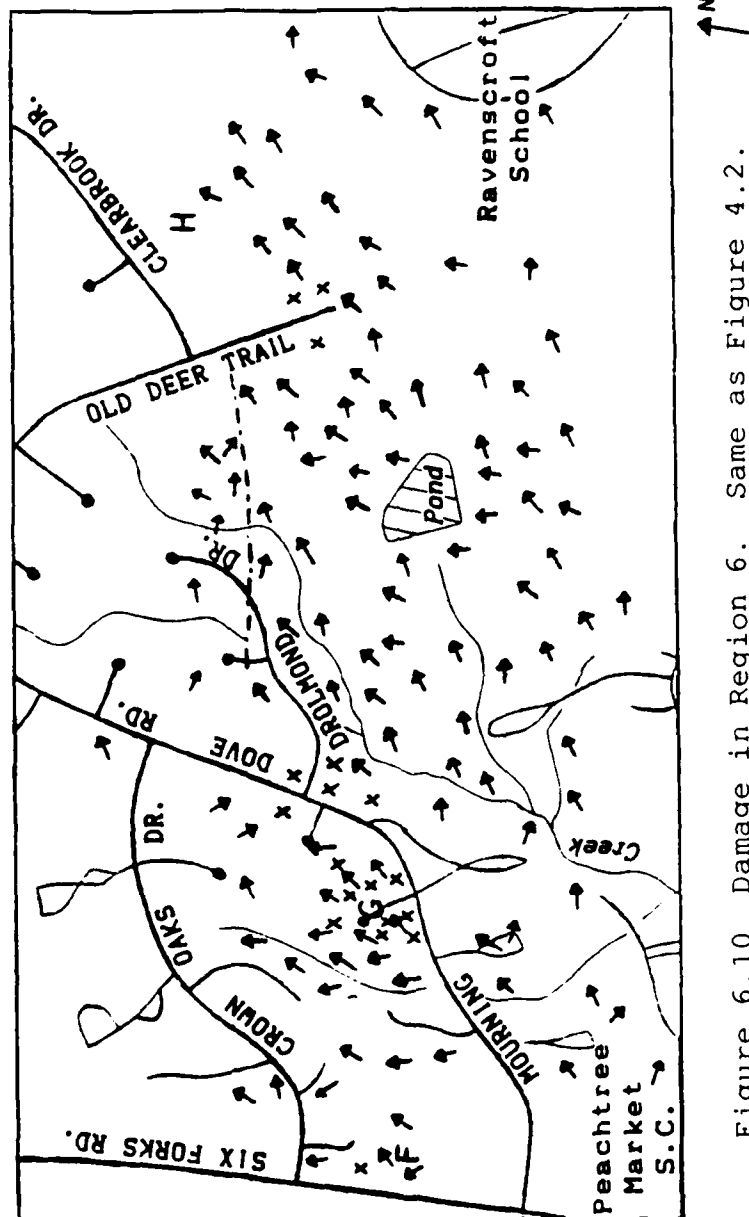


Figure 6.10 Damage in Region 6. Same as Figure 4.2.

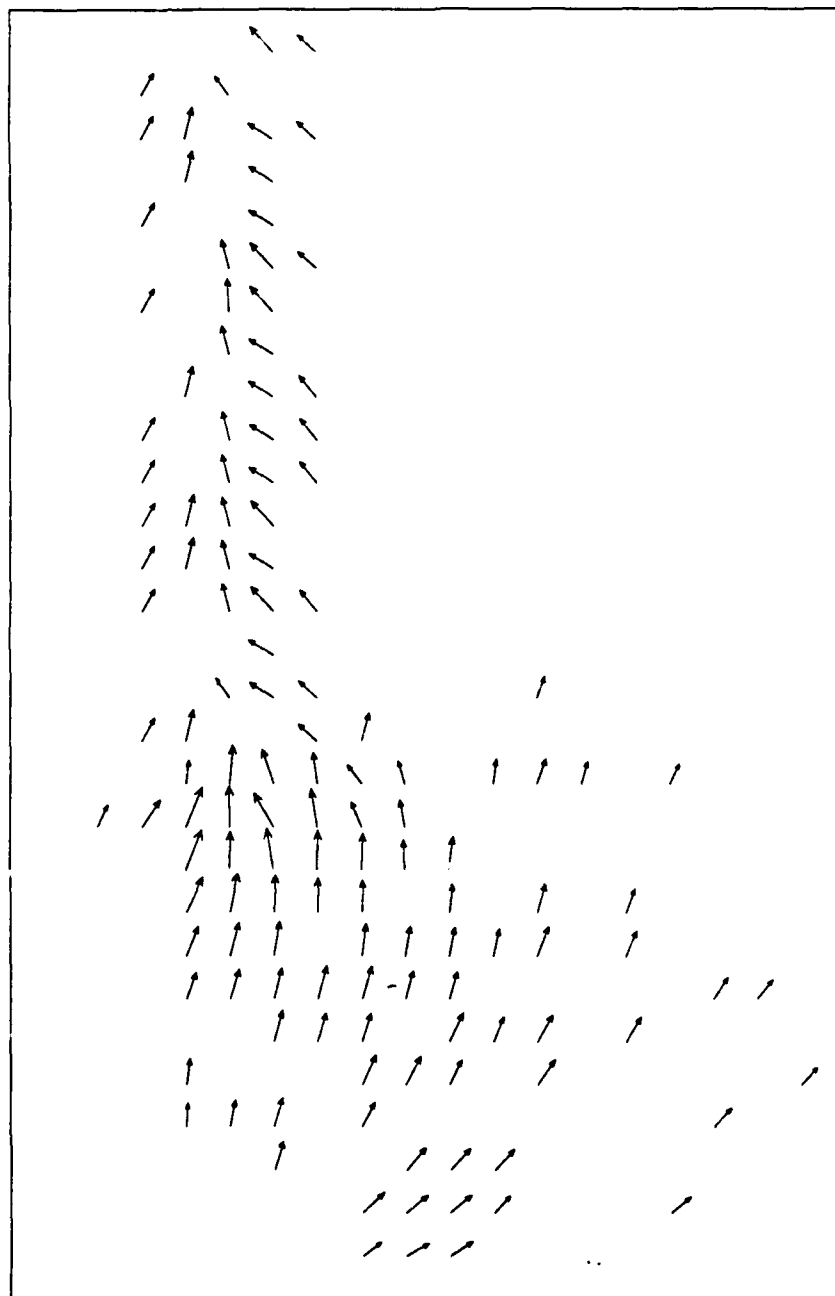


Figure 6.11 Model output with microburst to rear and immediate right of tornado. MB coordinates (23,30), initial tornado coordinates (25,20).

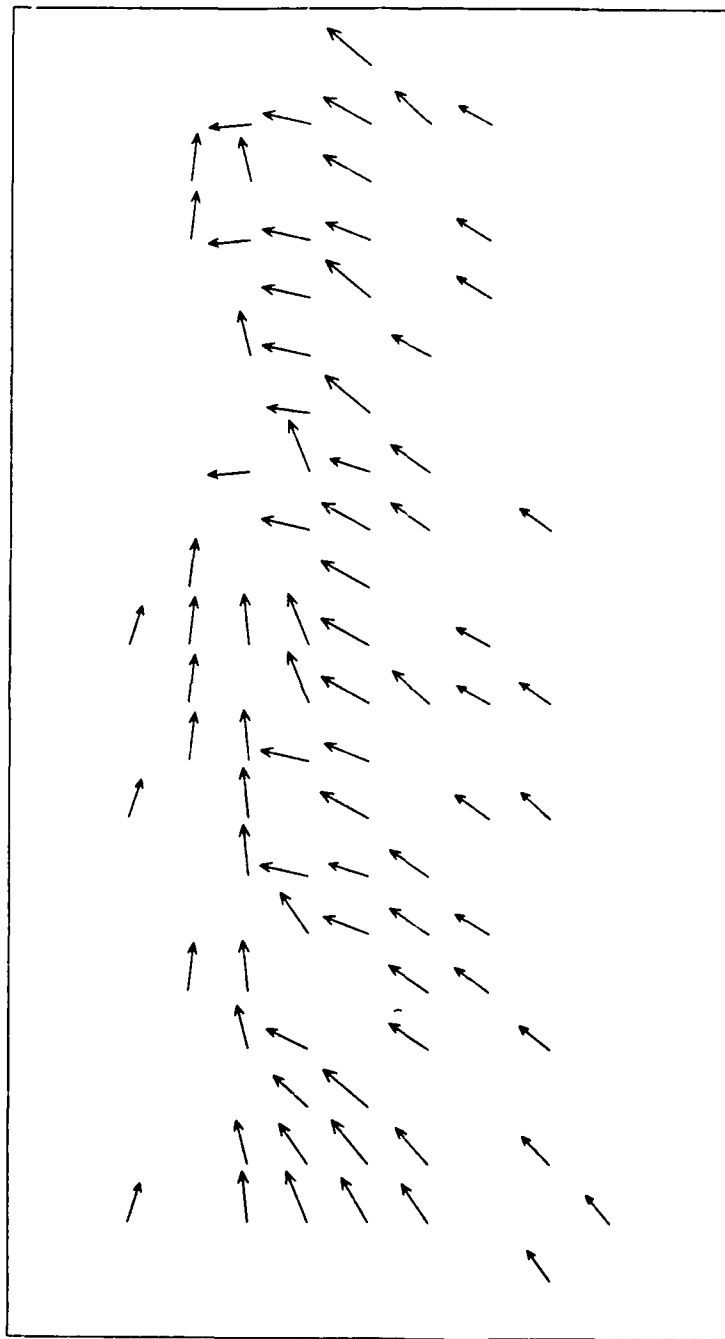


Figure 6.12 Model output with no microburst, with ambient wind 25 m s^{-1} from direction 40° less than tornado movement direction.

center of the storm. Neither accounts for the building destruction, done by winds blowing in the same direction as storm propagation, and the latter does not account for the wide damage track or the lack of strong southerly component on its right side.

A possible resolution is a pair of microbursts occurring in rapid sequence. The model, unfortunately, can generate only one microburst per run. An approximation would be to put the results from two runs over each other and create a composite. Figure 6.13 represents one such attempt. The aft microburst can account for the divergent flow in the townhouse complexes south of Mourning Dove Road, and the forward one (which, in this depiction, would have occurred first) can produce the broad southerly flow. It definitely appears that a number of things were going on simultaneously in this area, resulting in damage too complex for this model to resolve.

Beyond Falls of the Neuse Road, the damage becomes much more sporadic than previously, suggesting the possibility that the tornado had dissipated, and the damage that occurred was the result of microbursts alone. The model was run with no tornado present (accomplished by setting the maximum tornadic wind equal to the propagation speed, which causes m and Γ to be 0), and inserting a microburst. Even with the circulation component in the model's microburst, the model could not produce damage such as that observed in this area,

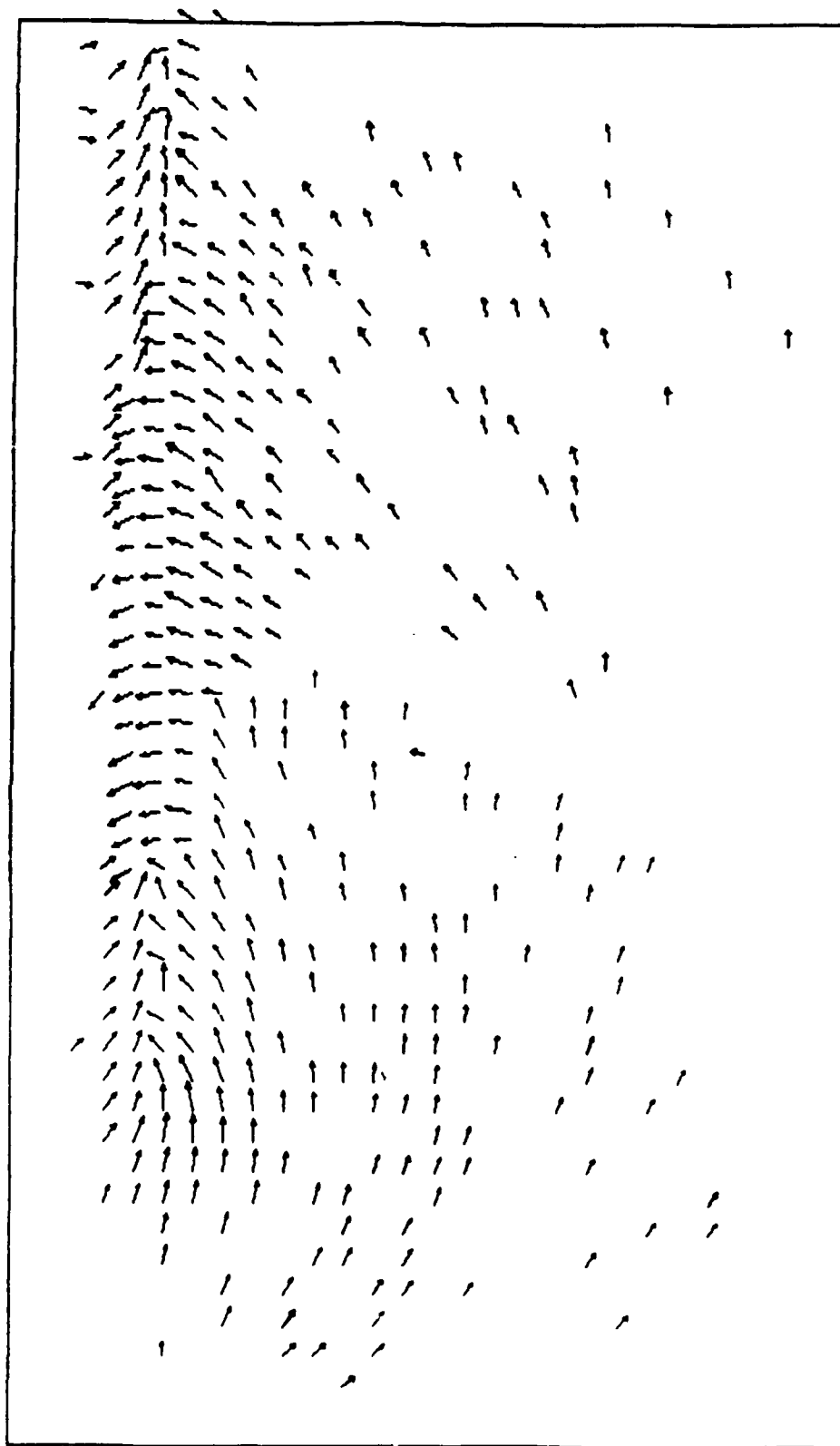


Figure 6.13 Composite showing model output with two microbursts, one at (25,30) and one at (10,25).

which continued to show different directions of damage on opposite sides of a center line. Figure 6.14 is output from one run. Thus, it must be that the damage, however spotty, was caused by a tornado. It must have been forming and dissipating through this area, with ground roughness possibly playing a role in its evolution.

6.3 Other Analyses of the Damage

Several other points can be made concerning damage in north Raleigh. First of all, there is no evidence that the tornado was ever anything more than a simple vortex. There were no cycloidal ground markings or unusual debris patterns that would indicate a multiple vortex storm. It is possible that a two-cell vortex may have been present during at least part of its lifetime, but this would not be reflected in the damage, since nearly all the damage occurs outside or at the rim of the tornado. Indeed, a variation of the model with a two-celled vortex with downflow at the center was attempted, with no observed difference in the results.

A very important effect of the presence of microbursts is to increase the intensity of the damage. A look at the areas where the microbursts are assumed to have occurred, based on the analysis of damage, indicates the most heavily damaged areas in Wake County were nearly always near a microburst, as shown in Figure 6.15. This implies that the tornado would not have been nearly as destructive as it was

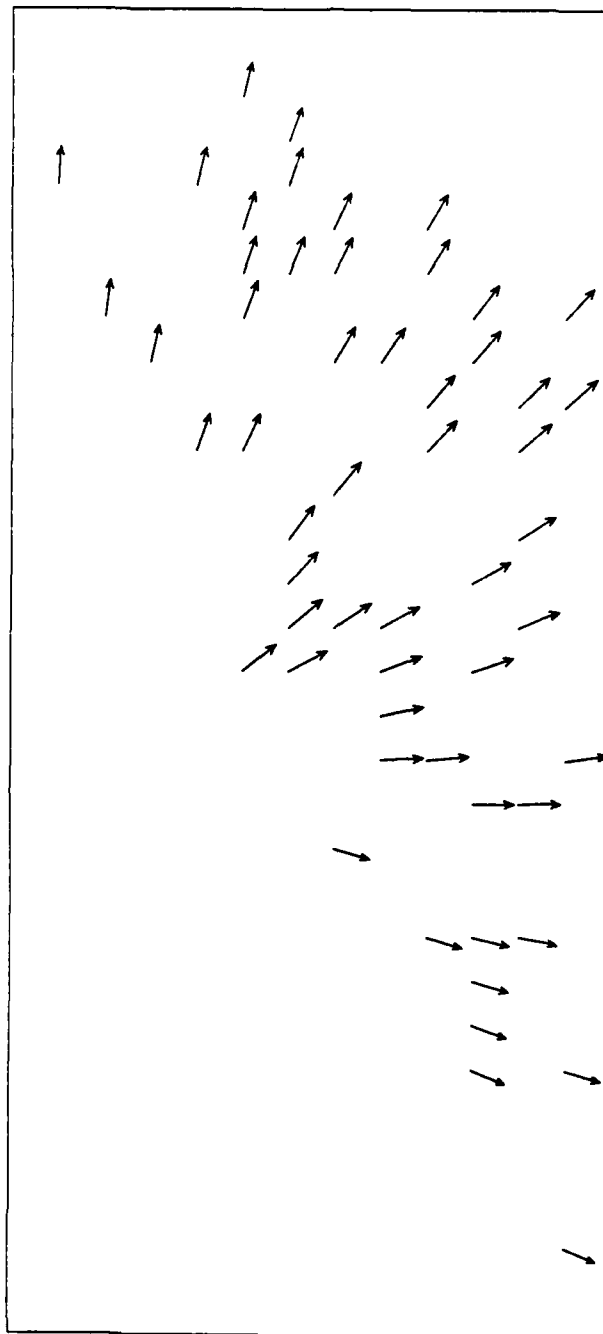


Figure 6.14 Model output showing microburst to right front of circulation center, with no tornado damage present.

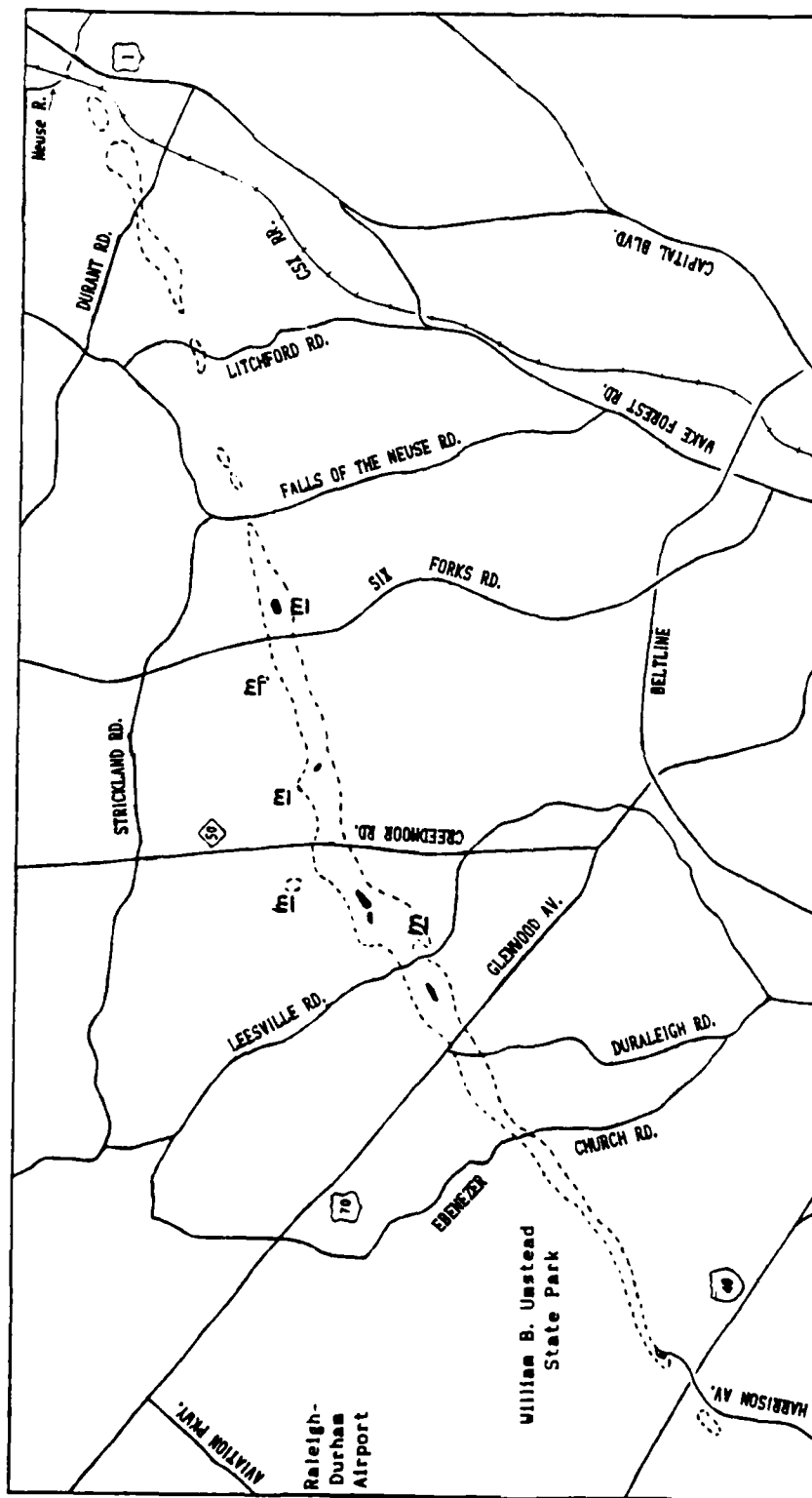


Figure 6.15 Locations of microbursts along damage track in north Raleigh, marked "m", with areas of F4 damage shown in black.

had the microbursts not occurred. Further evidence of this supposition is the fact that the input values for the tornadic winds used in the model runs never exceeded 75 or 80 m s^{-1} . Yet the output values obtained by adding a microburst, whose maximum outflow wind speed was 50 m s^{-1} or less, often exceeded 100 m s^{-1} . So, it is quite possible that this effect transformed an F2 tornado into an F4 storm.

The damage at the end of Old Deer Trail appears to indicate that a very small microburst, or "burst swath", occurred. A house in the middle of an area of heavy damage was left nearly undamaged, whereas the house immediately across the street was demolished; its debris blown in a direction away from the undamaged house (to the east-northeast). See Figure 6.16. Events such as this, discussed by Fujita and Wakimoto (1981) and Fujita (1985), are very localized, generally on a scale of 40 meters or less, but can produce extreme damage. This particular feature was located just to the right of the line of converging trees and may have been responsible for the area southeast of Clearbrook Drive with trees fallen indiscriminately over each other.

Additionally, areas such as the creek valley southwest of Greystone Lake and the "Y" shaped swath in the woods west of Creedmoor Road may also be indicative of the presence of microbursts. Airflow with a downward component would have been concentrated in the lower areas, while leaving the higher elevation areas less exposed. A similar pattern was

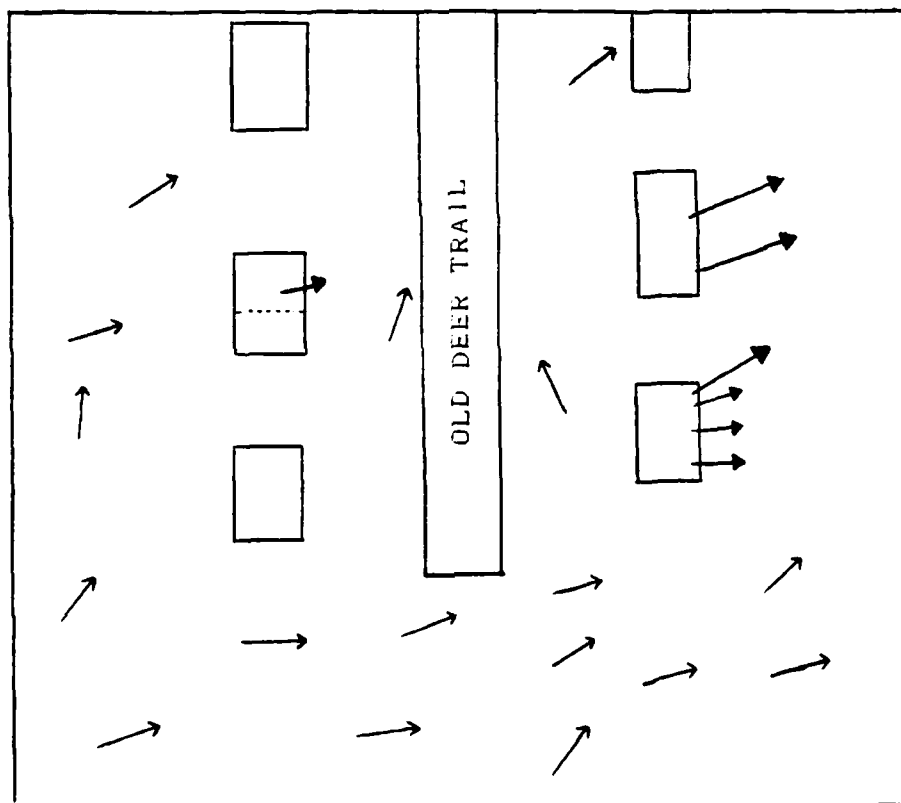


Figure 6.16 Close-in view of damage at the end of Old Deer Trail. Large head arrows show debris scatter from destroyed houses, small head arrows show downed trees. The bottom house (box shape) on the left was spared major damage. Tornado center moved just above this field of view.

observed in the South Hill, KY storm of 27 April 1971 (Fujita et al, 1971). As the areas in question are both south of the center of the tornado's path, this is further evidence of damage being affected by winds other than just the tornadic winds.

Many facets of the damage are similar to those observed in the Teton-Yellowstone Tornado of 1987 as surveyed by the University of Chicago (Fujita, 1989). That was also a long tracked storm, and was accompanied by numerous microbursts. Figure 6.17 shows the tornado relative location of the microbursts counted in the Wyoming storm. Most are on the right side of the tornado, with the right-front quadrant most preferred. The microbursts locations suggested in this study for the Raleigh storm are primarily in the right-front and left-rear quadrants of the tornado.

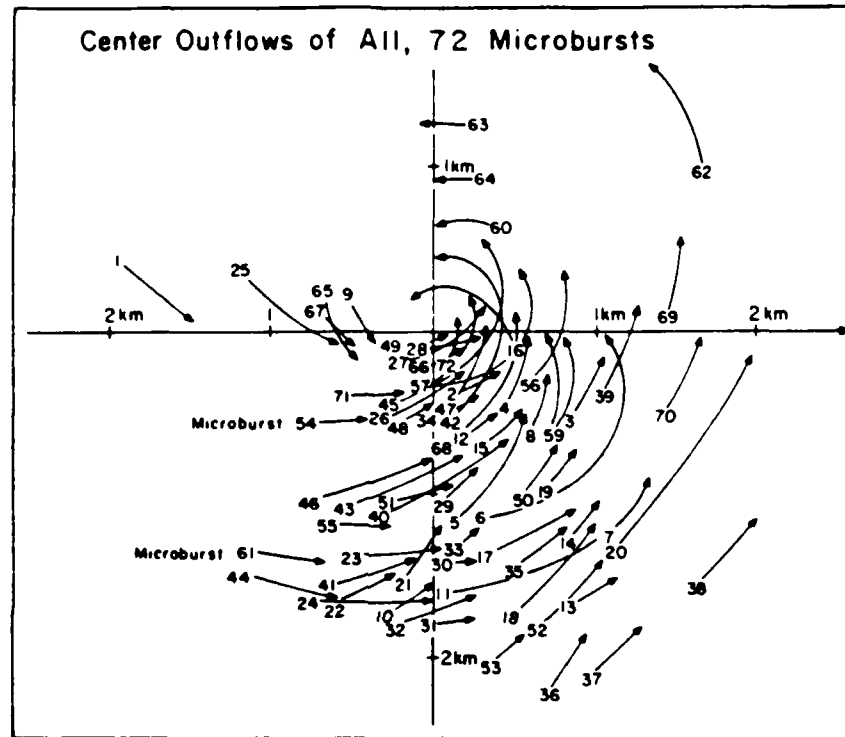


Figure 6.17 Tornado relative locations of microbursts in the Teton-Yellowstone tornado of 1987. (Fujita, 1989)

7. CONCLUSIONS AND FUTURE RESEARCH

7.1 Conclusions

The Raleigh tornado appears to have been accompanied by, and influenced by, a series of external winds, both on the same scale as the tornado (microbursts) and on a larger than tornado scale (ambient wind). These winds had a profound impact on the course of the tornado event as it transpired.

The evidence of the damage in north Raleigh, verified by eyewitness reports, indicates that a strong wind of mesoscale origin accompanied the tornado along its path. This wind was between 20 and 30 m s⁻¹ in speed and between 210° and 240° in direction. It was most likely associated with the outflow from the squall line which contained the Raleigh cell. Additionally, numerous microbursts appeared to have been present, some near enough to the tornado to affect its winds, and hence the orientation of the damage.

The presence of microbursts also seems to have greatly affected the intensity of the damage produced by the tornado. The most heavily damaged areas occurred near one or more microbursts. The model produced much higher winds with a microburst near the tornado than the winds of either the tornado or microburst on their own. Because of this, the severity of the tornado was greater than it would have been otherwise.

The two dimensional kinematic model devised to simulate damage from a tornado did an adequate job of simulating the

patterns of damage observed in north Raleigh. In addition to showing the basic pattern of damage that was established early in the life of the storm, it also did a reasonable job of recreating some of the observed deviations from this pattern by alternating the external wind profile, i.e. adding a microburst. This can be taken as further evidence that such features existed near the tornado.

The Raleigh tornado shared characteristics with other tornadoes studied in the literature. The strong inflow in several areas associated with microbursts are similar to the asymmetric inflows observed in other tornadoes, notably the Great Bend tornado of 1974 (Golden and Purcell, 1977). Damage was observed in several places to be more intense in lower elevation areas than on adjoining higher terrain, as in the South Hill tornado of 1971 (Fujita et al, 1971). The patterns of damage observed in Raleigh were similar to other tornadoes accompanied by nearby microbursts (Fujita, 1978 and 1989).

The presence of microbursts may also have been responsible for other facets of the Raleigh storm. In particular, they may have contributed to the longevity of the tornado in the manner described by Fujita (1989) in the Teton-Yellowstone tornado of 1987.

7.2 Future Research

Several implications for future research arise from this study. One important one would be a study on dynamic relationships between tornadoes and microbursts or other types of outflow in close proximity. Refinements could then be made to the tornado damage model. A dynamic wind flow would make it more representative of actual conditions.

Other refinements to the model could be the introduction of variable terrain features, such as elevation changes or changing roughness profile. The input wind speed values used for the microburst do not always seem representative of the output values, particularly when the microburst is on the left side of the tornado path, and so refinements to make it more user friendly are possible.

How the outflow features affected the formation and sustenance of the tornado is another possible area of study. The question of how these features can develop in close proximity to a tornado is another topic, as is how the synoptic situation contributed to the development of these features of the storm. By learning as much as possible from cases like this, it is possible to achieve a greater understanding of tornadoes in general.

REFERENCES

- Abbey, R. F. and T. T. Fujita, 1975: Uses of tornado path lengths and gradations of damage to assess tornado intensity probabilities. *Preprints: Ninth Conference on Severe Local Storms*, Amer. Met. Soc., 286-293.
- Agee, E. M., J. T. Snow, and P.R. Clare, 1976: Multiple vortex features in the tornado cyclone and the occurrence of tornado families. *Mon. Wea. Rev.*, **104**, 552-563.
- Anderson, C. E., 1990: Personal correspondence.
- Anderson, C. E. and M. W. Gunning, 1983: Mesoscale forcing factors involved in the long-lived Wichita Falls, Texas, tornadic storm. *Preprints: Thirteenth Conference on Severe Local Storms*, Amer. Met. Soc., 101-104.
- Barnes, S. L., 1978a: Oklahoma thunderstorms on 29-30 April 1970, part I: Morphology of a tornadic storm. *Mon. Wea. Rev.*, **106**, 673-684.
- Barnes, S. L., 1978b: Oklahoma thunderstorms on 29-30 April 1970, part III: Tornado characteristics inferred from damage tracks. *Mon. Wea. Rev.*, **106**, 697-703.
- Batchelor G. K., 1984: An Introduction to Fluid Dynamics. Cambridge Univ. Press.
- Benton, G. S. and A. M. Shapiro, 1988: A possible explanation for the sudden spin-up of tornadoes and other small atmospheric vortices. *Preprints: 15th Conference on Severe Local Storms*, Amer. Met. Soc., J93-J98.
- Brandes, E. A., 1984a: Relationships between radar-derived thermodynamic variables and tornado genesis. *Mon. Wea. Rev.*, **112**, 1033-1092.
- Brandes, E. A., 1984b: Vertical velocity generation and mesoscale sustenance in tornadic thunderstorms: the observational evidence. *Mon. Wea. Rev.*, **112**, 2253-2269.
- Browning, K. A., 1964: Airflow and precipitation trajectories within severe local storms which travel to the right of the winds. *J. Atmos. Sci.*, **21**, 634-639.
- Burgess, D. W. and R. J. Donaldson, 1979: Contrasting tornadic storm types. *Preprints: Eleventh Conference on Severe Local Storms*, Amer. Met. Soc., 189-192.

Byers, H. R., 1942: Nonfrontal thunderstorms. Misc. Report No. 3, Univ. of Chicago, 26 pp.

Byers, H. R. and P. R. Braham, 1949: The Thunderstorm. U.S. Govt. Printing Office, 287 pp.

Davies-Jones, R. P. and J. H. Golden, 1975: On the relation of electrical activity to tornadoes. *J. Geophys. Res.*, **80**, 1614-1616.

Dessens, J., 1971: Influence of ground roughness on tornadoes: a laboratory simulation. *J. Appl. Met.*, **11**, 72-75.

Forbes, G. S., 1981: On the reliability of hook echoes as tornado indicators. *Mon. Wea. Rev.*, **109**, 1457-1466.

Forbes, G. S. and R. M. Wakimoto, 1983: A concentrated outbreak of tornadoes, downbursts, and microbursts, and implications regarding vortex classification. *Mon. Wea. Rev.*, **111**, 220-235.

Fujita, T. T., 1973: Proposed mechanism of tornado formation from rotating thunderstorm. *Preprints: Eighth Conference on Severe Local Storms*, Amer. Met. Soc., 191-196.

Fujita, T. T., 1976: Spearhead echo and downburst near the approach end of a John F. Kennedy Airport runway. SMRP Res. Paper No. 137, Univ. of Chicago, 57 pp.

Fujita, T. T., 1978: Manual of downburst identification for Project NIMROD. SMRP Res. Paper No. 156, Univ. of Chicago, 104 pp.

Fujita, T. T., 1985: The downburst: microburst and macroburst. SMRP Res. Paper No. 210, Univ. of Chicago, 82 pp.

Fujita, T. T., 1989: The Teton-Yellowstone tornado of 21 July 1987. *Mon. Wea. Rev.*, **117**, 1913-1940.

Fujita, T. T., D. L. Bradbury, and P.G. Black, 1967: Estimation of tornadic windspeed from characteristic ground marks. SMRP Res. Paper No. 69, Univ. of Chicago, 99 pp.

Fujita, T. T., J. J. Tecson, and L. A. Schaal, 1971: Preliminary results of the Tornado Watch Experiment 1971. *Preprints: Seventh Conference on Severe Local Storms*, Amer. Met. Soc., 255-261.

- Fujita, T.T. and R. M. Wakimoto, 1981: Five scales of airflow associated with a series of downbursts on 16 July 1980. *Mon. Wea. Rev.*, **109**, 1438-1456.
- Goff, R. C., 1976: Vertical structure of thunderstorm outflows. *Mon. Wea. Rev.*, **104**, 1429-1440.
- Golden, J. H. and D. Purcell, 1977: Photogrammetric velocities for the Great Bend, Kansas, tornado of 30 August 1974: accelerations and asymmetries. *Mon. Wea. Rev.*, **105**, 485-492.
- Hjelmfelt, M. R., 1984: Radar and surface data analysis of a microburst in JAWS. *Preprints, 22nd Conference on Radar Meteorology*, Amer. Met. Soc., 64-69.
- Hoecker, W. H., 1960: Wind speed and air flow patterns in the Dallas tornado of April 2, 1957. *Mon. Wea. Rev.*, **88**, 167-180.
- Klemp, J. B., 1987: Dynamics of tornadic thunderstorms. *Ann. Rev. of Fluid Mech.*, **19**, 369-402.
- Krueger, S. K. and R. M. Wakimoto, 1985: Numerical simulation of dry microbursts. *Preprints, 14th Conference on Severe Local Storms*, Amer. Met. Soc., 163-166.
- Lemon, L. R. and C. A. Doswell, 1979: Severe thunderstorm evolution and mesoscale structure as related to tornado genesis. *Mon. Wea. Rev.*, **107**, 1184-1197.
- Letzmann, J., 1923: Das Bewegungsfeld in Fuss einer fortschreitenden Wind- oder Wasserhose. *Aeta Comm. Univer. Dorpat AIII*, 1-136.
- McCarthy, J., J. Wilson, and T. T. Fujita, 1982: The Joint Airport Weather Studies Project. *Bul. Amer. Met. Soc.*, **63**, 15-22.
- Mehta, K. C., J. E. Minor, and J. R. McDonald, 1976: Windspeed analysis of April 3-4 1974 tornadoes. *J. Struct. Div.*, **102**, 1709-1724.
- Miller, L. J., 1975: Internal airflow of a convective storm from dual-Doppler radar measurements. *Pure Appl. Geophys.*, **113**, 765-785.
- Miller, R. C., 1972: Notes on analysis and severe storm forecasting procedures at the Air Force Global Weather Central. Tech. Report 200, U. S. Air Force, Scott AFB.

- Minor, J. E., J. R. McDonald, and R. E. Peterson, 1982: Analysis of near-ground windfields. *Preprints: Twelfth Conference on Severe Local Storms*, Amer. Met. Soc., 289-292.
- Moller, A. R. and C. A. Doswell, 1988: A proposed advanced storm spotters training program. *Preprints: 15th Conference on Severe Local Storms*, Amer. Met. Soc., 173-177.
- (Raleigh, NC) News and Observer, 1989: Tornado! A Diary of the Destruction to Raleigh and surrounding North Carolina Counties. C. F. Boone, 64 pp.
- NOAA, 1988: Natural Disaster Survey Report to the Asst. Administrator for Weather Services--the North Carolina Tornadoes of November 28, 1988. U. S. Govt. Printing Office, 30 pp.
- Reynolds, G. W., 1959: A common wind pattern in relation to the classical tornado. *Bull. Amer. Met. Soc.*, **38**, 1-5.
- Rotunno, R. and J. B. Klemp, 1982: The influence of shear induced pressure gradient on thunderstorm motion. *Mon. Wea. Rev.*, **110**, 136-151.
- Rotunno, R., J. B. Klemp, and M. L. Weisman, 1988: A theory for strong, long-lived squall lines. *J. Atmos. Sci.*, **45**, 463-485.
- Sinclair, P. C., J.F.W. Purdom, and R. E. Dattore, 1988: Thunderstorm outflow structure. *Preprints: 15th Conference on Severe Local Storms*, Amer. Met. Soc., 233-239.
- Smull, B. F. and R. A. Houze, 1985: A midlatitude squall line with a trailing region of stratiform rain: radar and satellite observations. *Mon. Wea. Rev.*, **113**, 117-133.
- Storm Data, 1988, vol. **30** no. 11, 26-33, 56.
- Vasilov, S. V. and E. A. Brandes, 1984: An investigation of the transition from multicell to supercell storms. *Preprints: 22nd Conference on Radar Meteorology*, Amer. Met. Soc., 77-82.
- Wilhelmson, R. B. and J. B. Klemp, 1978: A three-dimensional numerical simulation of splitting that leads to long-lived storms. *J. Atmos. Sci.*, **35**, 1037-1063.

APPENDIX

Program for Tornado Damage Model

```

C      THIS PROGRAM SIMULATES THE FLOW
C      FIELD NEAR A VORTEX / SINK
C      SUPERPOSITION PROPAGATING IN AN
C      AMBIENT FLUID
C      *****COMPUTES DAMAGE VECTORS*****
C
C      VARIABLES AND ARRAYS
C
C      PARAMETER (NX=50,NY=50)
C
C      REAL MMAX,MAXVEL,MBMAX,MBVEL
C      REAL*4 X(NX),Y(100),U(NX,NY),V(NX,NY),UTOT(NX,NY),WORK(8000)
C      REAL*4 UMAX(NX,NY),VMAX(NX,NY),UTH(NX,NY),DAMT(NX,NY)
C      REAL*4 BUTH(NY,NY),BUMAX(NX,NY),BVMAX(NX,NY)
C      INTEGER*2 MAX,NX,NY)
C      CHARACTER*1 MBST
C      LOGICAL TRZONE
C
C      -NX AND NY ARE GRID SIZES.
C      -GLNGTH IS LENGTH OF GRID SPACING IN METERS.
C      -U, V ARE VELOCITY COMPONENTS; UTOT=SQRT(U**2+V**2).
C      -UMAX,VMAX,UTH ARE VALUES ASSIGNED TO POINTS WHOSE TOTAL
C      VELOCITY VALUE EXCEEDS A SPECIFIED THRESHOLD.
C      -VRAD IS THE VORTEX RADIUS IN METERS.
C      -UVORT IS THE Y-DIRECTION SPEED OF THE VORTEX IN M/SEC.
C      -DTMAX IS THE MAXIMUM VALUE OF THE COMPUTATIONAL TIME STEP.
C      -MMAX IS THE MAXIMUM SINK STRENGTH OF THE VORTEX.
C      -OMAX IS THE MAXIMUM CIRCULATION STRENGTH OF THE VORTEX.
C      -T IS THE ACCUMULATED TIME.
C      -UMICRO, VMICRO ARE THE MAXIMUM VELOCITY COMPONENTS ASSOCIATED
C      WITH THE MICROBURST.
C      -SUM IS DISTANCE TO TORNADO CENTER
C      -SUM1 IS DISTANCE TO CENTER OF MICROBURST OUTFLOW.
C      -OFB IS OUTFLOW BOUNDARY RADIUS OF THE MICROBURST.
C      -THRESH DETERMINES THE SPATIAL EXTENT OF THE PLOT.
C      -IMIN,IMAX,JMIN,JMAX ARE THE LIMITS OF GRIDPOINTS TO BE
C      INCLUDED IN THE PLOT.
C
C      *****INPUT VALUES FOR USE BY MODEL*****
C
C      RAD=0.017453292
C      PI=3.1415927
C
C      WRITE(6,*) 'PLEASE ENTER THE REQUIRED DATA AS REQUESTED'
C      WRITE(6,*) ' '
C      WRITE(6,*) 'INITIAL X-COORDINATE OF CENTER IS 29'
C      WRITE(6,*) 'ENTER INITIAL Y-COORDINATE OF CENTER'
C      READ(5,*) JCEN
C      WRITE(6,*) ' '
C      WRITE(6,*) 'ENTER VORTEX RADIUS, IN METERS'
C      READ(5,*) VRAD
C      WRITE(6,*) ' '
C      WRITE(6,*) 'ENTER # OF GRID POINTS PER VORTEX RADIUS'
C      READ(5,*) GRID
C      WRITE(6,*) ' '
C      WRITE(6,*) 'ENTER VORTEX TRANSLATIONAL SPEED, (M/S)'
C      READ(5,*) UVORT
C      WRITE(6,*) ' '
C      WRITE(6,*) 'ENTER DIRECTION FROM WHICH TORNADO IS MOVING'
C      READ(5,*) DIRT
C      WRITE(6,*) ' '
C      WRITE(6,*) 'ENTER ESTIMATED MAXIMUM WIND SPEED, (M/S)'
C      READ(5,*) MAXVEL
C      WRITE(6,*) ' '
C      WRITE(6,*) 'ENTER SWIRL RATIO: (TANG. VEL./RADIAL VEL.)'
C      READ(5,*) SWIRL
C      WRITE(6,*) ' '
C      GLNGTH=VRAD/GRID

```

```

IF (UVORT.EQ.0.0) THEN
  MTIME=1.0
  DTMAX=1.0
ELSE
  DTMAX=GLNGTH/UVORT
  WRITE(6,*) 'TIME STEP IS (IN SECONDS)'
  WRITE(6,*) DTMAX
  WRITE(6,*) ' '
  WRITE(6,*) 'ENTER NUMBER OF ITERATIONS TO BE PERFORMED'
  WRITE(6,*) 'MUST BE AN INTEGER VALUE.'
  READ(5,*) MTIME
  WRITE(6,*) ' '
ENDIF
WRITE(6,*) 'ENTER MINIMUM WIND SPEED FOR DAMAGE TO OCCUR, (M/S)'
READ(5,*) UDAM
WRITE(6,*) ' '
WRITE(6,*) 'ENTER AMBIENT WIND SPEED, (M/S)'
READ(5,*) AMB
WRITE(6,*) ' '
WRITE(6,*) 'ENTER AMBIENT WIND DIRECTION'
READ(5,*) DIRA
WRITE(6,*) ' '
WRITE(6,*) 'MICROBURST IN FIELD? (Y/N)'
READ(5,600) MBST
600 FORMAT (A1)
IF(MBST.EQ.'Y') THEN
  WRITE(6,*) ' '
  WRITE(6,*) 'ENTER X-COORDINATE OF MICROBURST CENTER'
  READ(5,*) IMB
  WRITE(6,*) ' '
  WRITE(6,*) 'ENTER Y-COORDINATE OF MICROBURST CENTER'
  READ(5,*) JMB
  WRITE(6,*) ' '
  WRITE(6,*) 'ENTER MAXIMUM MICROBURST WIND GUSTS'
  READ(5,*) MBMAX
  MBVEL=MBMAX
  IF(IMB.LT.25) MBVEL=MBVEL-UVORT
  WRITE(6,*) ' '
  WRITE(6,*) 'ENTER INITIAL MICROBURST OUTFLOW BOUNDARY RADIUS'
  READ(5,*) OFB
ENDIF
WRITE(6,*) ' '
WRITE(6,*) 'ENTER RANDOM NUMBER SEED'
WRITE(6,*) 'USE 6-DIGIT ODD INTEGER'
READ(5,*) ISEED
WRITE(6,*) ' '

C *****INITIALIZATION OF VALUES USED IN MODEL*****

IF(DIRA.GE.DIRT) THEN ' SETS AMB DIR RELATIVE TO TORNADO MOTION
  DIR=DIRA-DIRT
ELSE
  DIR=DIRA-DIRT+360.0
ENDIF

VR=SQRT(((MAXVEL-UVORT)**2)/((SWIRL**2)+1))
VT=SWIRL*VR
MMAX=2*PI*VRAD*VR
GMAX=2*PI*VRAD*VT
PRINT*, 'VR, VT=', VR, VT, ' SINK, CIRC=', MMAX, GMAX

UAMB=AMB*SIN(DIR*PI/180) ! AMBIENT WIND COMPONENTS
VAMB=AMB*COS(DIR*PI/180)

DO 1 I=1,NX
  X(I)=(FLOAT(I)-25)*GLNGTH ! VALUES ON X-COORDINATES
DO 2 J=1,NY
  UMAX(I,J)=0.0 ! INITIALIZES DAMAGE RESULTS
  VMAX(I,J)=0.0
  UTOT(I,J)=0.0
  MAX(I,J)=0
  DAMT(I,J)=UDAM+30*RAN(1SEED) ! INITIALIZES DAMAGE TEST ARRAY
2 CONTINUE ! RANDOM DAMAGE THRESHOLDS
1 CONTINUE

```



```

C ***MOVEMENT OF VORTEX AND EXPANSION OF MICROBURST WITH TIME***
      YO=-1.0*UVORT*T                                ! MOVEMENT OF TORNADO CENTER
      IF(MBST.EQ.'Y') THEN
        OFB=OFB+0.3*MBVEL*DTMAX                      ! EXPANSION OF OUTFLOW
        MBVEL=(MBMAX-UVORT)*(500/OFB)                ! DECREASE OF MB WIND
      ENDIF

500  CONTINUE

C *****FIXATION OF DATA FIELD, SO THAT PLOT CENTERS ON DAMAGED AREA*****
      THRESH=20.0
      IF(UDAM.GT.THRESH) THRESH=UDAM
      IF(AMB.GE.THRESH) THRESH=AMB+1

      IMIN=25
      IMAX=25
      IMN=25
      DO 51 J=1,(NY/2)                                ! NORMALIZES PLOT IN X-DIR
        DO 52 I=1,NX
          IF(UTM(I,J).LT.THRESH) THEN
            IF(I.GT.IMAX) GOTO 51
            IMN=I
          ELSE
            IF(IMN.LT.IMIN) IMIN=IMN
            IF(I.GT.IMAX) IMAX=I
          ENDIF
65      CONTINUE
52      CONTINUE
51      IF(IMIN.EQ.25) IMIN=1
      PRINT*,'IMIN=',IMIN,'      IMAX=',IMAX

      JMIN=50
      JMAX=0
      JMN=JCEN
      DO 60 I=1,NX                                ! NORMALIZES PLOT IN Y-DIR
        DO 65 J=1,NY
          IF(UTM(I,J).GE.THRESH) JMX=J
          IF(UTM(I,J).GE.THRESH) JMN=J-1
          IF(JMN.LT.JMIN) JMIN=JMN
          IF(JMX.GT.JMAX) JMAX=JMX
65      CONTINUE
60      CONTINUE
      IF(JMIN.EQ.0.OR.JMIN.EQ.JCEN) JMIN=1
      PRINT*,'JMIN=',JMIN,'      JMAX=',JMAX

      II=IMAX-IMIN+4
      JJ=JMAX-JMIN+2

      DO 70 I=1,II
        DO 75 J=1,JMAX+2
          BUMAX(I,J)=UMAX(IMIN+I-2,JMIN+J-1)
          BVMAX(I,J)=VMAX(IMIN+I-2,JMIN+J-1)
          BUTH(I,J)=UTM(IMIN+I-2,JMIN+J-1)
75      CONTINUE
70      CONTINUE

      PRINT*,'ELAPSED TIME=',T-DTMAX,'SECONDS'
      PRINT*,'MAX WIND=',UTMAX,'M/S'

C *****NCAR GRAPHICS SUBROUTINES FOR PLOTTING*****
C      CALL STRMLN(BUMAX,BVMAX,WORK,NX,II,JJ,0,IER)
C      CALL VELVCT(BUMAX,NX,BVMAX,NY,II,JJ,UDAM,0,0,0,0,0)
C      CALL CONREC(BUTH,NX,II,JJ,0,0,0,0,0,0)
      STOP
      END

```